UNIVERSITY OF SOUTHERN CALIFORNIA
Department of Civil Engineering

and

UNIVERSITY SS. CYRIL AND METHODIUS

Institute of Earthquake Engineering and Engineering Seismology (IZIIS)

IMPULSE RESPONSE ANALYSIS OF THE BORIK-2 13-STORY RESIDENTIAL BUILDING IN BANJA LUKA DURING 20 EARTHQUAKES (1974–1986)

by

Mihailo D. Trifunac, Maria I. Todorovska, Miodrag I. Manić, and Borko Đ. Bulajić

Report CE 07-02

July, 2007
Los Angeles, California

www.usc.edu/dept/civil_eng/Earthquake_eng/

ABSTRACT

The Borik-2 residential building, located in Banja Luka, Republic of Srpska (One of the two State Entities of the state of Bosnia and Herzegovina, in former Yugoslavia) is a rare example of an instrumented reinforced-concrete building that has been shaken by a significant number of small earthquakes and by one intermediate-size earthquake. It was not damaged by any of these earthquakesand only in the case of the largest, M=5.4, of 8/13/1981 did it possibly approach damaging levels of response. During the other 19 recorded events, the motions were small. These recordings are invaluable for validation of structural models and for structural health-monitoring methods, and they are described in this report.

In a new method, which was recently developed and tested for two buildings in Southern California, we measure the wave travel times of vertically propagating waves in a building by working with plots of impulse response functions computed by deconvolution of the recorded earthquake response. We use these travel times to infer the local (between sensors) and global changes in structural stiffness from one earthquake event to another, and with time during strong levels of shaking for large events. The measured wave travel times are also used to estimate the fundamental fixed-base frequency of the building, f_1. These estimates of f_1 can be compared with the estimates of the soil-structure system frequency f_{sys} during the same earthquakes and during forced and ambient vibration tests. For the building described in this report, the average value of f_1 during the strong EW motion of event EQ 11 (8/13/1981) decreased by about 16%, while the corresponding f_{sys} dropped by about 22%. For the NS response during the same event, the corresponding reductions were 18% and 31% respectively.

In agreement with our previous studies (Todorovska and Trifunac 2006, 2007a,d), this analysis confirms that monitoring only the changes of f_{sys} can be unreliable for structural health monitoring, while monitoring changes of f_1, over suitably chosen time windows (before, during, and after excitation by strong earthquake motions) can be a powerful and robust tool for structural health monitoring. Also, we emphasize that for verification of mathematical models of structures that employ the fixed-base assumption (no soil-structure interaction), structural stiffness should be calibrated with respect to f_1 and not f_{sys}.

Keywords: Earthquake response, damage detection, structural health monitoring, wave propagation times, impulse response function, Borik-2, Banja Luka

TABLE OF CONTENTS

1. INTRODUCTION

The Borik-2 residential building is a rare example of an instrumented reinforced-concrete building that approached the damaging level of response but did not experience the structural damage during the 12-year period 1974–1986. What is interesting about this building is that excellent strong-motion data from 20 earthquakes are available for this period (between April of 1974 and October of 1986). Forced vibration tests and one ambient vibration test of the building have also been conducted and can be used for relative comparison with the results based on earthquake response.

For structures supported by soils, which is typical for most residential areas, the soil-structure interaction is an integral part of the dynamic response (Luco et al. 1986). For a soil-structure system, the peaks of the transfer function of the relative response occur at the frequencies of the soil-structure system, rather than at the frequencies of the fixed-base building. Although the two sets of frequencies are related, it is difficult to determine experimentally the fixed-base frequencies from recorded seismic response unless the structure is appropriately instrumented. At present, the configuration of instruments in typical buildings is incomplete for such soil-structure interaction studies (Trifunac and Todorovska 2001). Under these circumstances, observed reductions in f_{sys}, the first frequency of the soil-structure system, have often been erroneously interpreted to be *entirely* due to loss of structural stiffness (e.g., Browning et al. 2000; De la Llera et al. 2001; Islam 1996; Li and Jirsa 1998). Aničić et al. (1990), Fajfar et al. (1987) and Petrović (1989) make the same mistake in their analysis of Borik-2 building by calibrating their structural models to f_{sys} rather than to f_1. As we will show in the following, the Borik-2 building has f_{sys} near 1.3 Hz, while its f_1 is close to 2 Hz. Since the building stiffness is proportional to the frequency squared, is can be seen that the models used by Aničić et al. (1990), Fajfar et al. (1987) and by Petrović (1989) have the overall stiffness too small, by a factor of about 2.5. Since their engineering models are used to verify the adequacy of structural design and to calibrate building dynamic response in general, it is seen that neglecting the role of soil-structure interaction in the dynamic response of this structure can lead to significant errors. For reliable health monitoring, and for the correct calibration of the structural models in general, it is therefore essential to be able to monitor f_1, the fundamental fixed-base frequency, separately from f_{sys}, the first frequency of the soil-structure system (Todorovska and Trifunac 2006, 2007a).

Snieder and Şafak (2006) used impulse response functions, computed by deconvolution from small amplitude seismic response, to analyze one-dimensional wave propagation in Millikan Library in Pasadena, California. Todorovska and Trifunac (2006, 2007a) proposed the use the

impulse response functions for monitoring the time changes in the response of structures experiencing damaging motions. They estimated f_1 from the travel time of shear waves, which propagate along the building height, and which require at least the recorded horizontal motion at the ground floor and at the roof. In this work, we apply their procedure to estimate f_1 from the recorded data of the NS and EW responses of the Borik-2 reinforced-concrete building during 20 earthquakes. We will estimate the variations of f_1 from one earthquake to another, and during the largest earthquake, and *calibrate* the detected changes in terms of the observed lack of documented damage. Such calibration is essential for future uses of f_1 as a tool for real-time structural health monitoring. This procedure was applied previously to estimate f_1 for (1) the Imperial County Services Building (a 6-story reinforced-concrete structure in El Centro, California, severely damaged by the Imperial Valley earthquake of October 15, 1979, and later demolished), and (2) the 7-story Van Nuys Hotel, in Van Nuys, California. The observed changes in f_1 as function of the level of response, and in relation to f_{sys} and the observed damage, are described in Todorovska and Trifunac (2006, 2007a,d).

As we noted in our previous work, the changes in f_1 reflect changes in the *global* stiffness of the structure. Due to the redundancy of civil engineering structures, however, these changes are often small if the damage is localized, and, hence, are difficult to detect (see Chang et al. 2003, and Doebling et al. 1996, for detailed state of the art reviews on this topic). Wave propagation methods, however, make it possible to detect local changes in stiffness with relatively few sensors by detecting changes in travel times of seismic waves between sensors.

There are only a few publications on wave propagation methods for analyses of building response, other than nondestructive testing, for structural health monitoring and damage detection in civil structures (Kanai 1965, Todorovska and Lee 1989, Todorovska and Al Rjoub 2006, Todorovska and Trifunac 1989, 1990). Şafak (1999) presented a layered continuous model to detect damage by tracing changes in the parameters in the layers. Ivanović et al. (2001) used strong-motion data recorded in a 7-story RC building in Van Nuys during the 1994 Northridge earthquake, and cross-correlation analysis (to estimate time lags between motions recorded at different levels). Trifunac et al. (2003) analyzed changes in wave numbers (inversely proportional to the wave velocities) of waves propagating between different building stories. Gicev and Trifunac (2007a,b) used the energy and power of nonlinear waves to identify the location of damage. Ma and Pines (2003) proposed a method based on a lumped-mass building model and propagation of de-reverberated waves to identify the damage. The first applications of the impulse response functions computed by deconvolution (Snieder and Şafak 2006) to detect local changes in stiffness, and for earthquake damage detection in general, appear to be in our recent studies of the Van Nuys 7-story hotel (Todorovska and Trifunac 2006, 2007a) and of the Imperial County Services Building (Todorovska and Trifunac 2007b,c,d).

In this report, we present a brief description of the Borik-2 building and the recorded strong-motion data. Then we review the methodology and present the results, analysis, and conclusions.

2. THE BUILDING AND THE STRONG MOTION DATA

The data studied in this paper were recorded by the strong-motion accelerograph network that

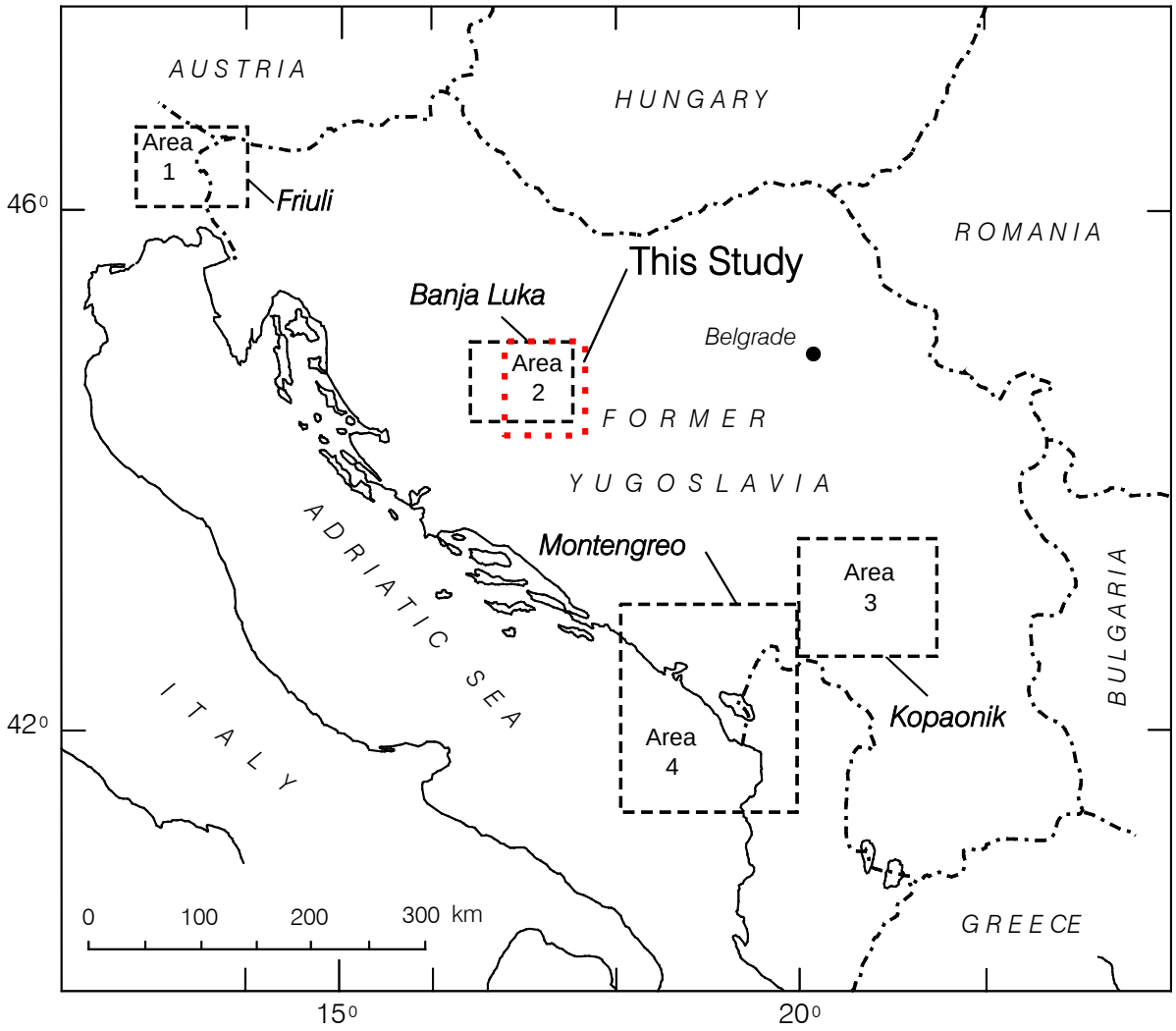

Fig. 2.1. Four areas in the former Yugoslavia that experienced concentrated earthquake activity during the period from the mid-1970s to the early 1980s. The building studied in this work, Borik-2, is located in Banja Luka, which is in Area 2.

started to operate in former Yugoslavia in 1973 (Jordanovski et al. 1987). The free-field data from this network were digitized at the University of Southern California in the Department of Civil Engineering, using automatic digitization and software methods described by Trifunac and Lee (1979). For the period between 1975 and 1983, these data were recorded mainly in four

areas of former Yugoslavia that experienced the earthquake activity: Friuli, Banja Luka, Kopaonik, and Montenegro (Fig. 2.1) (Trifunac and Ivanović (2003a,b). In this paper, we

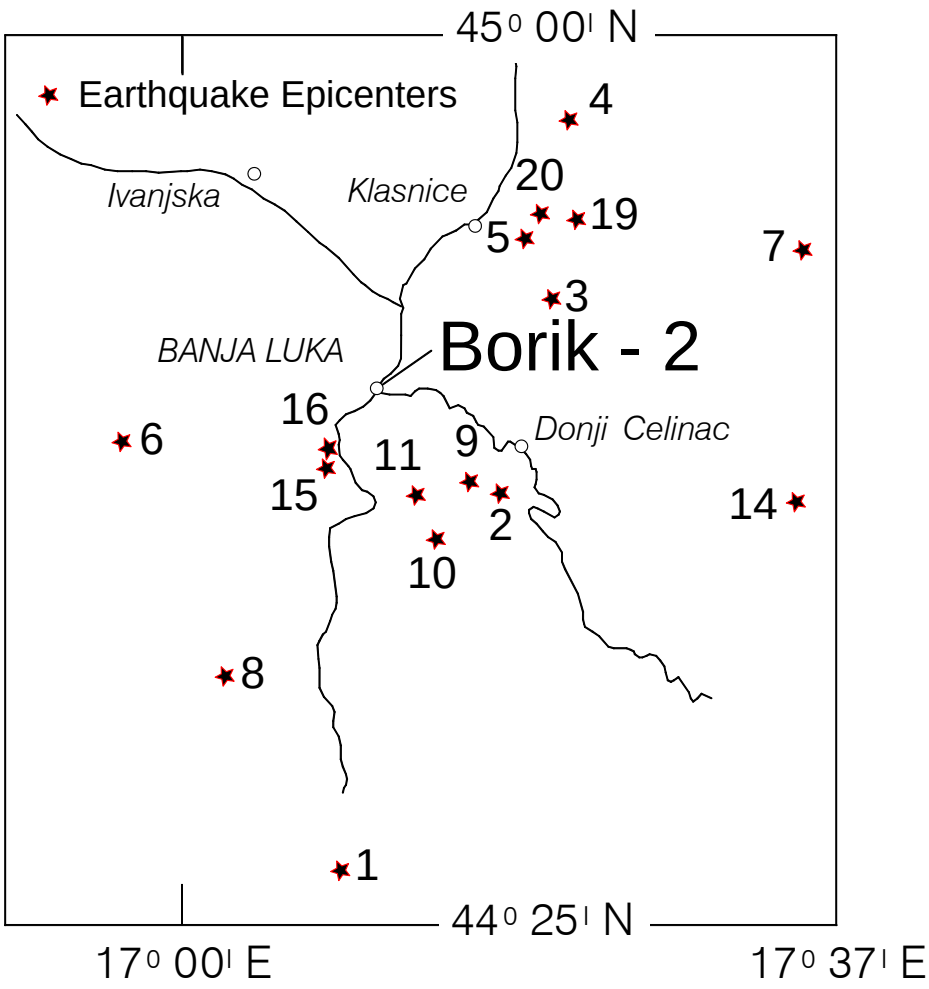

Fig. 2.2. Geographical distribution of the earthquakes that triggered the strong-motion instruments in the Borik-2 building. Four additional earthquakes used in this study are not shown.

analyze only accelerograms recorded in the Borik-2 building in Banja Luka. These data were digitized and processed by the authors during the summer of 2006 using the flat-bed scanner and the digitization procedure described by Lee and Trifunac (1990). Fig. 2.2 shows the epicenters of 16 identified earthquakes used in this study and their relative positions with respect to the site of the Borik-2 building.

2.1 The Building

The structure we study is a 14-story apartment building located in the settlement "Borik" (44° 46′ 15.35′′ North, and 17° 12′ 20.02′′East) in the city of Banja Luka, Republic of Srpska (Bosnia and Herzegovina), referred to in this work as Borik-2 (Fig. 2.1.1a,b,c,d,e,f). The building is 17.84 × 17.84 m in plan and has a basement, 13 floors, and a roof. Each of the 13 floors is 2.80 m high, the basement is 2.47 m high, and the construction on the roof (terrace plus the building for the lift equipment) is 3.40 m high. Figure 2.1.1 shows: (a) the foundation layout, (b) a plan view of a typical floor, (c) a cross-section view of the building frame, (d) a view of the building from southwest, (e) a satellite image of its surroundings, and (f) a northwesterly view of its surroundings from above.

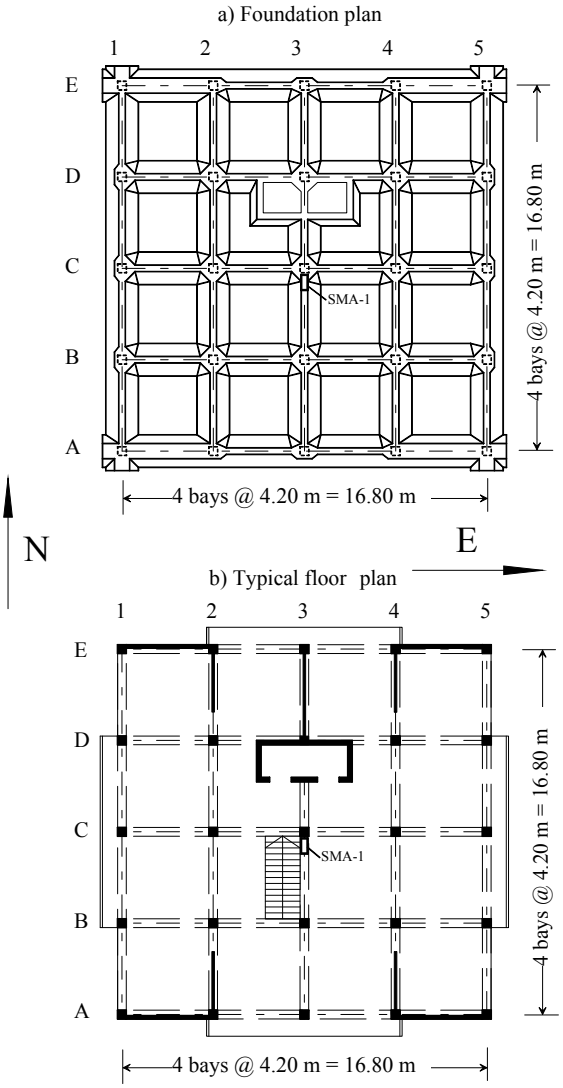

Fig.2.1.1a,b. Foundation plan (top), typical floor plan (bottom).

The foundation is constructed as a strip footing with a constant height, connected in the two orthogonal directions by a grid of beams. The foundation level for all strip footings is –4.24 m (from the ground level). Typical framing consists of columns spaced at 4.20 m centers in both the transverse and longitudinal directions.

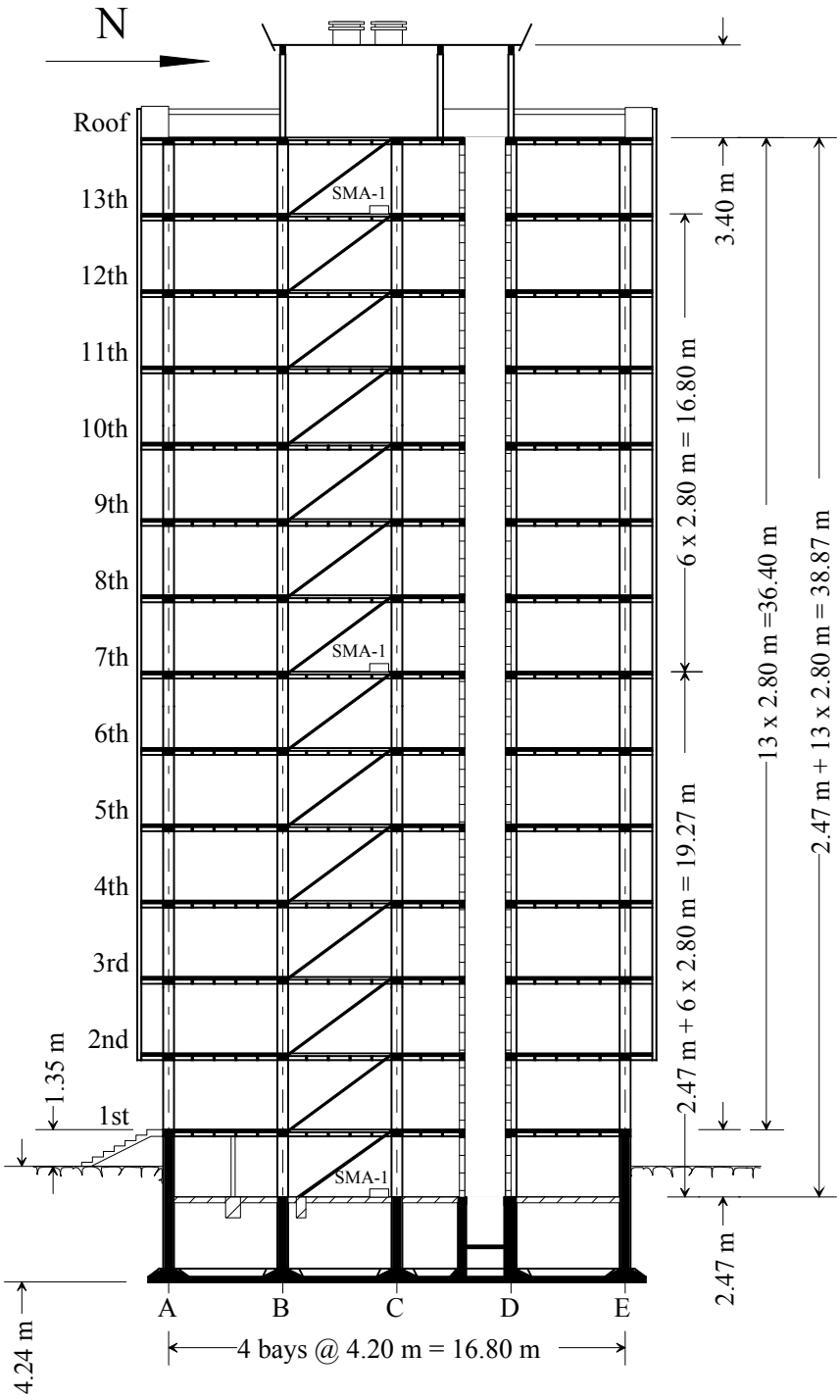

Fig.2.1.1c. North-south cross section of Borik-2 building.

Fig.2.1.1d View from South-West.

The building was constructed in 1972 using the IMS (Institute for Testing of Materials, Belgrade, Serbia) system of construction (Petrović 1982; Dimitrijević 1982; 2002; Vojnović 1982). This system consists of prefabricated reinforced-concrete columns and floor diaphragms and cast-in-

Fig.2.1.1e. Borik-2 and neighboring buildings (satellite view).

place reinforced-concrete shear walls. The connection between the columns and floor diaphragms is attained solely by the friction due to horizontal pre-stressing of the floor diaphragms. The floor diaphragms are reinforced-concrete prefabricated cassette ceilings with the total height of 22 cm at all floors. Spandrel beams surround the perimeter of each slab and comprise the cables for the horizontal pre-stressing of the whole floor diaphragm system. The shear walls have a constant thickness of 15 cm, from the basement to the roof, and are made of the relatively constant quality of the reinforced concrete, with the cylinder compressive strength measured in these walls being in the range of 33 to 48 MN/m^2. The percent of reinforcement in the shear walls ranges from 0.92 to 2.54% in the E-W direction and from 2.74 to 4.73 % in the

N-S direction. The columns also have a constant cross section of 38 × 38 cm, with the prefabricated continuation at each third floor. All columns are reinforced with $4\phi 18$, and the cylinder compressive strength measured in the ground floor columns was in the range from 62 to 64 MN/m^2. The measured values of the modulus of elasticity were in the range from 3.3×10^4 to 4.4×10^4 MN/m^2 (Fajfar et al. 1987).

Fig.2.1.1f. Panoramic view of Borik-2 building, in Banja Luka.

The “non-structural” elements include (1) light partition walls, (2) a brick masonry lift shaft, and (c) the prefabricated reinforced concrete: parapets, face elements, and a staircase. The roof diaphragm is constructed as a cast-in-place reinforced-concrete structure.

2.2 Site Conditions

The building is situated on soil with favorable (in the engineering sense) conditions, with considerable gravel deposit. The geotechnical soil profile beneath the Borik-2 building is shown

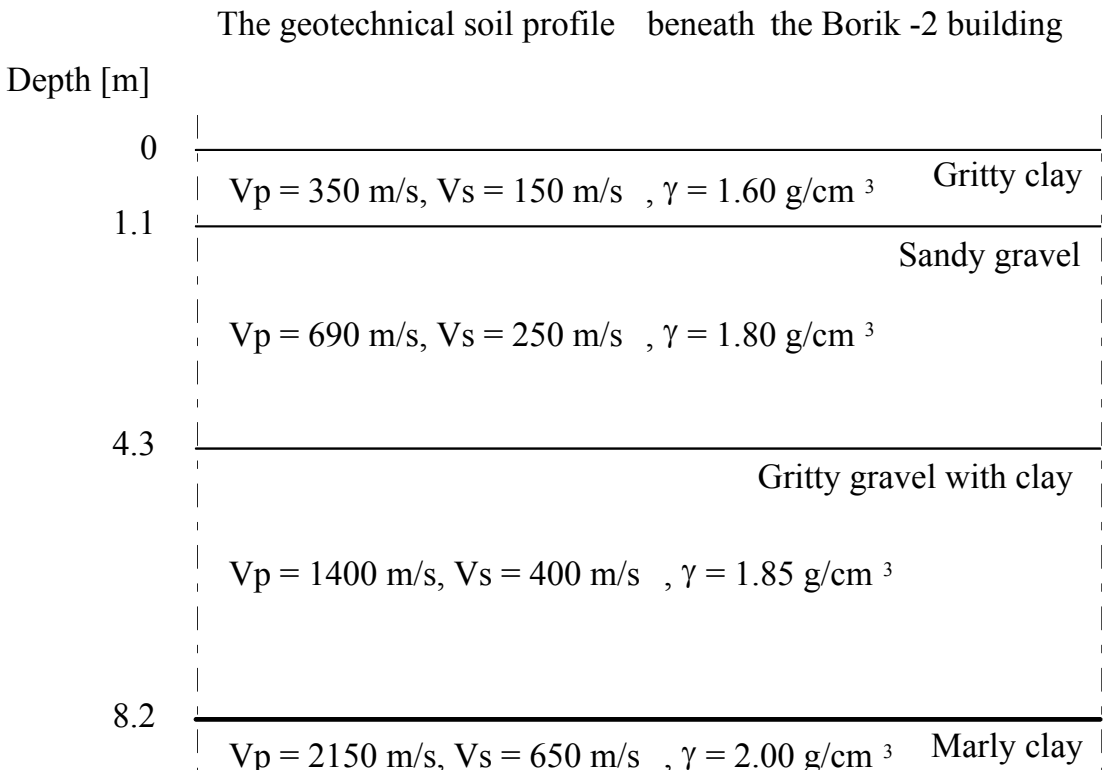

Fig.2.2.1 The geotechnical soil profile beneath the Borik-2 building.

in Figure 2.2.1. The equivalent shear wave velocity in the top 30 m is near 475 m/s, which is about 60% higher than the typical value of 300 m/s in Southern California. Furthermore, since the footing of Borik-2 building is at –4.24 m, the foundation is only about 4 m above the Marley clay, which has shear wave velocity of 650 m/s, and consequently the representative shear modulus of the soil around the foundation is 3 to 5 times larger than at the building sites we studied in Southern California (Todorovska and Trifunac 2006, 2007a). Therefore the nonlinearities in the soil response at the site of the Borik-2 building will occur at relatively higher levels of shaking.

2.3 Forced Vibration Experiments

For dynamic testing by forced vibrations, harmonic sinusoidal force is generated by specially constructed vibrators (e.g., see Appendix A in Luco et al. 1986). For the testing of the Borik -2, the GSV-101 GEOTRONIX (USA) vibrators were used. By gradually increasing the excitation frequency and measuring the amplitudes of response of the structure at the selected points, frequency response curves can be constructed from which resonant frequencies of the structure can be defined.

Two forced-vibration tests were carried out in the Borik-2 building by the staff of the Institute of Earthquake Engineering and Engineering Seismology—IZIIS, Skopje (Petrovski et al. 1975). The building was first studied in July 1972, before the installation the of majority of the partition walls and other nonstructural elements, and again four months later, in October 1972, after the installation of almost all nonstructural elements. Masses of the building during the first and the second test were estimated, respectively, to be 59% and 81% of the final mass in the completed stage.

Table 2.3.1. Forces, Frequencies, and Peak Displacements at Resonance, During Forced-Vibration Tests in Borik-2 Building, in October 1972.

Direction	Approximate force at resonance (lb/kg)	Resonant frequency (Hz)	Peak displacement at Roof (cm)
EW	730/330	1.343	0.180
	440/200	1.360	0.120
	260/115	1.376	0.076
NS	440/200	1.345	0.112
	350/160	1.372	0.085
	260/115	1.380	0.068

After the second forced-vibration test, when the state of the Borik-2 building was assessed to be similar to the expected one during the serviceability period of the building, the dynamic

characteristics in the two orthogonal directions and torsion were defined. The corresponding natural frequencies in the E-W direction were f_1 = 1.31 Hz, f_2 = 5.57 Hz; in the N-S direction they were f_1 = 1.30 Hz, f_2 = 5.06 Hz; and torsion was measured at f_1 = 1.50 Hz and f_2 = 6.08 Hz. The viscous damping coefficients were evaluated to be 2% on the average. For evaluation of the damping coefficient, the two methods were simultaneously used: (1) the half-power method and (2) the logarithmic decrement method.

The results of the forced-vibration tests indicated pronounced nonlinear response for different amplitudes of forcing function and some coupling between the translational and torsional responses. In Table 2.3.1, we summarize the results based on Fig. 3.9 (for EW) and Fig. 3.11 (for NS) in Trajkovski (1992), who describes the experiments from October 1972 for different amplitudes of the harmonic force. The transition of the resonant curves from low to high forcing functions is not continuous for the Borik-2 building, as one would expect for a gradually softening system (e.g., Hudson 1970). For both EW and NS excitation, the measured resonant curves show a clear peak at 1.38 Hz for the smallest periodic excitation (115 kg). With increasing force, this peak disappears and a new one emerges at 1.34 Hz for EW response (for the force of 330 kg), and at 1.35 Hz for NS response (for the force of 200 kg). This behavior suggests the opening and closing of some "gaps" at different force (deformation) amplitudes, and a highly complex dynamic system. It would, of course, be of considerable interest to determine whether such behavior occurs also during transient earthquake excitation, but at present the data we have is not sufficiently detailed to study this further.

2.4 Strong-Motion Records

In October 1972, as a part of the instrument network for recording strong earthquake ground motion on the territory of former the Yugoslavia, three strong-motion SMA-1 accelerographs were installed in the Borik-2 building (at the foundation level, at the 7th, and at the 13th floors) to record the response during future earthquakes. The location of these instruments is shown in Figs. 2.1.1b,c.

Table 2.4.1. Earthquakes recorded in Borik-2 during the instrumentation period 1972–1990.

#	EQ ii	Date	Time [GMT]	Epicentral Coordinates	Hypocentral Depth [km]	*M*	I_0
1	EQ 01	4/12/1974	06:24	44 27 00N, 17 09 00E	Unknown	2.8	5 MCS
2	EQ 02	4/23/1974	03:45	44 42 00N, 17 18 00E	Unknown	3.0	5 MCS
3	EQ 03	2/17/1975	14:24	44 49 29N, 17 00 21E	0	3.3	6 MCS

4	EQ 04	8/09/1975	08:46	44 56 44N, 17 22 35E	0	Unknown	4 MCS
5		10/08/1975	12:15	44 48 00N, 17 18 00E	Unknown	2.7	5 MCS
6	EQ 05	4/20/1977	00:31	44 51 56N, 17 19 40E	9.8	4.7	6 MCS
7		04/28/1977	03:41	44 55 02N, 17 20 59E	14.0	4.0	4 MCS
8	EQ 06	2/17/1979	22:06	44 44 07N, 16 56 24E	10.0	3.7	6 MCS
9	EQ 07	9/07/1979	12:57	44 51 24N, 17 35 07E	10.0	4.0	5 MCS
10	EQ 08	8/08/1980	16:35	44 34 48N, 17 02 24E	0	3.5	Unknown
11	EQ 09	7/24/1981	02:53	44 42 36N, 17 16 12E	5.0	3.0	Unknown
12	EQ 10	7/24/1981	02:55	44 40 12N, 17 14 24E	10.0	2.9	Unknown
13	EQ 11	8/13/1981	02:58	44 42 00N, 17 13 12E	7.0	5.4	8 MCS
14	EQ 12	8/13/1981	Unknown	Epicenter Unknown	Unknown	Unknown	Unknown
15	EQ 13	8/13/1981	Unknown	Epicenter Unknown	Unknown	Unknown	Unknown
16	EQ 14	8/13/1981	04:37	44 41 24N, 17 34 48E	7.0	3.5	5 MM
17	EQ 15	8/13/1981	11:13	44 43 12N, 17 13 12E	10.0	2.8	Unknown
18	EQ 16	8/14/1981	04:44	44 43 48N, 17 13 12E	10.0	3.2	5 MM
19*	EQ 17	(8/13/1981 – 8/21/1981)	Unknown	Epicenter Unknown	Unknown	Unknown	Unknown
20*	EQ 18	(8/13/1981 – 8/21/1981)	Unknown	Epicenter Unknown	Unknown	Unknown	Unknown
21*		(8/13/1981 – 8/21/1981)	Unknown	Epicenter Unknown	Unknown	Unknown	Unknown
22*	EQ19	8/21/1981	03:30	44 52 48N, 17 22 12E	10.9	3.5	5 MM
23*		8/30/1981	03:11	44 58 47N, 17 21 14E	10.0	2.8	Unknown
24*		(8/30/1981– 11/21/1981)	Unknown	Epicenter Unknown	Unknown	Unknown	Unknown
25		06/14/1982	18:21	44 38 58N, 17 12 00E	0.0	Unknown	4 MCS

26	07/03/1982	03:41	44 46 49N, 17 08 48E	0.0	3.4	5 MCS
27	09/07/1982	21:22	44 57 24N, 17 24 17E	0.0	Unknown	Unknown
28	10/12/1982	01:34	44 50 37N, 17 21 23E	10.0	3.4	5 MM
29	11/22/1982	18:57	44 35 05N, 16 49 48E	10.0	2.9	Unknown
30	09/02/1984	15:14	44 52 56N, 17 16 32E	0.0	4.2	6 MM
31 EQ 20	10/11/1986	01:09	44 52 56N, 17 20 49E	3.1	3.7	5 MM

* Due to a malfunction in the recording system on the 7th floor, for these earthquakes only motions at the foundation level and on the 13th floor were recorded.

The first recorded strong-ground-motion record in the Borik-2 building was obtained on April 12, 1974, and the last one on October 11, 1986. The largest recorded motions are those of the August 13, 1981 (02:58 h, GMT), from the Banja Luka earthquake. Table 2.4.1 gives the list of 31 earthquakes for which records in this building are known to have been recorded during the instrumentation period (October 1972 to end of the 1990). The right-hand side of column 1 in Table 2.4.1 shows the 20 earthquakes chosen for this study, which are identified as EQ 01 through EQ 20. The remaining 11 records were too small to provide reliable information for this work.

During the Banja Luka, Yugoslavia, earthquake of August 13, 1981 (02:58 h, GMT), with magnitude M = 5.4, the epicenter of which fell in the Banja Luka seismic source area (Fig. 2.2, event #13 i.e. EQ 11), structural responses at the foundation level and on the 7th and the 13th floor were recorded. Several days after the earthquake, detailed inspection of the building was carried out, and neither structural nor nonstructural damage (except for minor damage on the terrace, at the top of the building, Čaušević 1988) were observed, which shows that the building has worked essentially in the "elastic range" during all recorded strong earthquakes thus far. However, in one of the later studies, Fajfar et al. (1987) suggested that local cracking might have occurred in some shear walls (at the 1st story and from 7th to the 10th stories) and in some columns (10th to 14th stories). Inspection of the soil conditions in the vicinity of the Borik-2 showed no traces of nonlinear soil behavior close to the building.

Figures 2.4.1 and 2.4.2 show computed relative displacements (in cm) of the 13th floor relative to the basement, versus time (in seconds) for the NS and EW responses, for all 20 earthquakes chosen for this study (EQ 01 to EQ 20). For all of the events, the vertical scales in Figs. 2.4.1 and

2.4.2 are the same and show the range up to 0.5 cm, except for EQ 11, for which this range is 5 cm. It can be seen that, except for EQ 05, most peak relative displacements are less than 0.1 cm. During event EQ 11, the peak relative displacement in the NS direction reached about 4.2 cm.

Thus, if we neglect the contribution of soil structure interaction and consider the average overall drift between the basement and the 13th floor, we find that it was smaller than about $3 \cdot 10^{-5}$ during 19 small events, and less than 10^{-3} during the NS response to the EQ 11 event. Because for typical reinforced-concrete buildings structural damage begins to occur for the drift amplitudes comparable to and exceeding about 10^{-2} (Trifunac and Ivanović 2003c), it is not surprising that the earthquake EQ 11 did not result in any apparent structural damage.

Figures 2.4.3 (a through e) show Fourier amplitude spectra of recorded NS accelerations at the 13th floor. Figures 2.4.4 (a through e) show the same for EW recorded accelerations. Because accelerations emphasize high frequencies, we will use these plots to identify the system frequencies f_{sys}, which correspond to higher modes. Figures 2.4.5 (a through e) and Figs. 2.4.6 (a through e) show the Fourier amplitude spectra of relative displacements (at the 13th floor relative to the basement). We will be using these plots to identify the lowest system frequencies. All spectra for NS motions are plotted for frequencies between 0 Hz and 6 Hz. Spectra for EW motions had a few higher frequency peaks and are plotted from 0 Hz to 7 Hz.

Figure 2.4.7 summarizes the information that can be deciphered from the spectra in Figs.2.4.3 through 2.4.6. It presents frequencies of all identifiable spectral peaks versus the event number (EQ 01 through EQ 20, or just 1 through 20 as shown in this figure). All peaks associated with NS response are shown with full circles, and those with EW and torsional response are indicated by open circles. The results of forced-vibration tests in October 1972 and of ambient vibration tests in June 1983 are also shown. The observed trends and the changes in system frequencies are suggested by continuous (for NS) and dashed lines (for EW). These trends are interrupted by event 11, which contributed the largest excitation in this data set. Following event 11, a minor drop in the fundamental system frequency, from near 1.3 Hz (before the earthquake) to about 1.15 Hz (after the earthquake), is evident. The drop of the second system frequencies, from about 4.6 Hz to 4.0 Hz for NS response, and from about 5.0 Hz to 4.7 Hz for EW response, is more apparent. All of these system frequencies begin essentially at the frequencies measured during the forced-vibration experiment in October 1972 and then gradually decrease and level off during events 5 through 10. After what appears to be a permanent drop, during event 11, these frequencies are again nearly constant during the remaining events, 13 through 20. The gradual decrease during events 1 through 5, and the largest drop during event 11, are apparently associated with cracking of structural concrete, of non-structural elements, and of partition walls.

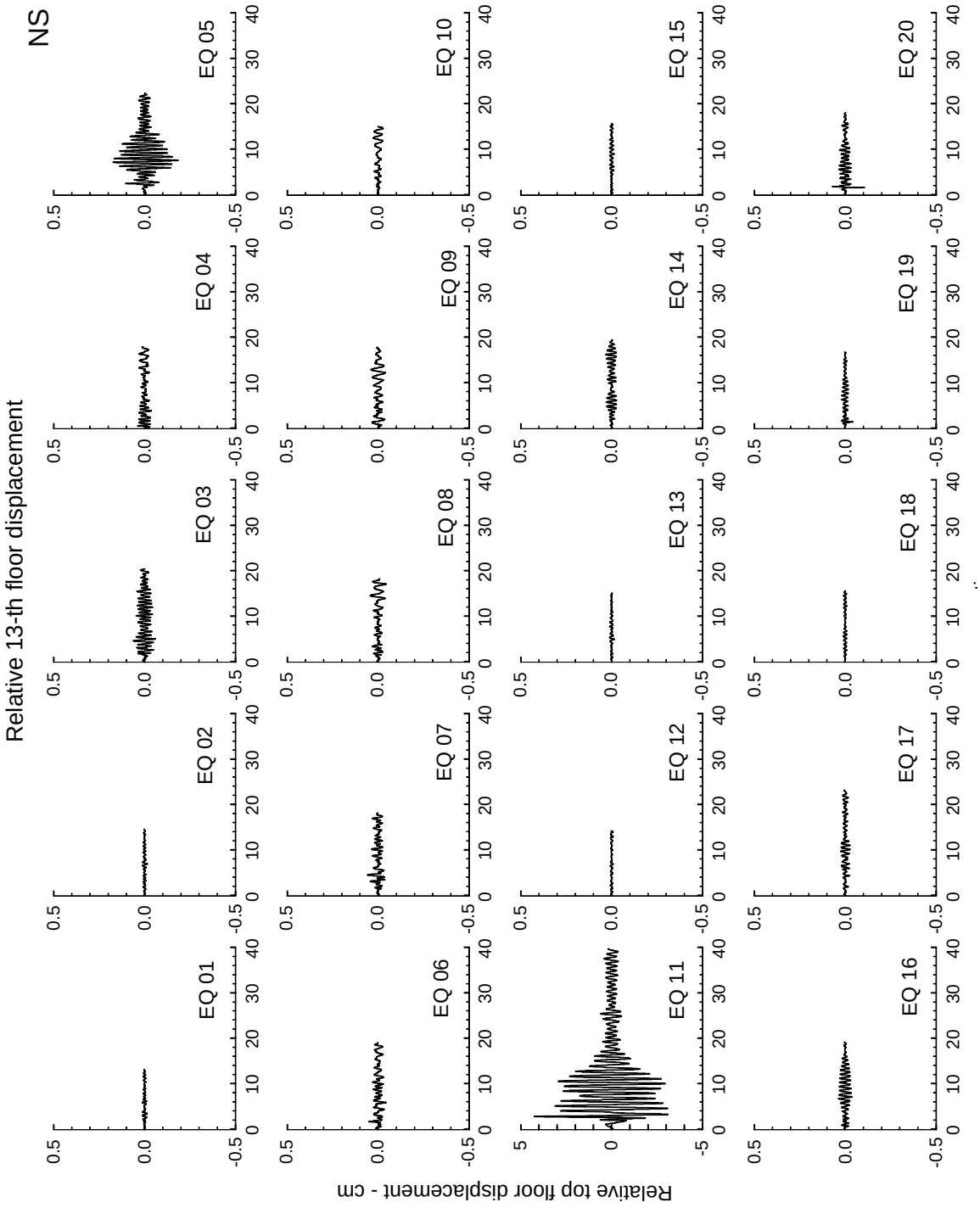

Fig.2.4.1. Computed from recorded accelerograms, the relative NS displacements on 13^{th} floor in the Borik-2 building.

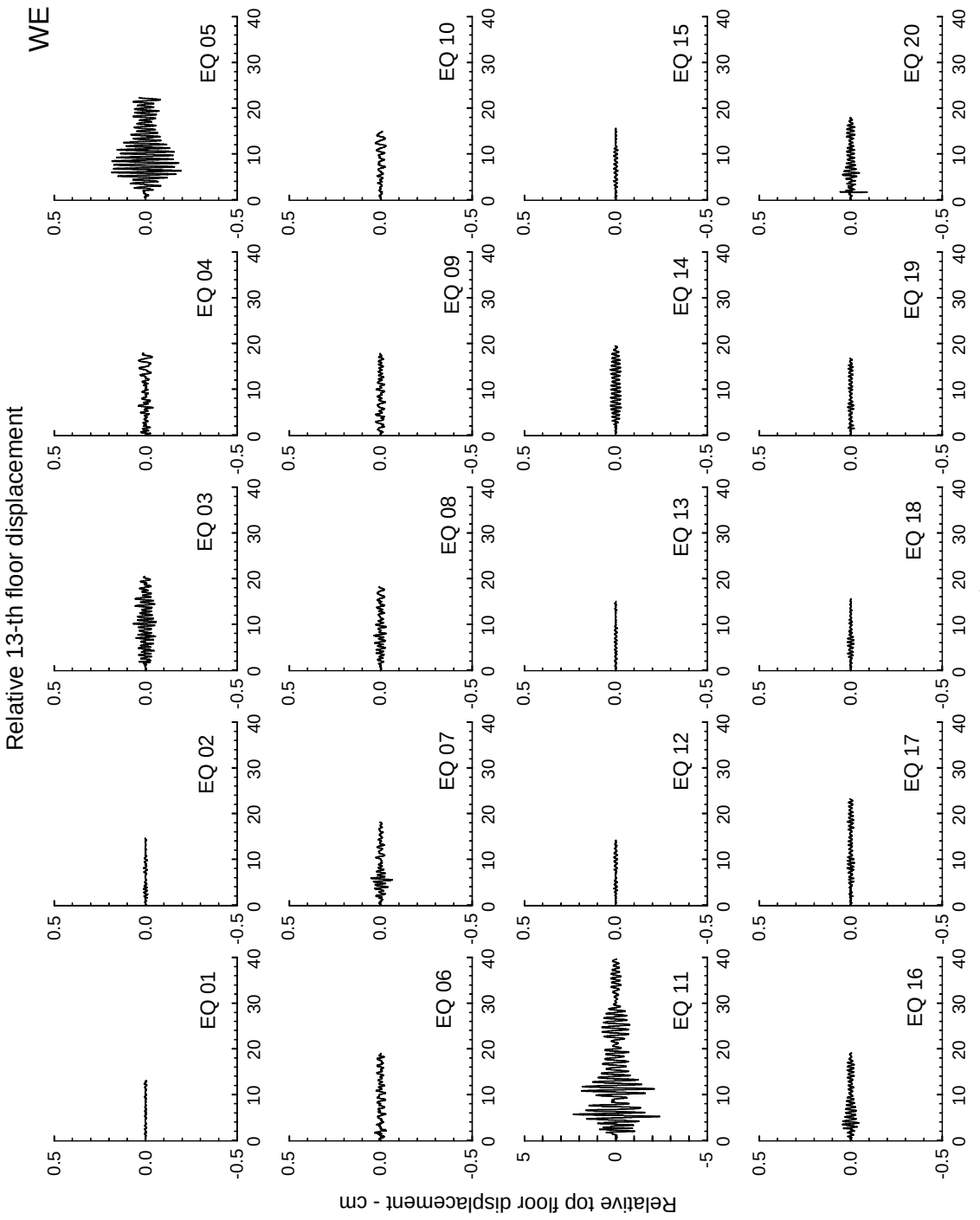

Fig.2.4.2. Computed from recorded accelerograms, the relative EW displacements on the 13th floor in the Borik-2 building.

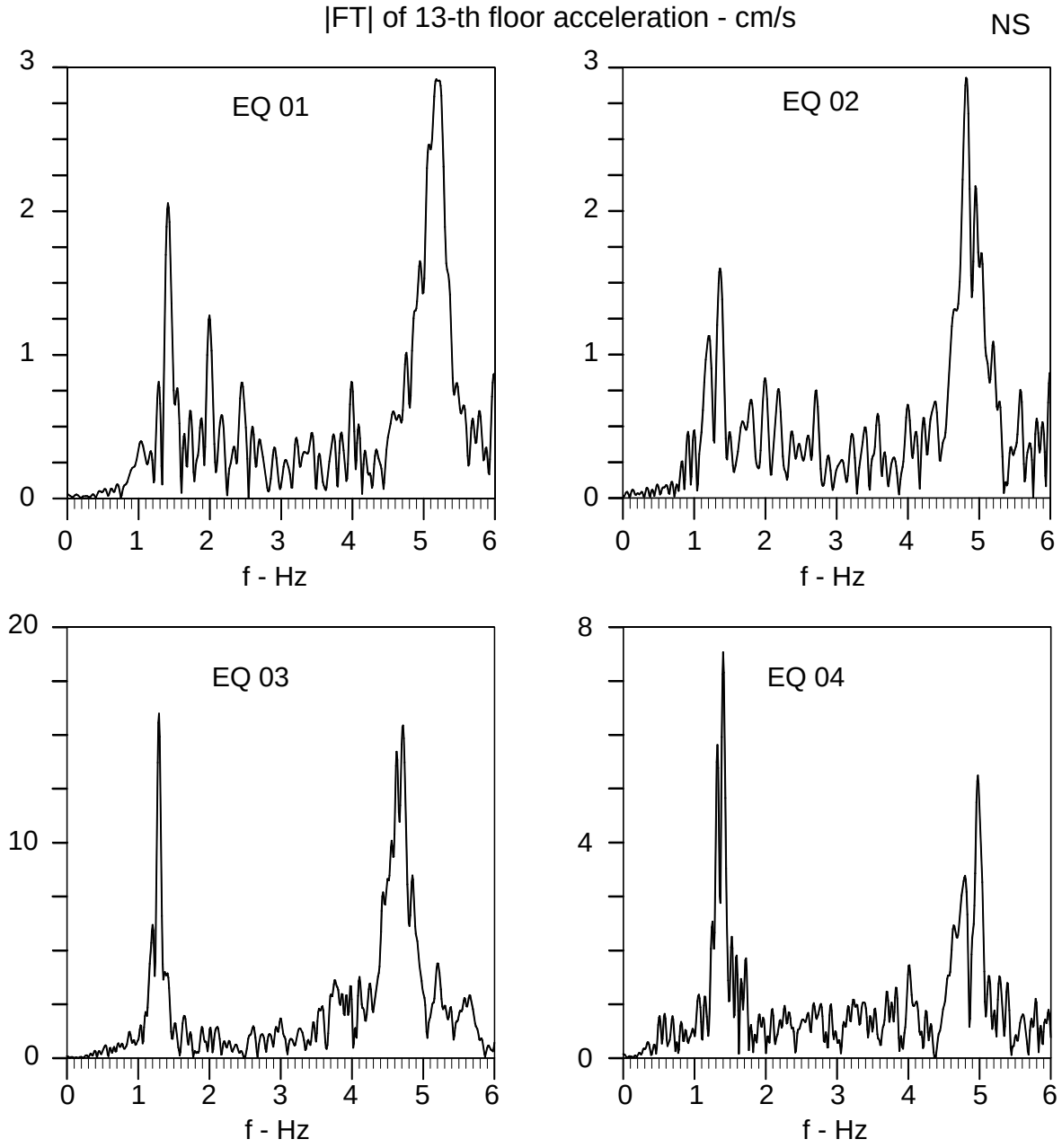

Fig.2.4.3a. Fourier amplitude spectra of recorded NS accelerations at 13th floor in the Borik-2 building, for earthquakes EQ 01 through EQ 04.

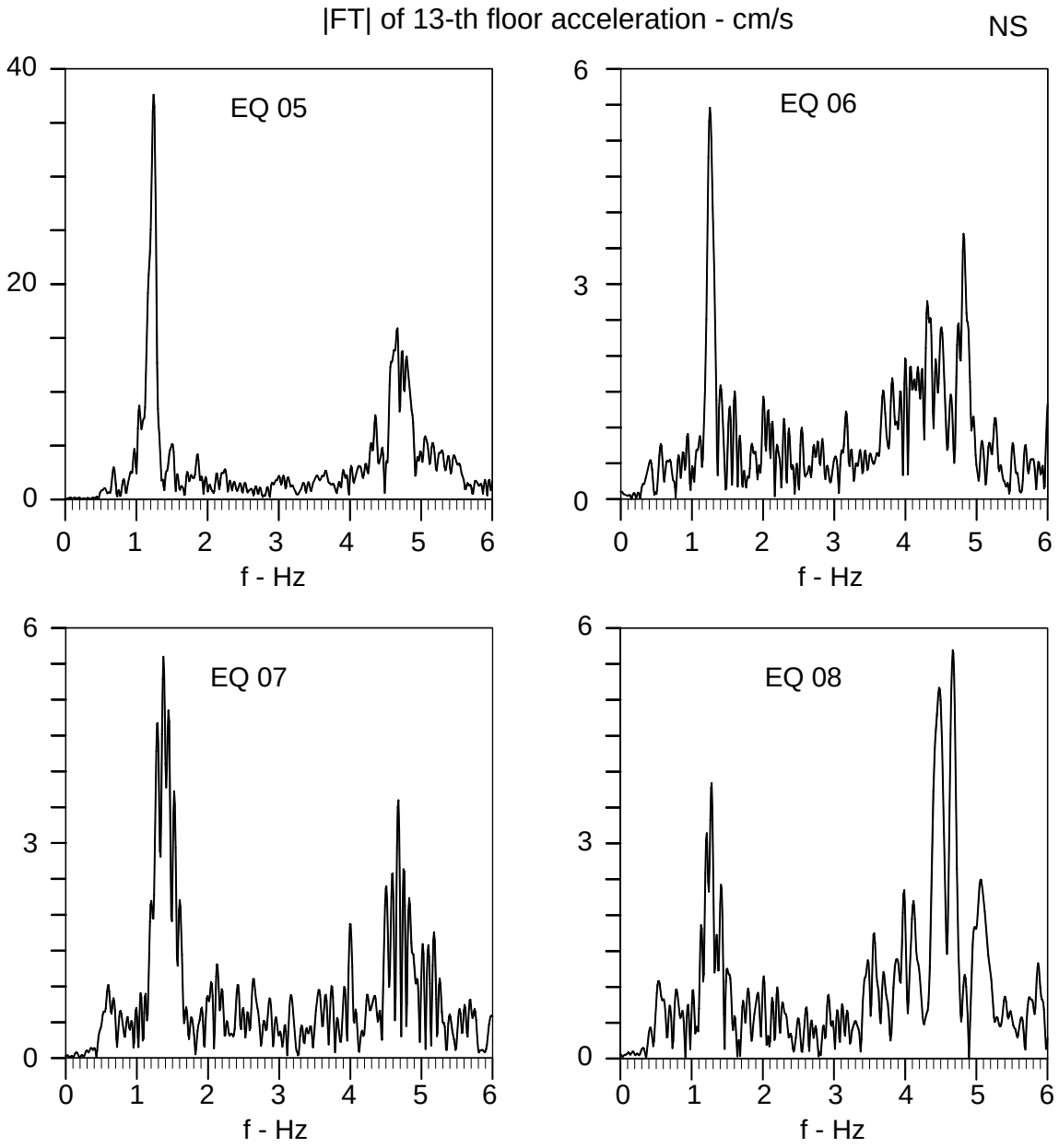

Fig.2.4.3b. Same as Fig.2.4.3a, but for EQ 05 through EQ 08.

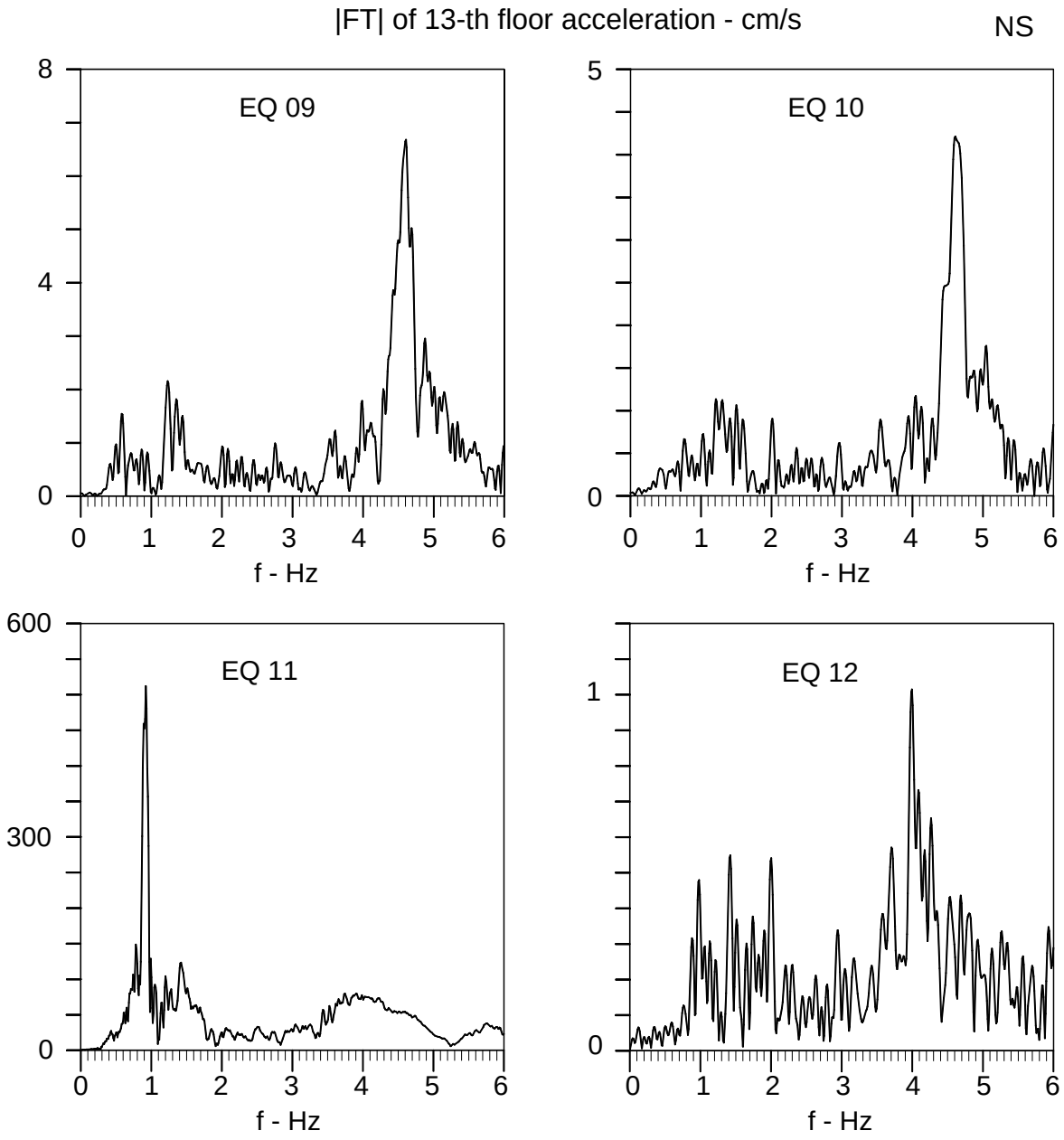

Fig.2.4.3c. Same as Fig.2.4.3a, but for EQ 09 through EQ 12.

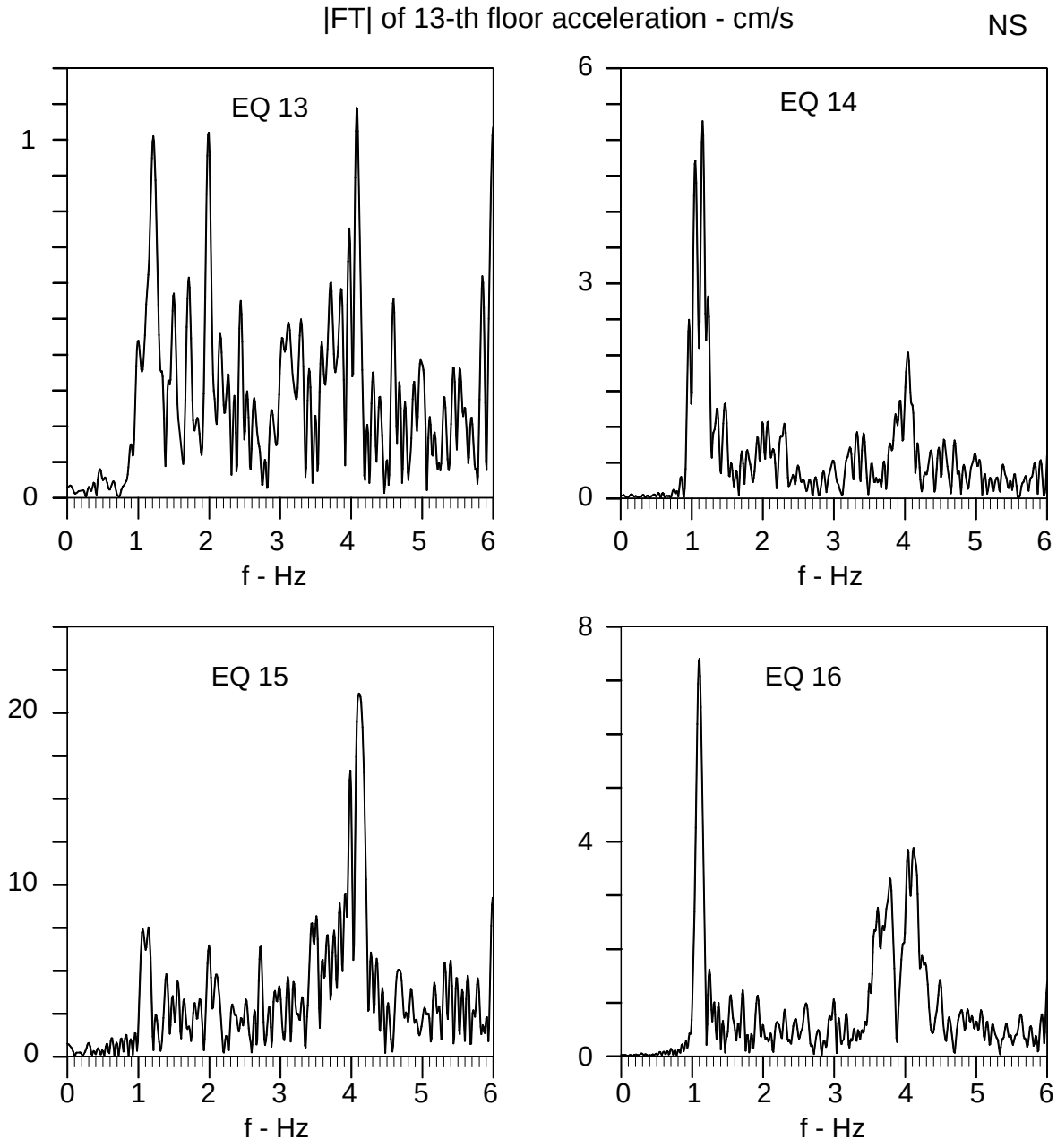

Fig.2.4.3d. Same as Fig.2.4.3a, but for EQ 13 through EQ 16.

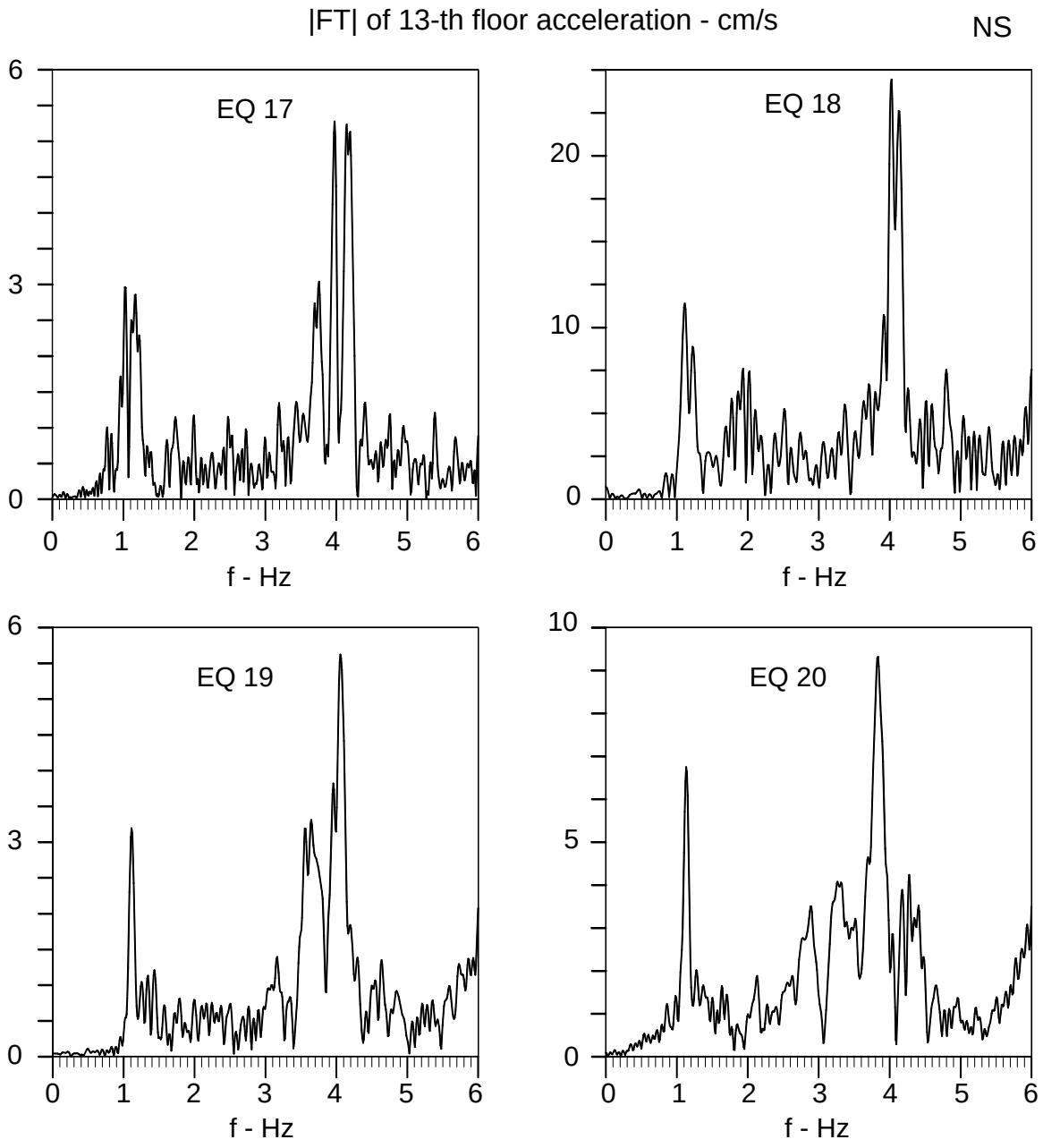

Fig.2.4.3e. Same as Fig.2.4.3a, but for EQ 17 through EQ 20.

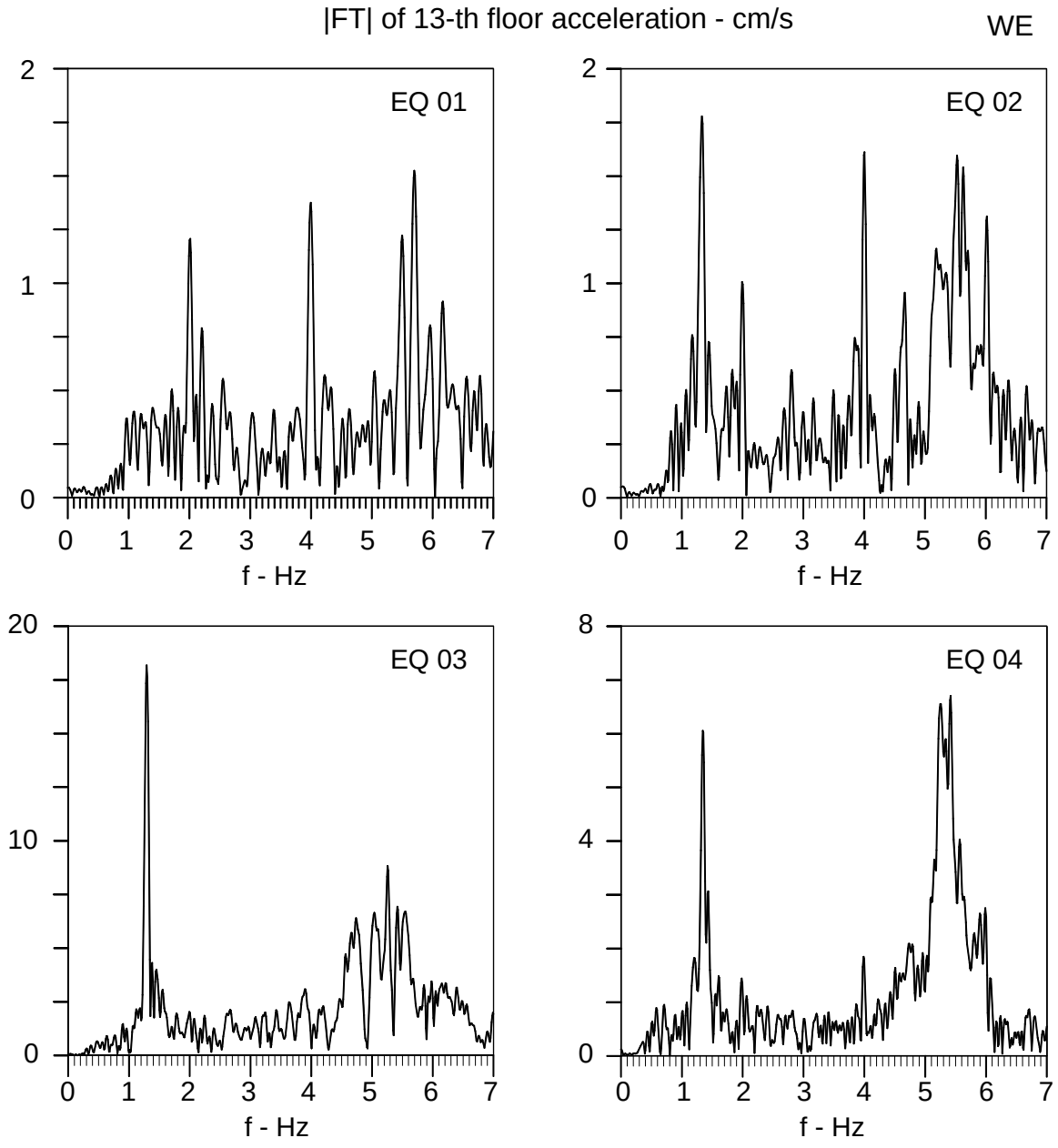

Fig.2.4.4a Fourier amplitude spectra of recorded EW accelerations on the 13th floor in the Borik-2 building, for earthquakes EQ 01 through EQ 04.

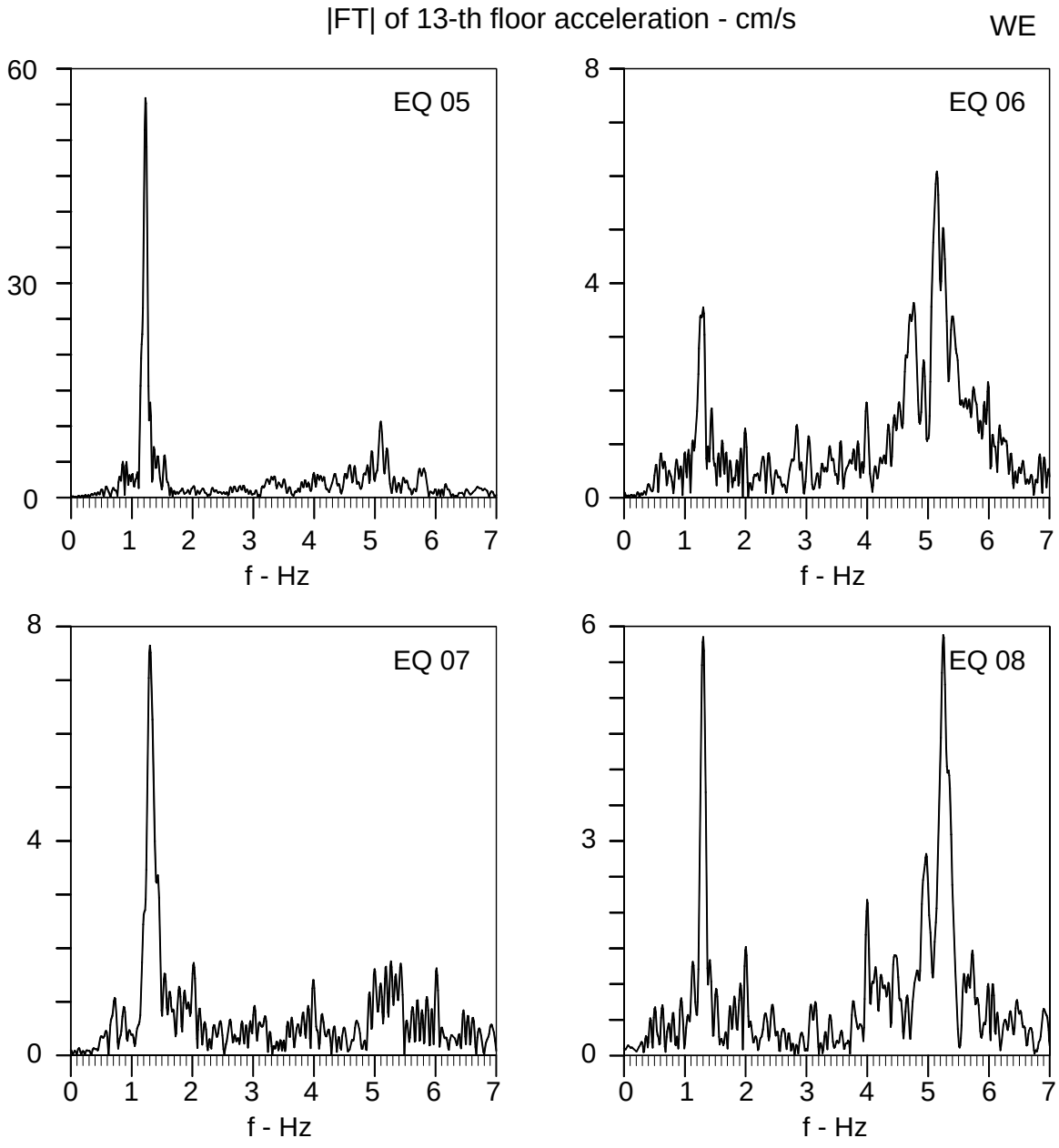

Fig.2.4.4b. Same as Fig.2.4.4a, but for EQ 05 through EQ 08.

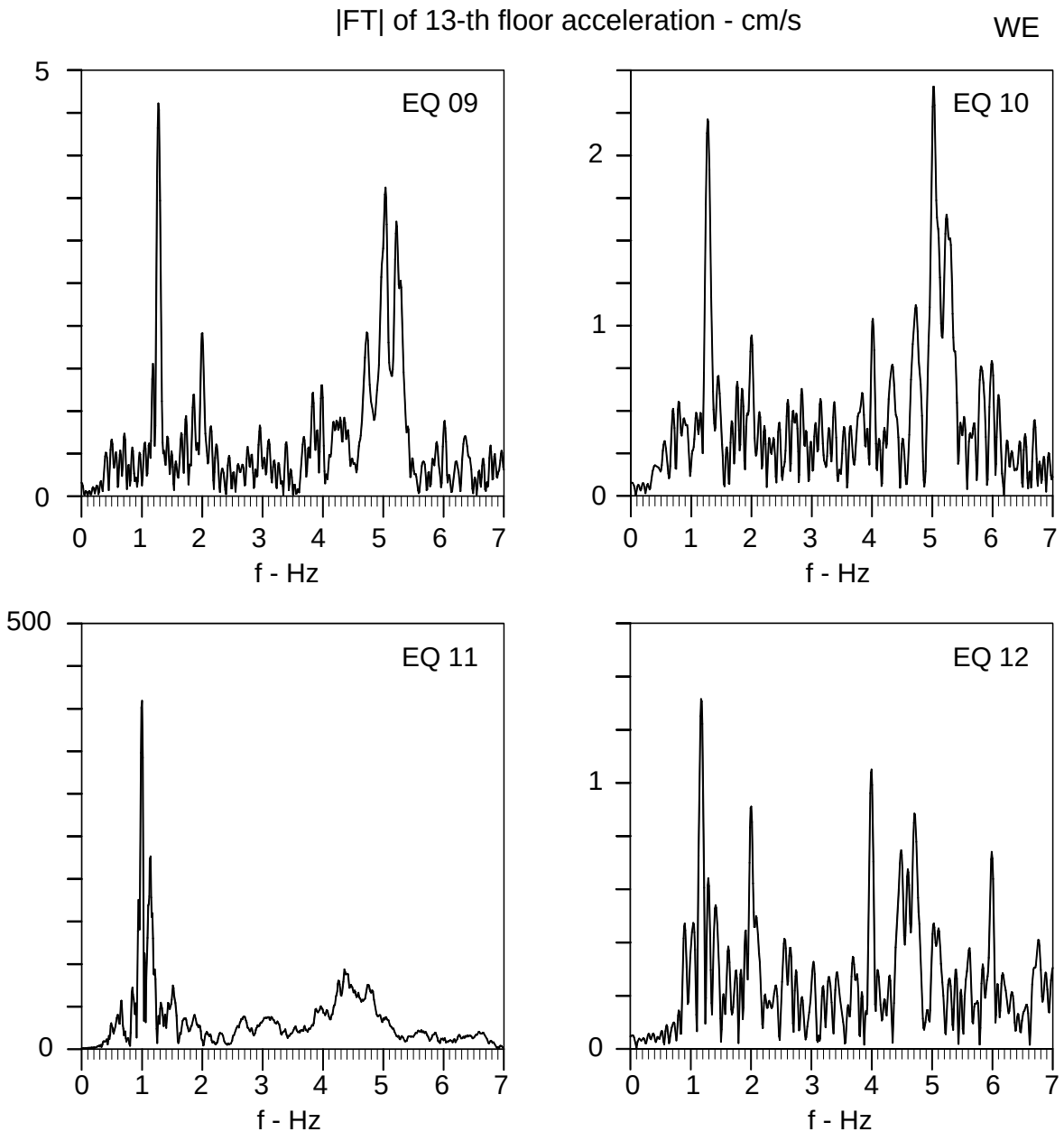

Fig.2.4.4c. Same as Fig.2.4.4a, but for EQ 09 through EQ 12.

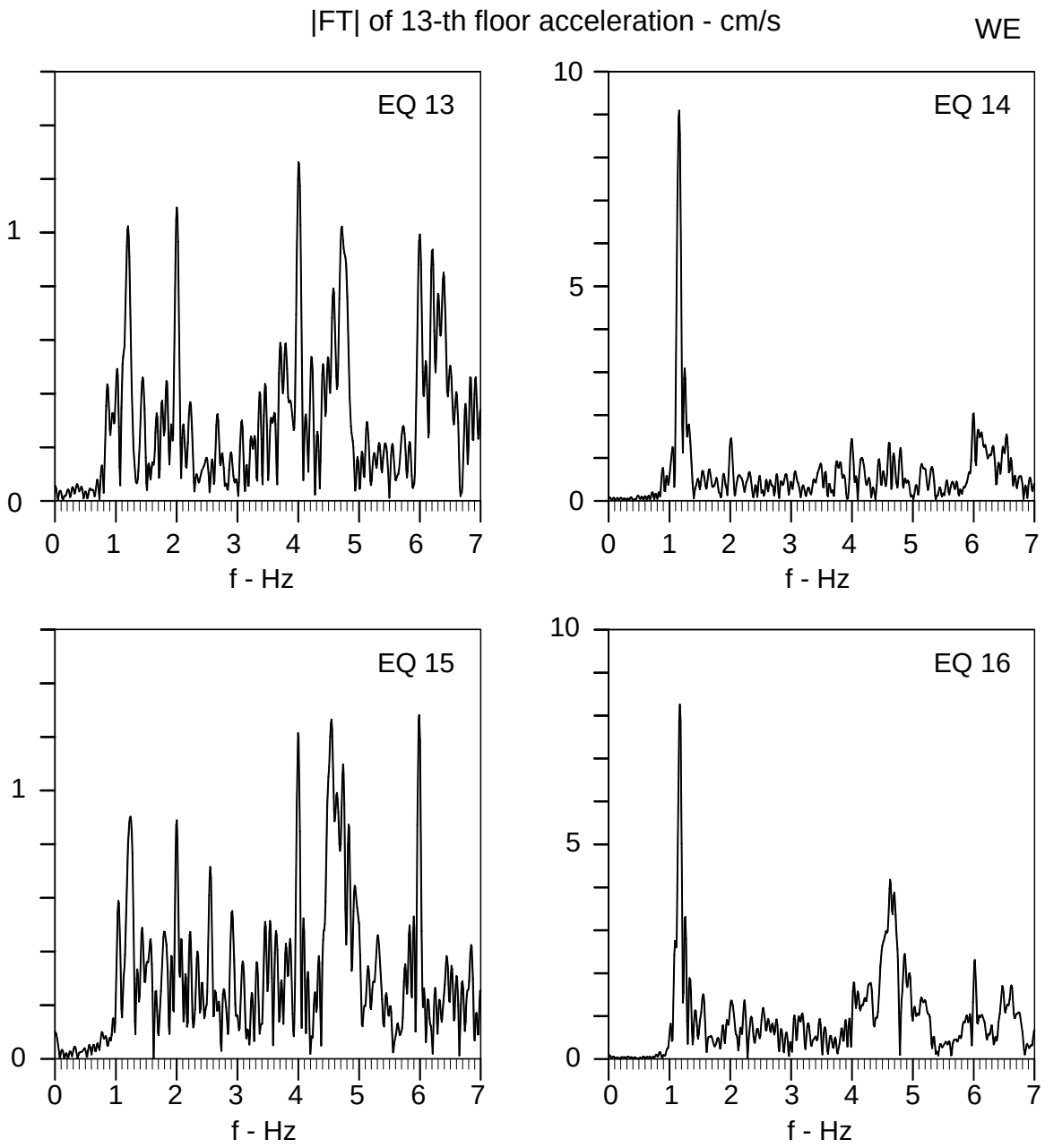

Fig.2.4.4d. Same as Fig.2.4.4a, but for EQ 13 through EQ 16

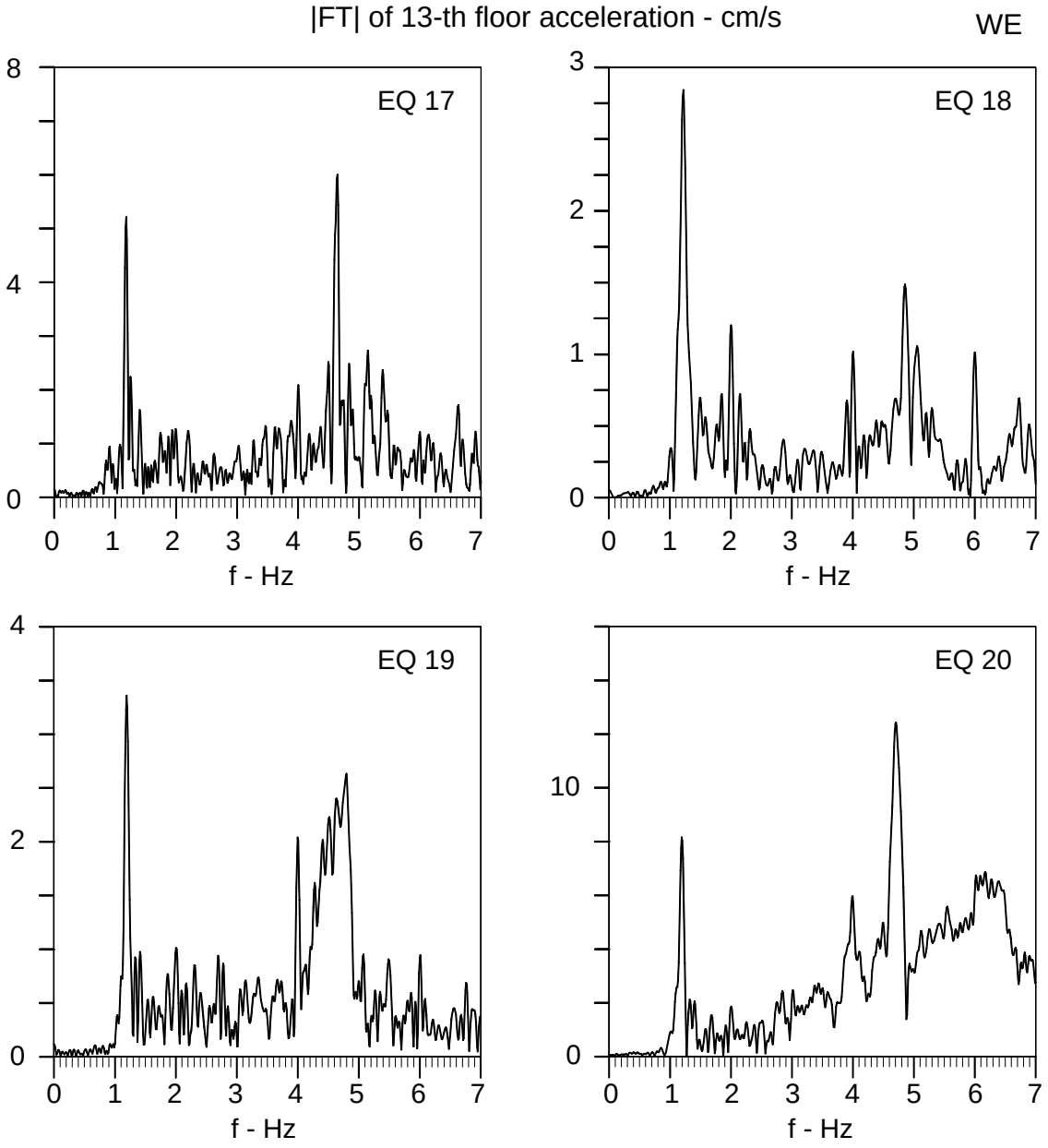

Fig.2.4.4e. Same as Fig.2.4.4a, but for EQ 17 through EQ 20.

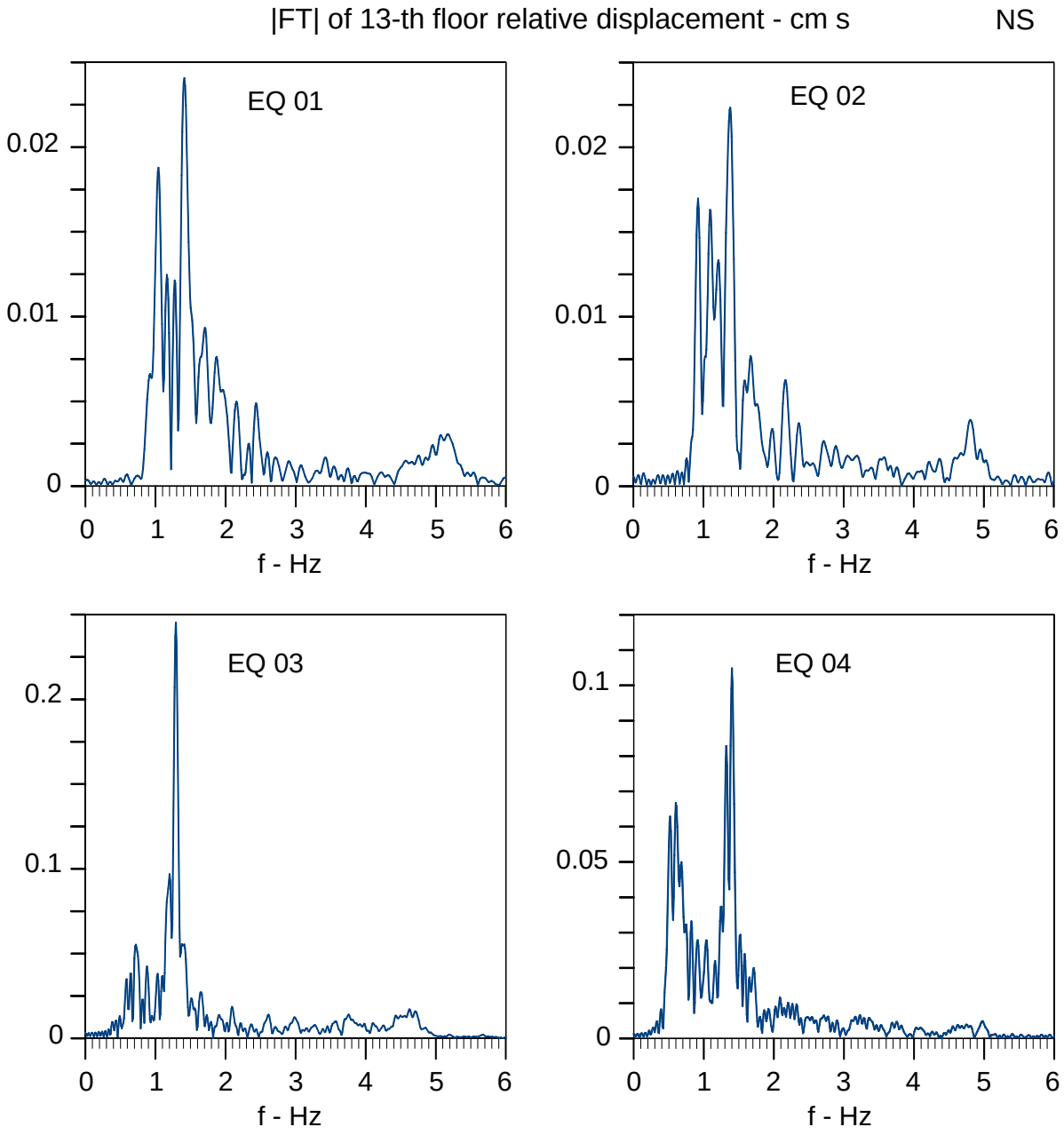

Fig.2.4.5a Fourier amplitude spectra of computed relative NS displacements on the 13th floor of the Borik-2 building, for earthquakes EQ 01 through EQ 04.

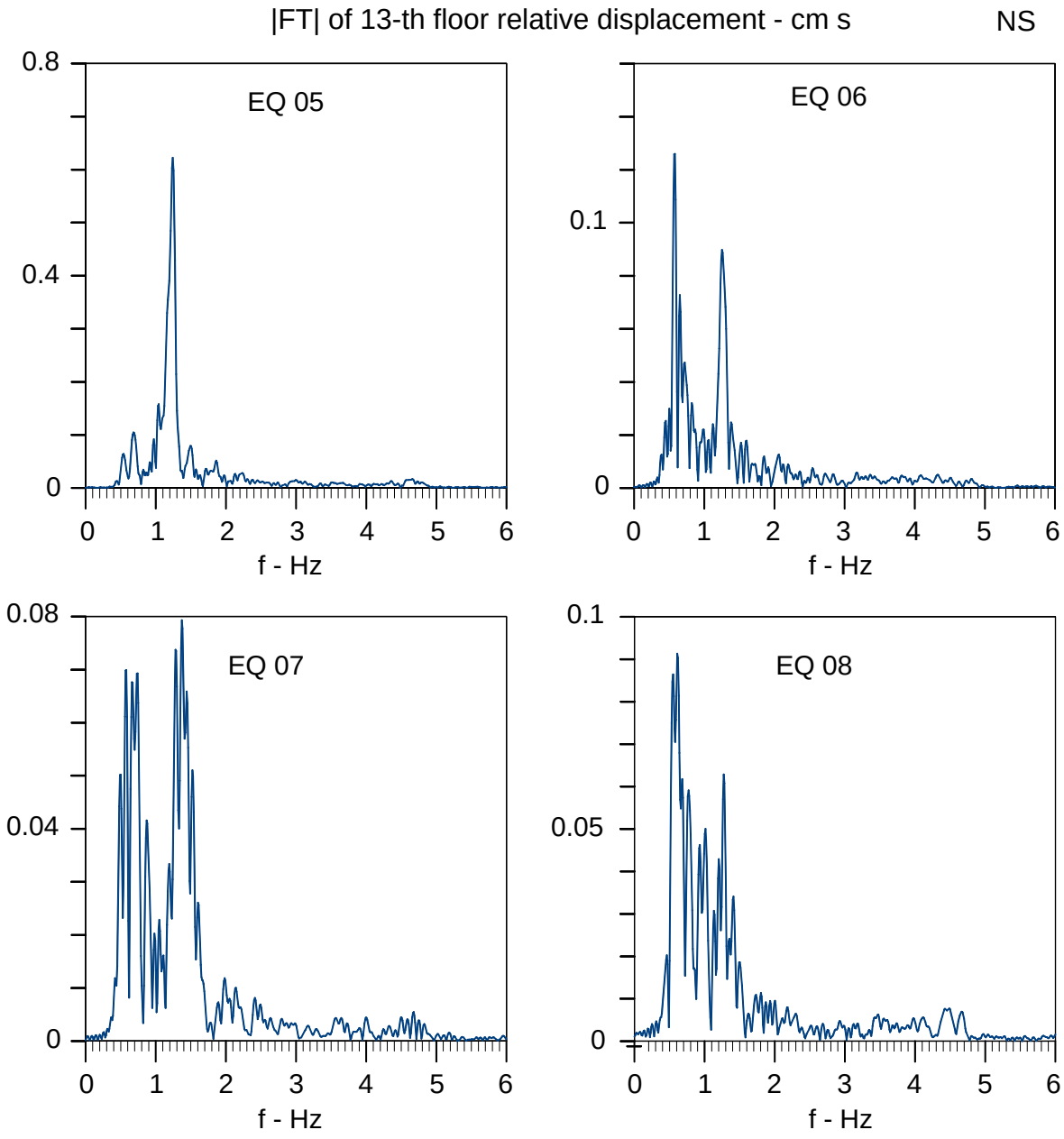

Fig.2.4.5b. Same as Fig.2.4.5a, but for EQ 05 through EQ 08.

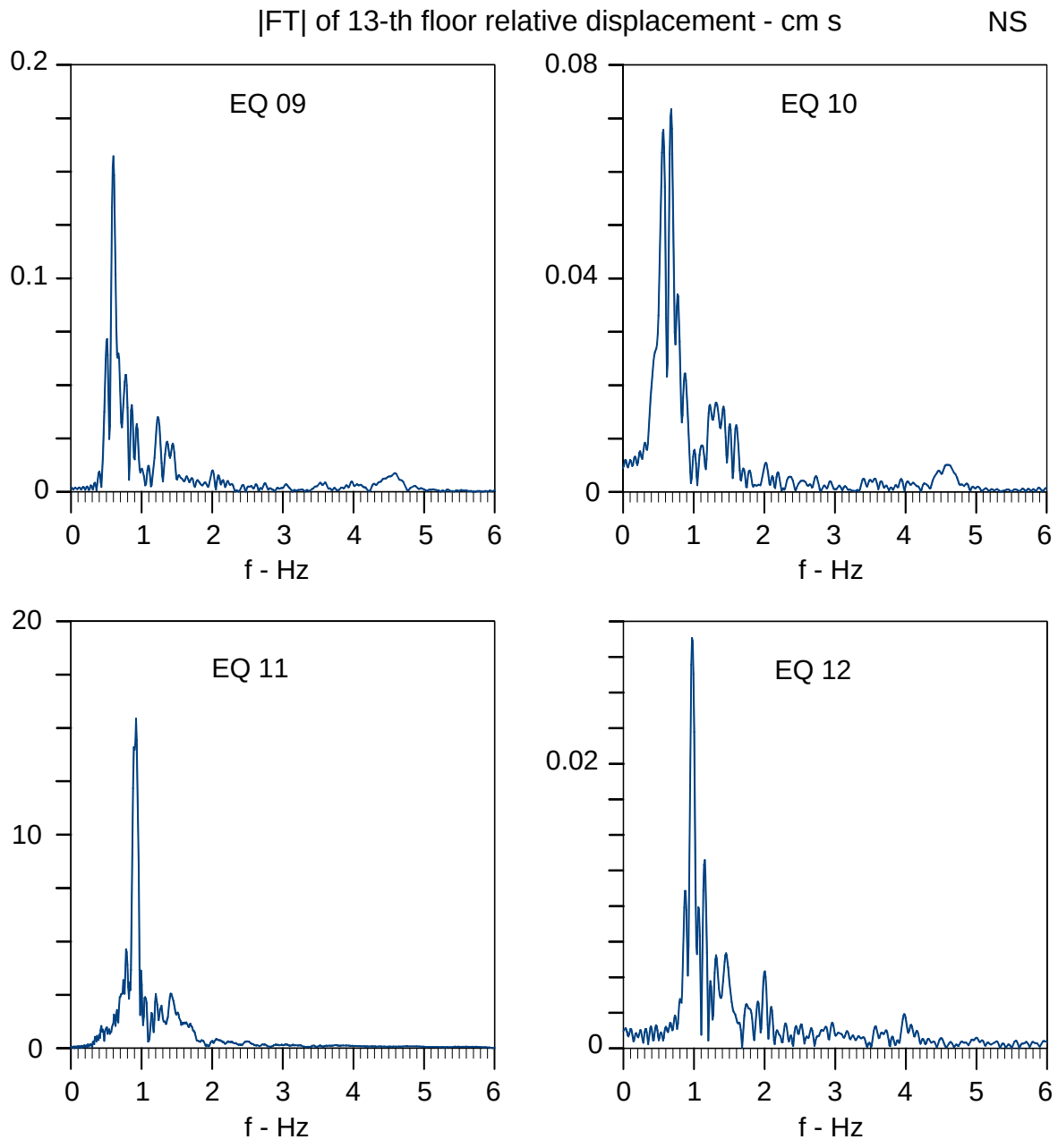

Fig.2.4.5c. Same as Fig.2.4.5a, but for EQ 09 through EQ 12.

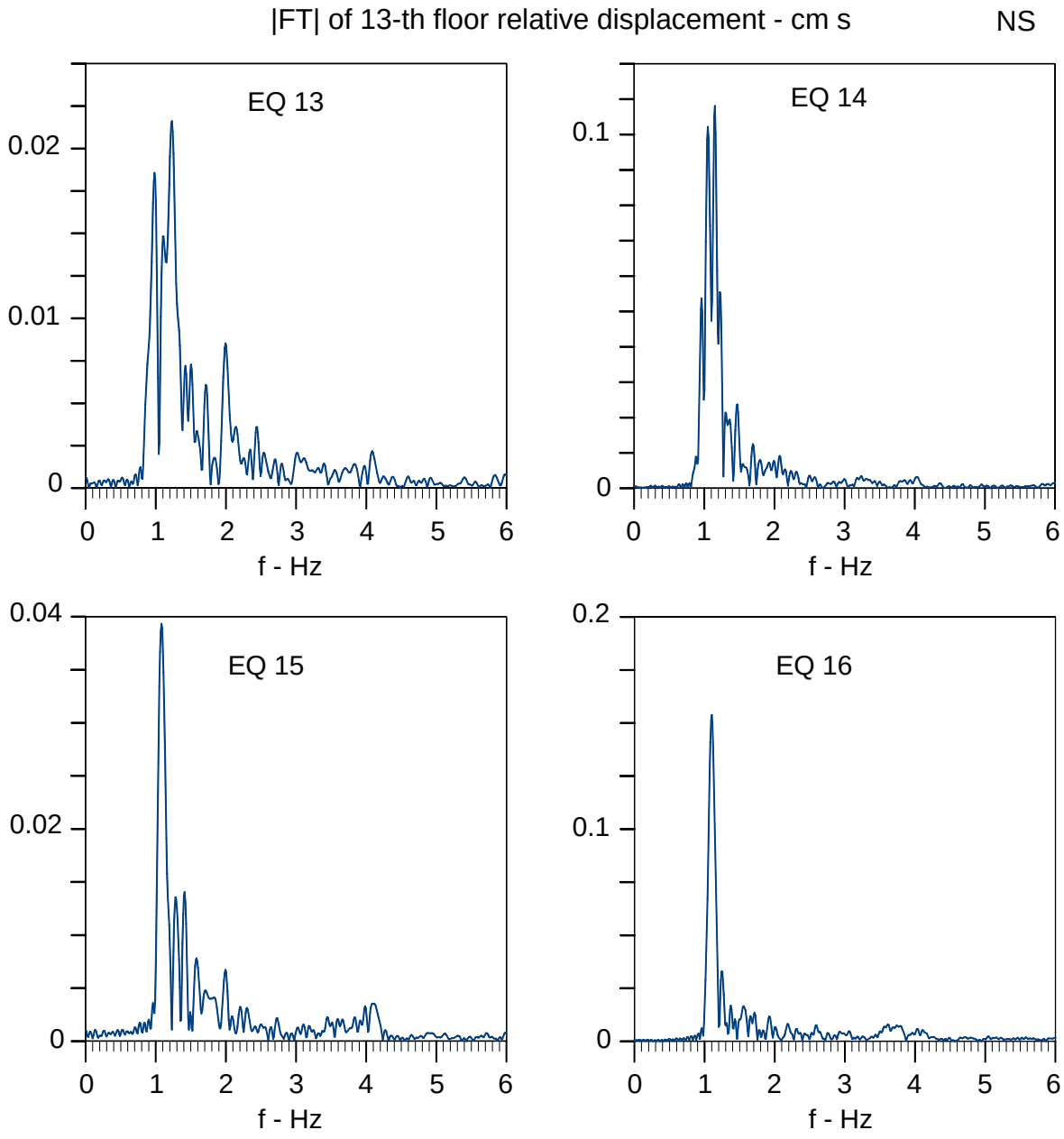

Fig.2.4.5d. Same as Fig.2.4.5a, but for EQ 13 through EQ 16.

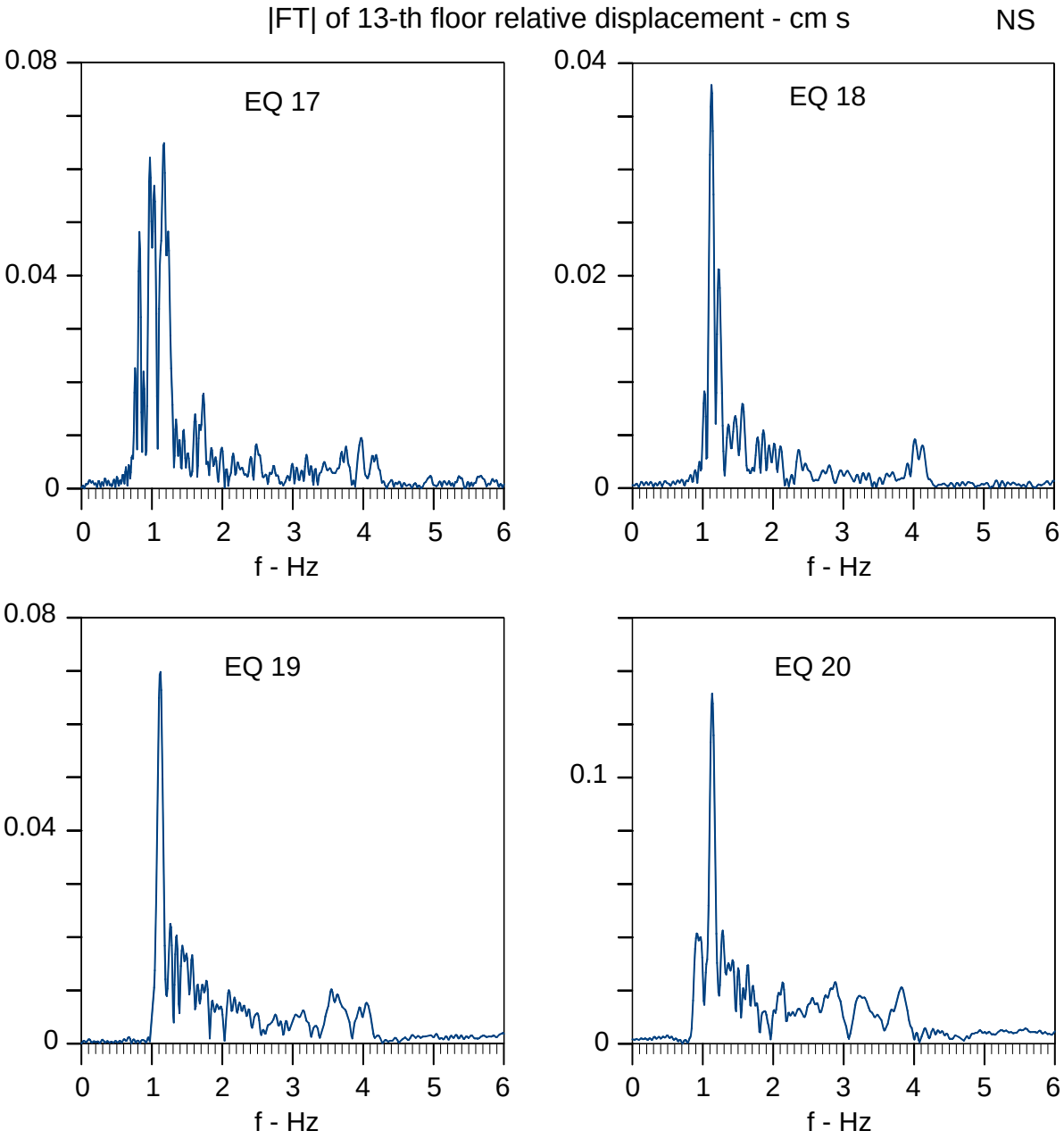

Fig.2.4.5e. Same as Fig.2.4.5a, but for EQ 17 through EQ 20.

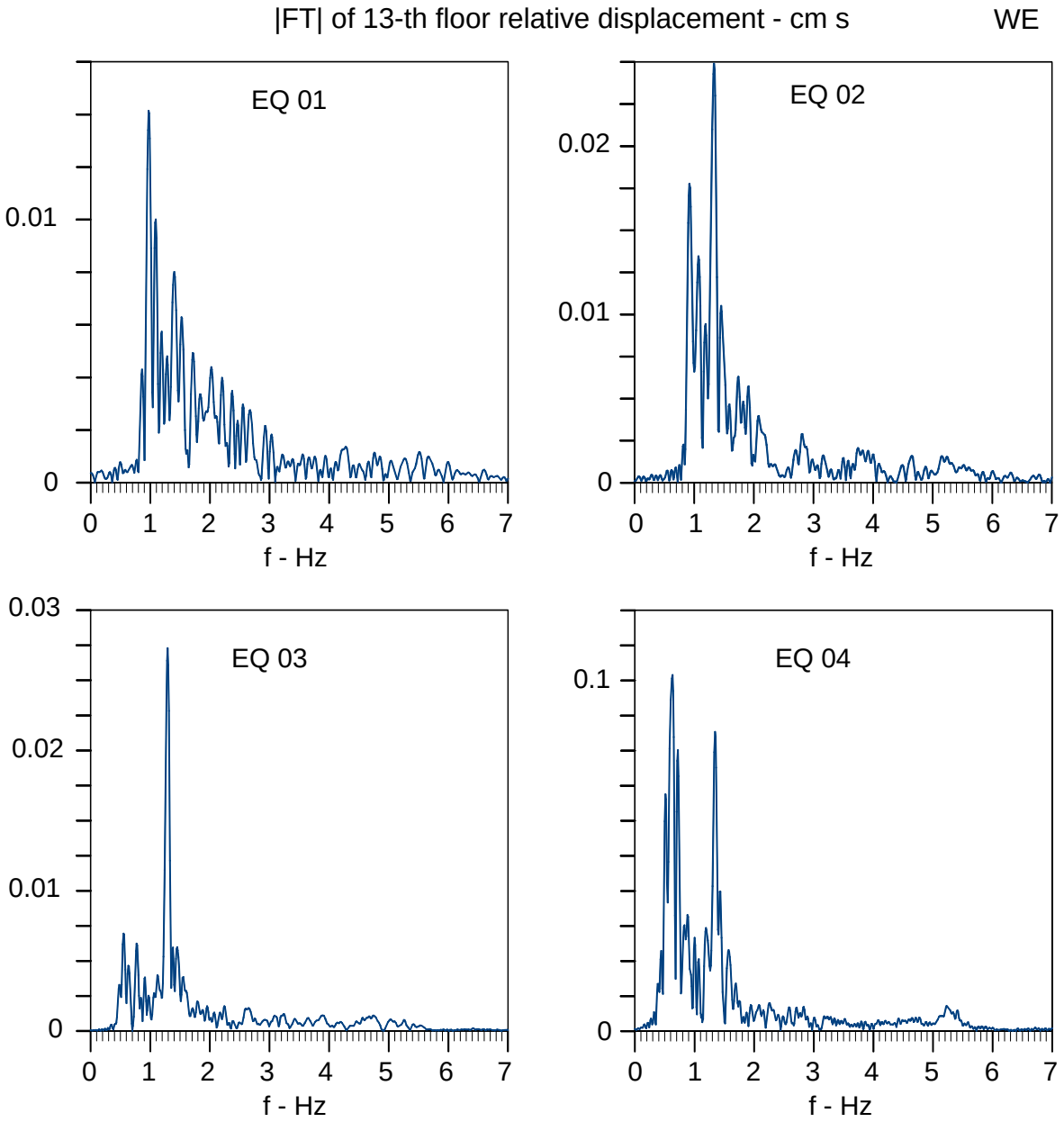

Fig.2.4.6a Fourier amplitude spectra of computed relative EW displacements on the 13th floor of the Borik-2 building, for earthquakes EQ 01 through EQ 04.

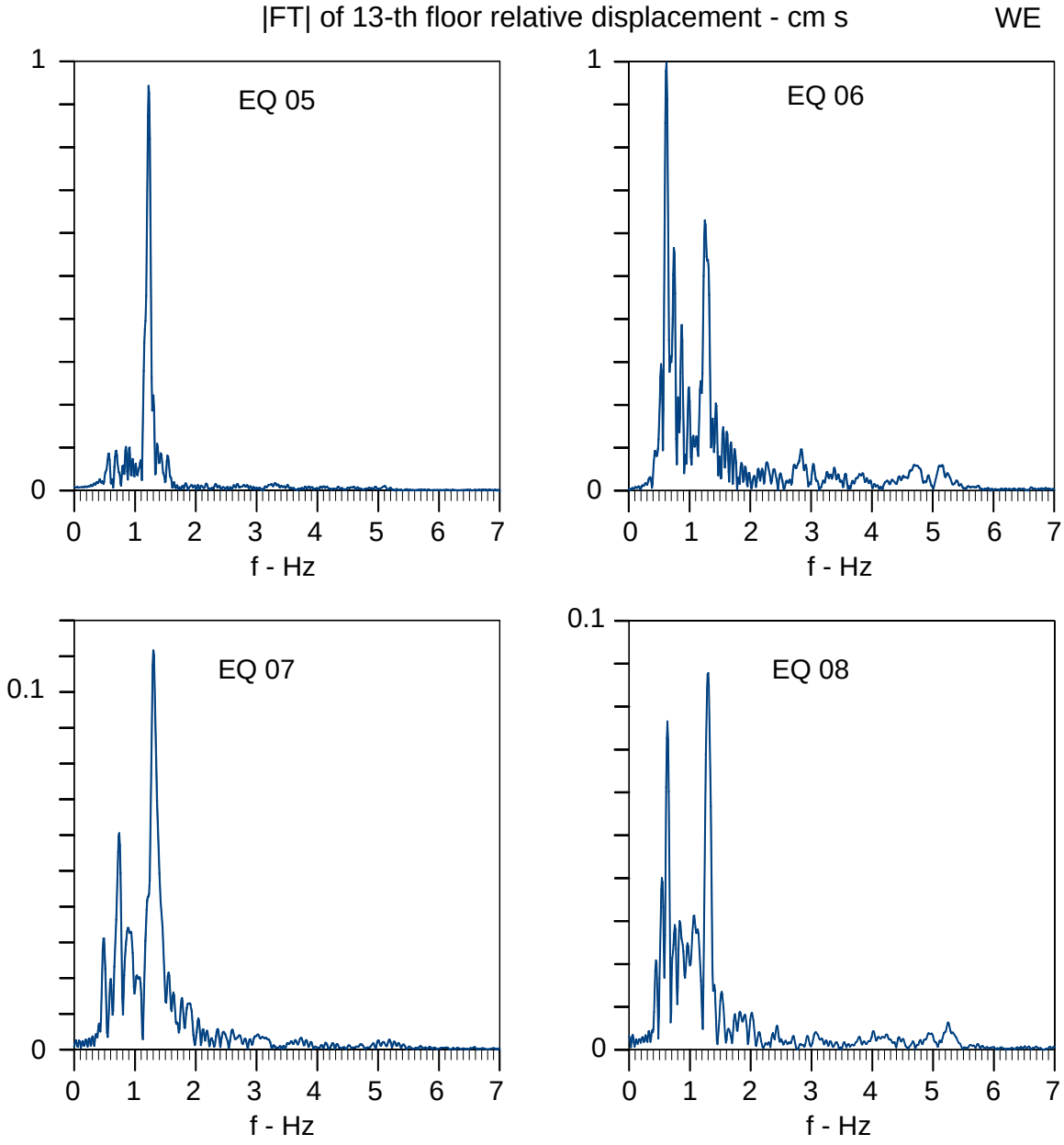

Fig.2.4.6b. Same as Fig.2.4.6a, but for EQ 05 through EQ 08.

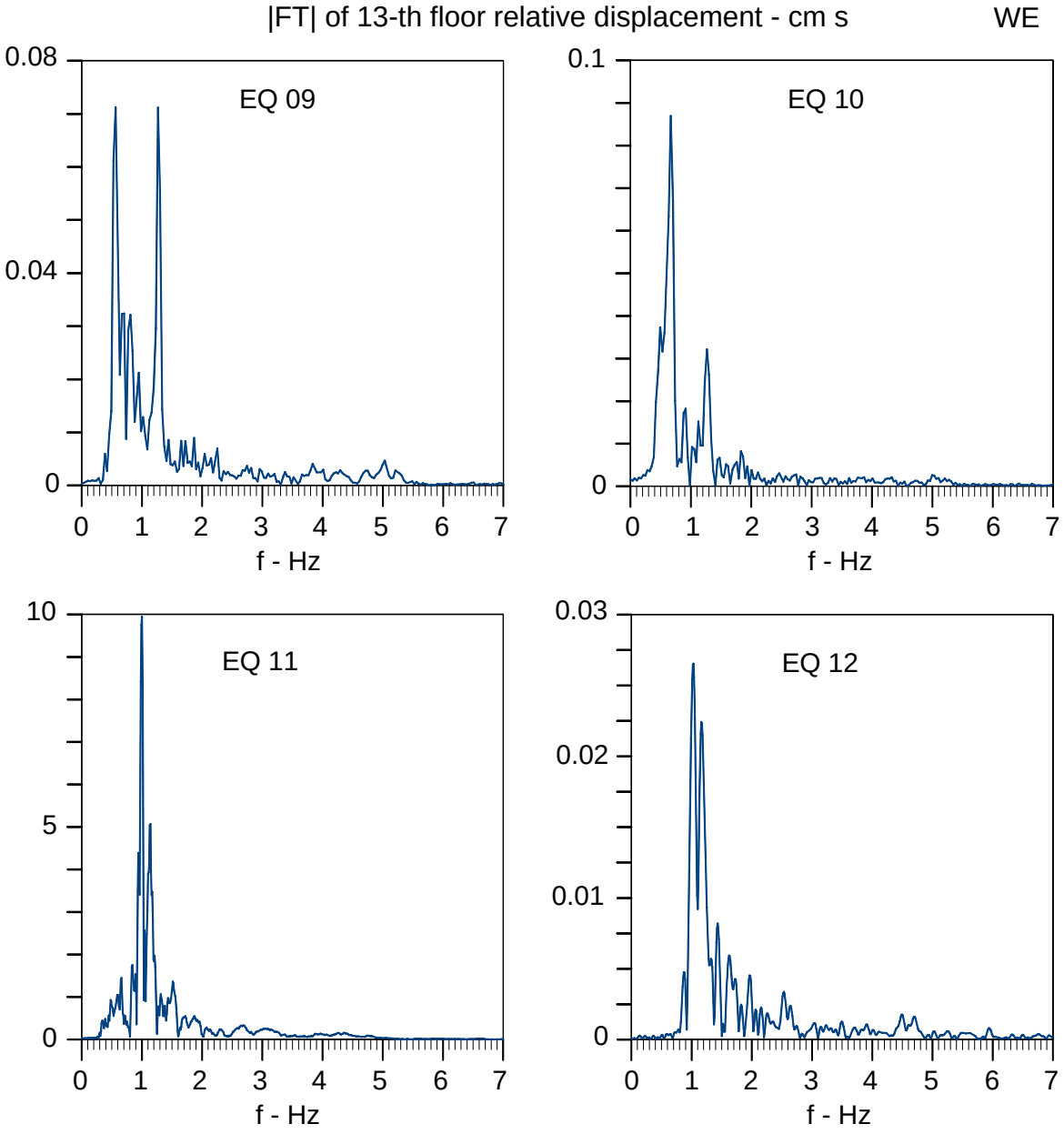

Fig.2.4.6c. Same as Fig.2.4.6a, but for EQ 09 through EQ 12.

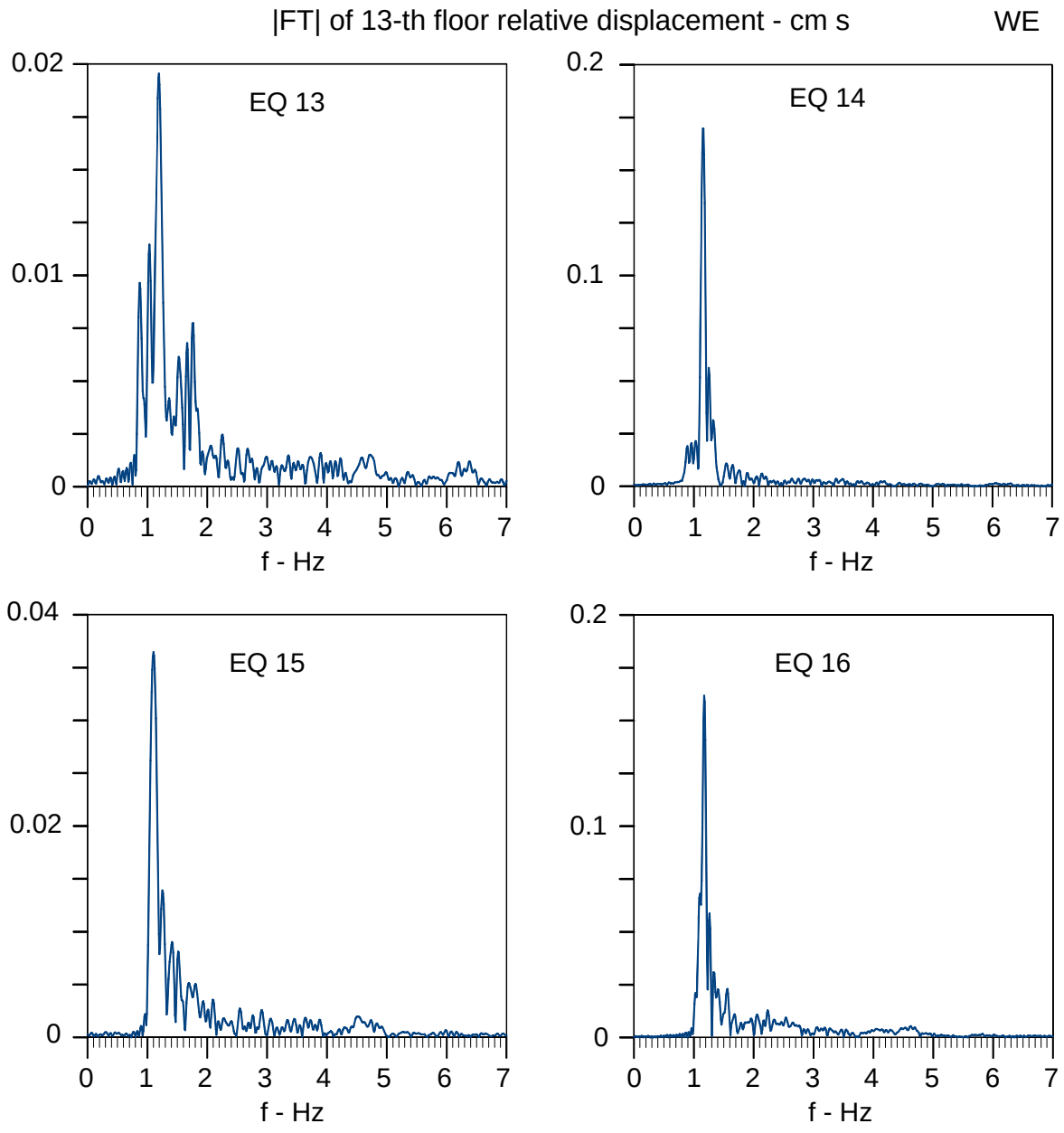

Fig.2.4.6d. Same as Fig.2.4.6a, but for EQ 13 through EQ 16.

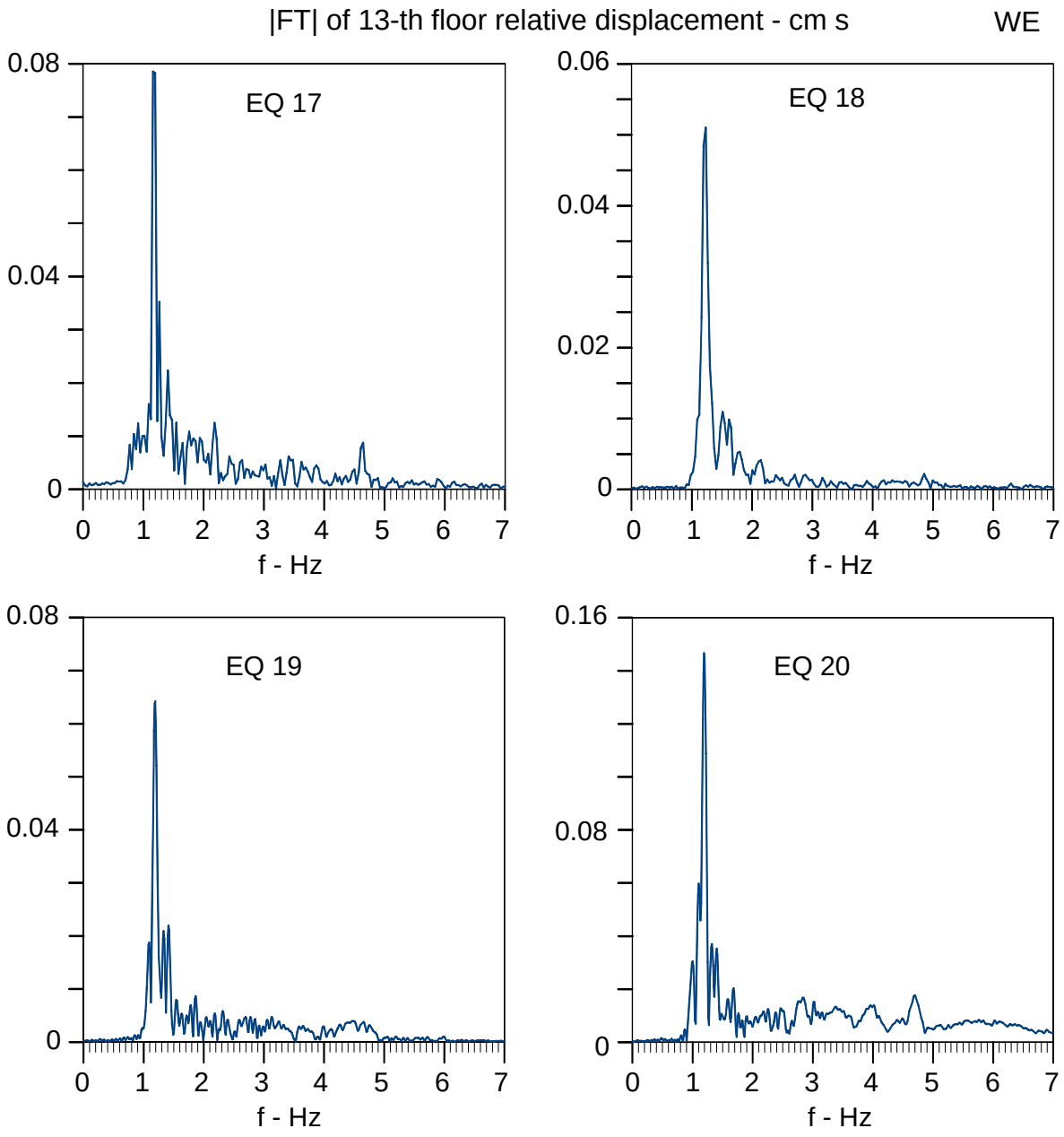

Fig.2.4.6e. Same as Fig.2.4.6a, but for EQ 17 through EQ 20.

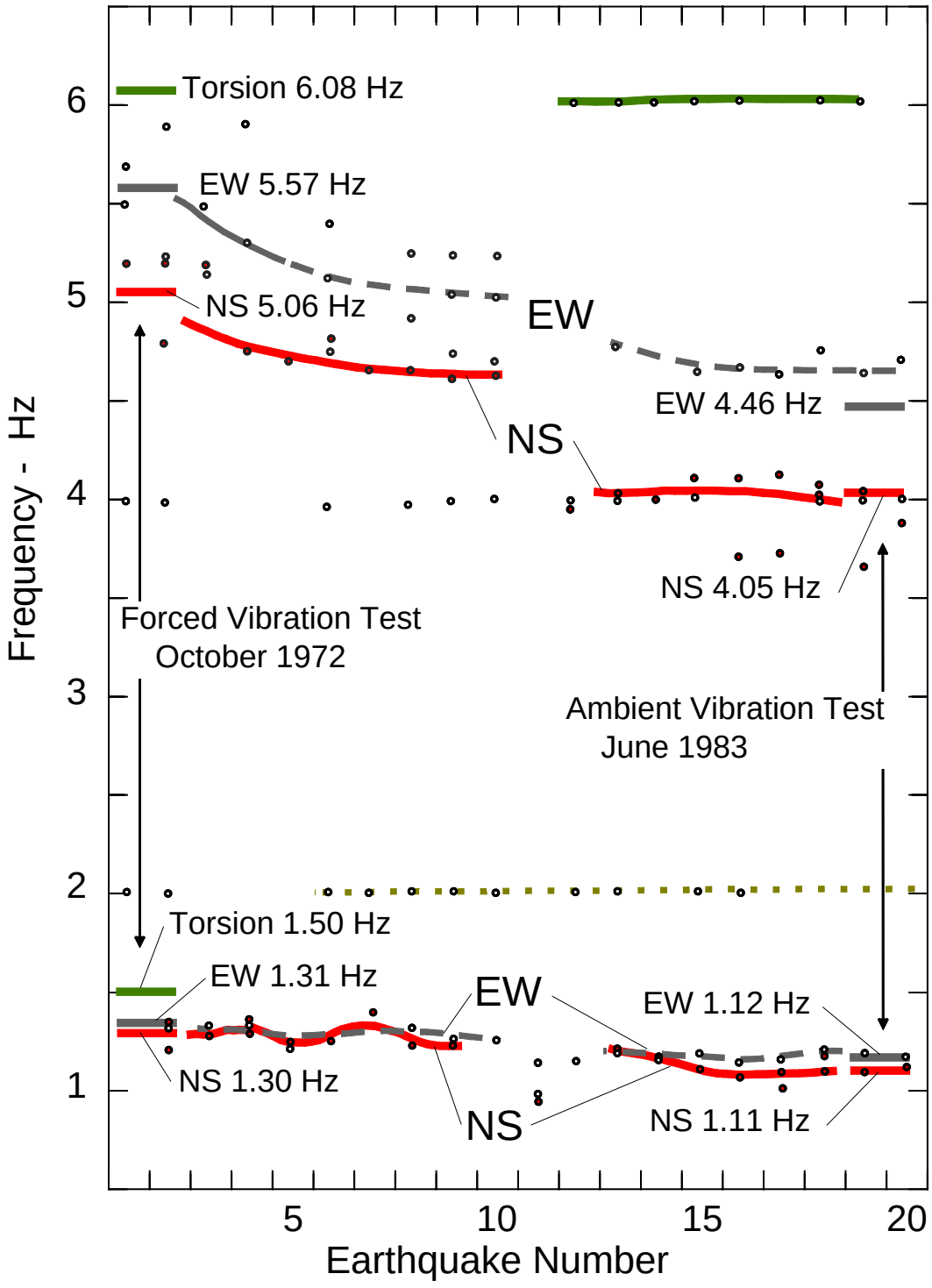

Fig.2.4.7 Comparison of the two first system frequencies as seen (a) during forced vibration tests of Borik-2 building in October 1972, (b) during the 20 earthquakes studied in this work, and (c) during ambient vibration experiment in June 1983. Torsinal frequencies, measured in 1972, are also shown for completeness of this presentation.

All the observed system frequencies start out near the system frequencies measured during the forced-vibration tests in 1972. The ambient vibration test in 1983 shows frequencies lower than those preceding event EQ 11 but consistent with those measured during events 19 and 20. Only the measured second EW system frequency, during the ambient vibration test in 1983, is slightly smaller than the same frequency inferred from the Fourier spectral peaks during events 19 and 20. Figure 2.4.7 also shows the recurring spectral peaks near 2 Hz and 4 Hz. The trend of these peaks is not changed by event 11, and at this time we do not have a plausible interpretation of what these peaks represent.

2.5 Ambient Vibration Experiments

In June 1983, almost two years after the Banja Luka earthquake of August 1981, the staff of the

Table 2.5.1. System frequencies evaluated by using different experimental techniques.

System frequency	Direction	Method of Evaluation		
		Forced Vibrations October, 1972	Ambient Vibrations June, 1983	SMA-1 Records (August1981 Earthquake)
1st mode	E-W	1.31	1.12[1] (1.28)[2]	1.00
	N-S	1.30	1.04 (1.22)	0.87
	Torsion	1.50	--- (1.40)	-
2nd mode	E-W	5.57	4.24 (5.12)	4.34
	N-S	5.06	3.84 (4.48)	4.00
	Torsion	6.08	--- (5.90)	-

[1] Taškov and Krstevska (1983). It appears that in their report the geographic orientation of the building is erroneously rotated by 90º relative to the correct one. Consequently, we replaced the reported results for EW with those for NS and vice versa.

[2] Brackets show frequencies supposedly measured during this experiment, as reported in Jurukovski et al. (1984), Fajfar et al. (1987) and Aničić et al. (1990).

Institute of Earthquake Engineering and Engineering Seismology (IZIIS) from Skopje carried out ambient vibration tests of the Borik -2 building to determine the dynamic characteristics of the structure after the earthquake (Taškov and Krstevska 1983). They reported the following system frequencies for E-W: f_1 = 1.12 Hz, f_2 = 4.24 Hz; and for N-S: f_1 = 1.04 Hz, and f_2 = 3.84 Hz. For reasons we cannot decipher at the time of this writing, Jurukovski et al. (1984), Fajfar et al. (1987) and Aničić et al. (1990) reported different values for the same experiment: E-W, f_1 = 1.28 Hz, f_2 = 5.12 Hz; N-S, f_1 = 1.22 Hz, f_2 = 4.48 Hz; and torsion, f_1 = 1.40 Hz, f_2 = 5.90 Hz, respectively. Table 2.5.1 summarizes these system frequencies and compares them with other different experimental estimates.

2.6 Previous Work

IMS is a prefabricated construction system consisting of precast concrete columns, waffle floor slabs, edge girders, stairs, and wall panels. The frame structure carries gravity loads, while shear walls are main lateral load-resisting elements. The main characteristic of this technology is that the key structural elements are joined together by pre-stressing in two orthogonal horizontal directions. The IMS system has been used in the former Yugoslavia since the 1960s, and it can be found in many major cities like Belgrade (50% of apartments in New Belgrade), Novi Sad, Niš, Banja Luka, Sarajevo, Tuzla, etc. The IMS system was also used in China, Cuba, Egypt, Georgia, the Philippines, and Russia. It is estimated that to date more than 400,000 housing units (~2.5 million m² of built area) have been constructed using the IMS system. Consequently, the system had to be extensively tested and continues to be developed further at the Institute for Testing of Materials in Belgrade, Serbia (e.g. Petrović 1982; Dimitrijević 1982; 2002; Vojnović 1982). Because the IMS system was exposed to moderate earthquake shaking during the Banja Luka earthquake of 1981, and because the Borik-2 building had instruments in the basement and on the 7th and 13th floors, it is of interest to summarize here some of the previous studies of this building.

In this summary of the previous work, for consistency and continuity we will use the same notation as used by the authors of the papers we cite. They use f_1 and f_2 indiscriminately to designate the first and second (computed or observed) frequencies, either when they describe the full-scale experimental results, or for the mathematical models they proposed to represent the Borik-2 building. When they discuss fixed-base building models, f_1 and f_2 represent fixed-base characteristic frequencies of their building models. When they consider soil-structure interaction, or when they describe the strong-motion recorded data, their f_1 and f_2 represent $f_{sys,1}$ and $f_{sys,2}$, which are the first two system frequencies of the soil-structure system. In contrast, throughout this work, we will use f_1 and f_2 to designate only the fixed-base building frequencies,

determined either from the recorded data or as characteristics of the fixed-base mathematical models of this building. We will use f_{sys} to represent the soil-structure system frequency.

Jurukovski et al. (1984) presented a system identification analysis for the NS response of the Borik-2 building. They adopt a simple lumped-mass model, allow only horizontal degrees of freedom for each mass (for floors 1 through 14), and in modeling soil-structure interaction they consider translational and rotational stiffness and degrees of freedom for the foundation mass only. To develop the models, they (1) use the results of forced vibration and ambient vibration tests, (2) adopt damping, rocking stiffness, and translational stiffness of the foundation mass as unknown parameters, and (3) perform iterative search for their optimal values. They determine the optimal values for the response during 1981 earthquake. Jurukovski et al. (1984) do not discuss the logic behind their use of fixed-base conditions to formulate the "structural model," and while they iterate to find the optimum values only for the damping and the equivalent soil stiffness they do acknowledge that further modeling refinements are necessary. In their conclusions, Jurukovski et al. (1984) state that "a certain time after the earthquake, the dynamic system is strengthened and brought to its original position again," but they provide no evidence or references to support their claim. It is not clear from their comments whether this "strengthening" occurs in the structure, in the soil, or in both.

Jurukovski et al. (1984) is chronologically the first paper we find that cites frequencies for the ambient vibration test in the Borik-2 building (values shown in brackets in column 4 in Table 2.5.1), that are different from the values contained in the report by Taškov and Krstevska (1983). Jurukovski et al. (1984) also report the values of torsional frequencies, which are not mentioned by Taškov and Krstevska (1983). Taškov is the second author of the Jurukovski et al. (1984) paper, so it is surprising that the report by Taškov and Krstevska (1983) is not cited.

In Section 1.3.3 of "Selected Chapters on Earthquake Engineering" (Odabrana Poglavlja iz Zemljotresnog Građevinarstva), Petrović (1989) develops an equivalent continuous Bernoulli beam theory for analysis of natural periods of a symmetric building that is fixed at its base. He than shows an example, with geometric and material properties, that corresponds to the characteristics of the Borik-2 building. He shows how, using his tables, one can compute f_1 = 1.27 Hz for this building, and he comments that for the same building, numerical analysis using a digital computer and matrix representation of the stiffness matrix gives f_1 = 1.20 Hz. By referring to the latter as an "exact" value, he notes that the difference relative to his approach using tables is only 5.5%.

Fajfar et al. (1987) present dynamic response analysis of the Borik-2 building using a fixed-base, discrete linear model, with properties that they develop and calibrate in terms of the results of the forced-vibration experiments in 1972, the earthquake response in 1981, and the ambient

vibration tests in 1983. They use the geometry of the mode shapes determined during the forced- and ambient vibration tests of Borik-2 building to justify their assumption that the effects of soil-structure interaction for this building can be neglected. They do not comment that their justification could be valid only in a special case, if the rocking component of soil-structure interaction could be shown to be equal to zero (this of course never happens with real buildings, where the rocking component of foundation motion is the primary contributor to the total response). Their results imply "practically linear structural behavior" during the 1981 earthquake, with only minor excursions to non-linear range in the deformations of the shear walls (in the first story and from the 7^{th} to the 10^{th} stories). Table 2.6.1 summarizes the observational data they use (system frequencies in Hz) during forced vibrations in 1972, earthquake response in 1981, and ambient vibration testing in 1983 (they give no specific reference to identify the source of the system frequencies for ambient vibration experiments in 1983 and only state that the tests were performed by IZIIS, Skopje). Table 2.6.2 gives the corresponding frequencies determined by their model studies.

Table 2.6.1. System Frequencies (Hz) Observed During Different Full-Scale Experiments.

System Frequency	Direction	Forced Vibrations (October 1972)	Ambient Vibrations (June 1983)	SMA-1 Records (August 1981 Earthquake)
1^{st} mode	E-W	1.30-1.37	1.28	0.98-1.00
	N-S	1.30-139	1.22	0.91
	Torsion	1.49-1.56	1.41	-
2^{nd} mode	E-W	5.56	5.00	4.35-4.76
	N-S	4.76-5.00	4.55	4.17-4.35
	Torsion	5.88-6.25	5.88	-

Fajfar at al. (1987) reach the following conclusions. (1) The differences among different experiments and earthquake response resulted almost entirely from changes in masses and from the influence of the non-structural elements in the response. The stiffness was significantly higher during small amplitudes of response and was much smaller during large earthquake

response. (2) Large earthquake excitation amplitudes near 5 Hz contributed to strong excitation of the second mode, and this had significant influence on all internal forces. The displacement time history, however, was not significantly influenced by the second mode. (3) Without experimental data, only rough predictions of structural behavior during earthquakes are possible.

Table 2.6.2. Model Frequencies (Hz), Evaluated by Analysis, for the Conditions During the Tests of October 1972 and June 1983, and Recorded Earthquake Response in August 1981.

System Frequency	Direction	Forced Vibrations (October, 1972)	Ambient Vibrations (June, 1983)	SMA-1 Records (August1981 Earthquake)
1st mode	E-W	1.33	1.20	0.97-1.06
	N-S	1.32	1.19	0.89-0.93
	Torsion	1.59	1.43	-
2nd mode	E-W	6.25	5.55	5.26-5.55
	N-S	5.26	4.76	3.85-4.17
	Torsion	7.69	7.14	-

In the book entitled “Earthquake Engineering” by Aničić et al. (1990), on pages 247–252 we find what appears to be a summary of work by Fajfar et al. (1987). The building described in this book is referred to as a “building of IMS type in Banja Luka,” but from the material presented it seems that the authors are describing the Borik-2 building in Banja Luka. The authors describe their model, which includes walls as cantilevers, with T cross-sections, and a frame consisting of columns and inter-story floor slabs. They assume that the soil-structure interaction can be neglected because “the experimental results have shown that it plays a minimal role.” but they do not cite a source of experimental observations that would confirm this. They assume the contribution of nonstructural members to the overall stiffness of the building model to be in the range from 30% (for EW) to 40% (for NS) for weak motions (for modeling the observed system frequencies during the forced-vibration test in 1972 and for those of ambient vibration testing in 1983), and only 8% to 18% (for both NS and EW motions) during the earthquake event EQ 11, in 1981. They conclude that the behavior of the building was essentially linear during the

earthquake event, with the exception of "a few places" in the structure where slight nolinearity may have occurred, but they do not state where those places were in the building. Aničić et al. (1990) summarizes their results in two tables, which are reproduced here as Tables 2.6.1 and Table 2.6.2.

Table 2.6.3. System Frequencies, in Hz, for Ambient Vibration Tests in June 1983, in the Borik-2 building, as Reported in Taškov and Krstevska (1983), Jurukovski et al. (1984), Fajfar et al. (1987), and Aničić et al. (1990).

System Frequency	Direction	Taškov and Krstevska (1983)	Jurukovski et al. (1984)	Fajfar et al. (1987)	Aničić et al. (1990)
1st mode	E-W	1.12 [1.12][1] (1.10)[2]	1.28	1.28	1.28
	N-S	1.04 [1.11][1] (1.09)[2]	1.22	1.22	1.22
	Torsion	-	1.40	1.41	1.41
2nd mode	E-W	4.24 [4.46][1] (4.33)[2]	5.12	5.00	5.00
	N-S	3.84 [4.05][1] (3.95)[2]	4.48	4.55	4.55
	Torsion	-	5.90	5.88	5.88

[1]Average values based on 5 to 7 data points in the report by Taškov and Krstevska (1983).

[2] Average values, based on re-examination (by M. Manić in June 2007) of 5 to 7 recordings, at different floors, with clear local peaks in the Fourier amplitude spectra as plotted in the report by Taškov and Krstevska (1983).

Aničić et al. (1990) conclude that the modeling tools they describe are capable of determining the dynamic characteristics of buildings shaken by small and moderate earthquakes. They note

that during small amplitudes of excitation (forced- and ambient vibration tests) nonstructural members and partition walls contribute significantly to the stiffness of the models. They observe that the good predictions of the response they found in this case imply that this can be achieved by using the results of full-scale experimental observations, and that this shows the adequacy of their simple models. They note, however, that in the absence of full-scale recorded motions this may be possible only approximately. In connection with their last comment, the reader may wish to peruse the report by Kojić et al. (1984).

In Table 2.6.3, we summarize the differences among the reported values of the system frequencies for the ambient vibration test in June 1983 in the Borik-2 building. It seems that Fajfar et al. (1987) and Aničić et al. (1990) adopted the values reported by Jurukovski et al. (1984), except for the 2nd system frequencies. All of the 1st system frequencies are essentially the same. The minor differences appear to result from the use of only two significant figures in Aničić et al. (1990), who report periods, and then rounding off to three significant figures, after inversion to frequencies. What is remarkable in this comparison is (1) how different the values used by Jurukovski et al (1984), Fajfar et al. (1987), and Aničić et al. (1990) are relative to those reported by Taškov and Krstevska (1983), and (2) that these authors all report the values for torsional frequencies, while Taškov and Krstevska (1983) do not. Thus, from the published papers and reports we have that deal with the Borik-2 building it is not possible to determine the source for the tosional frequencies cited and used by Jurukovski et al (1984), Fajfar et al. (1987), and Aničić et al. (1990).

In Fig. 2.6.1, we illustrate these differences graphically. Horizontal bars show the range between the minimum and maximum values, while open and closed circles show computed averages based on the measured data (open circles for T&K–Data represent the data in the Taškov and Krstevska (1983) report as interpreted by Manić in the summer of 2007, and solid circles represent data as reported by Taškov and Krstevska (1983)). The horizontal bars labeled "Manić" represent the same data, but as re-interpreted by Manić in 2007, while the short vertical bars show his averages. The number of measured values used to compute the averages (5, 7, and 11) is shown in Fig. 2.6.1. The frequencies of the peaks were read by Manić from spectral amplitudes, for recordings on the terrace, the roof, and the 7th, 4th, and 1st floors. We did not include the measurements for the basement. The points labeled J&al. correspond to the values

reported in Jurukovski et al. (1984), while the points labeled F&A are from Fajfar et al. (1987) and Aničić et al. (1990). Finally, the observed frequencies during EQ 19 (8/21/1981) and EQ 20

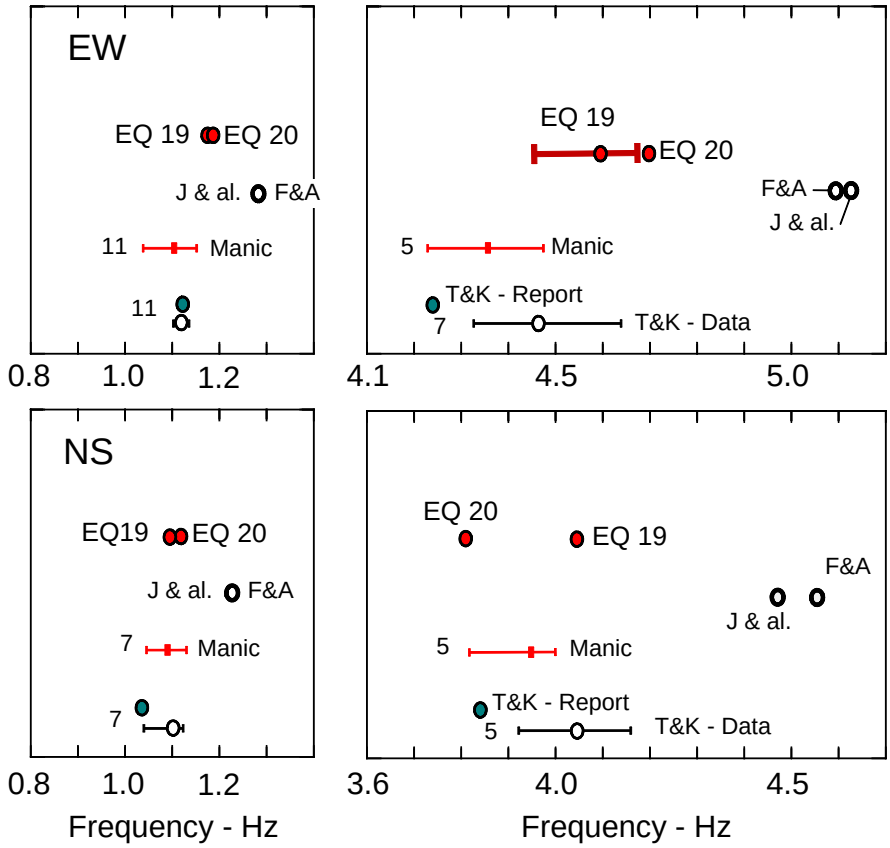

Fig.2.6.1. Comparison of different estimates of the two lowest system frequencies for EW and NS vibrations of the Borik-2 building. Bottom bars and open circles (T&K–Data) show the range and the average values as we found those in the report by Taškov and Krstevska (1983). Full circles above (T&K–Report) show the values they reported. The range bars above, with average values shown by small solid rectangles (Manić), represent our interpretation of the spectra of ambient vibration measurements in Taškov and Krstevska (1983). The numerals in the bottom two rows show the number of spectral peaks defining the range and the average values. The pair of solid circles on the top shows the frequencies of the spectral peaks in the recorded motions during EQ 19, which occurred before, and EQ 20, which occurred after the ambient vibration test in June 1983.

(10/11/1986) (see Figs. 2.4.3e and 2.4.4e) are included because those preceded and followed the ambient vibration tests of June 1983. All peaks we found in the Fourier amplitude spectra of recorded earthquake accelerations were sharp and clearly defined. Only the peak for the 2nd system frequency during EQ 19 was broad and not well defined. The horizontal bar in the top right part of Fig. 2.6.1 for EQ 19 shows the width of this peak.

As can be seen from Fig. 2.6.1, the data in Taškov and Krstevska (1983) for the first two system frequencies are consistent with what we found during two small earthquakes (EW 19 and EQ 20). The system frequencies reported by Jurukovski et al. (1984), Fajfar et al. (1987), and Aničić et al. (1990), which were used as starting conditions for their analyses, are inconsistent with both earthquakes and ambient vibration tests. Therefore, their analyses and conclusions are not valid for the Borik-2 building and will have to be considered only in a qualitative sense. In their report, Taškov and Krstevska (1983) chose to present system frequencies somewhat smaller than the average values based on their measurements, except for the fundamental EW system frequency. It is not clear from their report why this was done.

3. METHODOLOGY

3.1 One-Dimensional, Continuous-Wave Propagation Model of a Building

An incident wave at the base of a building will propagate up and will be delayed and attenuated at observation points at different heights along the building. At the top, it will be reflected and will be seen delayed at consecutive observation points as it moves down toward the base again.

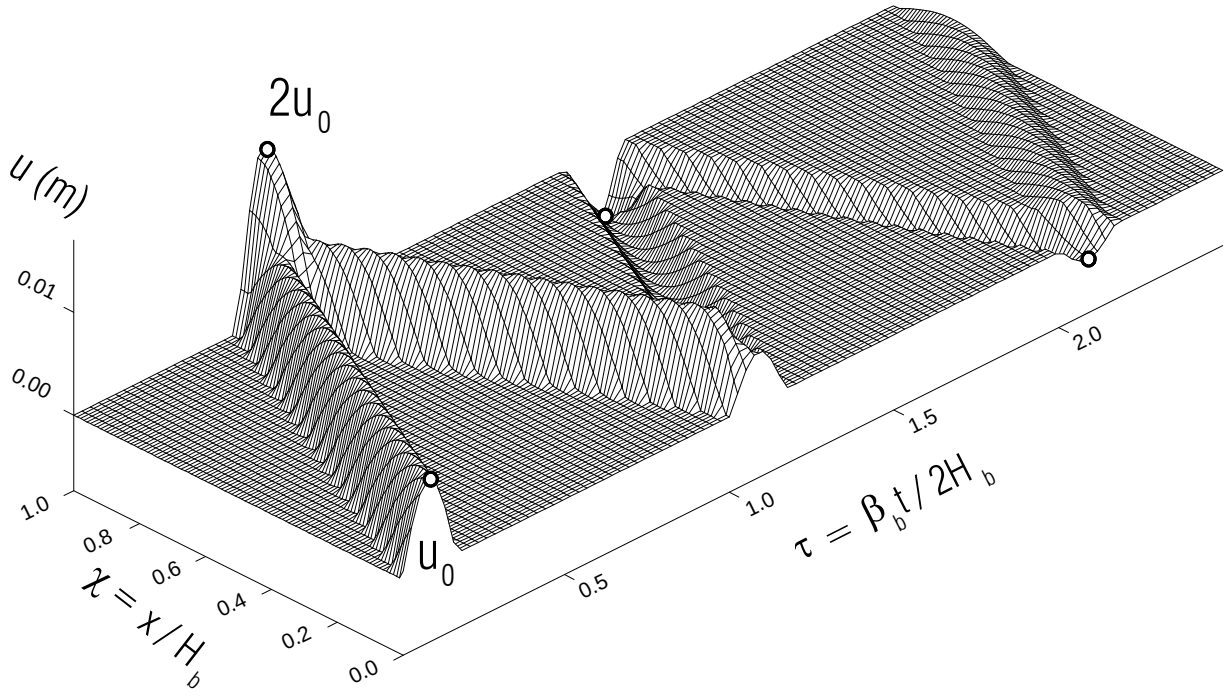

Fig.3.1.1 Displacements in a shear building caused by a pulse, with amplitude u_0, incident from soil into the building (at $x/H_b = 0$), and propagating up and down. The resulting motion is shown versus dimensionless height x/H_b and dimensionless time $\tau = \beta_b t/2H_b$. The building has constant rigidity and wave velocity, β_b, throughout its height H_b.

After reaching the base, it will be partially reflected and will again propagate up. After many such reflections, the motion resulting from constructive interference will dominate the response. In Fig. 3.1.1, we illustrate this for a homogeneous linear shear building with constant rigidity and wave velocity, β_b, throughout its height H_b. In this figure, we show the displacement field resulting from an incident pulse with amplitude u_0, and we plot the displacement versus dimensionless building height x/H_b and versus dimensionless time $\tau = \beta_b t/2H_b$. In a real

building, variations in wave speed and in rigidity, at different floors, will create additional reflections and changes in wave amplitude every time the wave crosses a jump in the material properties (Fig. 3.2.1), and the resulting wave motion will appear more complicated, but it will maintain the same general character as illustrated in Fig. 3.1.1. The displacements accompanying the wave motion up and down the building will be further complicated when nonlinear deformations occur along the wave path. The reader can find examples of such nonlinear waves in a building in the papers by Gičev and Trifunac (2007a,b). In this work, we will interpret the computed impulse response functions only terms of the equivalent linear representation.

The time delay between the motions at different stories can be observed by a naked eye in some earthquake records in tall buildings, but to measure such delays it is better to use some appropriate signal processing tool, the most common one being cross-correlation analysis. In this work, we use deconvolution analysis (Snieder and Şafak 2006; Todorovska and Trifunac 2006, 2007a,d). For completeness of this presentation we reproduce here the basic theory as outlined in Todorovska and Trifunac (2006).

3.2 Impulse Response Computation

We assume that the building is a linear time-invariant system with a single input—the ground motion, $u_{\text{ref}}(t)$—and multiple outputs—the story responses, $u_{\text{i}}(t)$ (Fig. 3.2.1). In time, this input and the outputs are related by

$$u_i(t) = (u_{\text{ref}} * h_i)(t) = \int_0^t u_{\text{ref}}(\tau) h_i(t-\tau)\, d\tau \quad , \tag{3.1}$$

and in the frequency domain by

$$\hat{u}_i(\omega) = \hat{u}_{\text{ref}}(\omega)\hat{h}_i(\omega) \, , \tag{3.2}$$

where $*$ indicates convolution and the hat indicates Fourier transform. Function $h_i(t)$ is the impulse response function and represents the response at level i to input that is a Dirac delta function, $\delta(t)$:

$$u_{\text{ref}}(t) = \delta(t) \quad \Leftrightarrow \quad u_i(t) = h_i(t) \, . \tag{3.3}$$

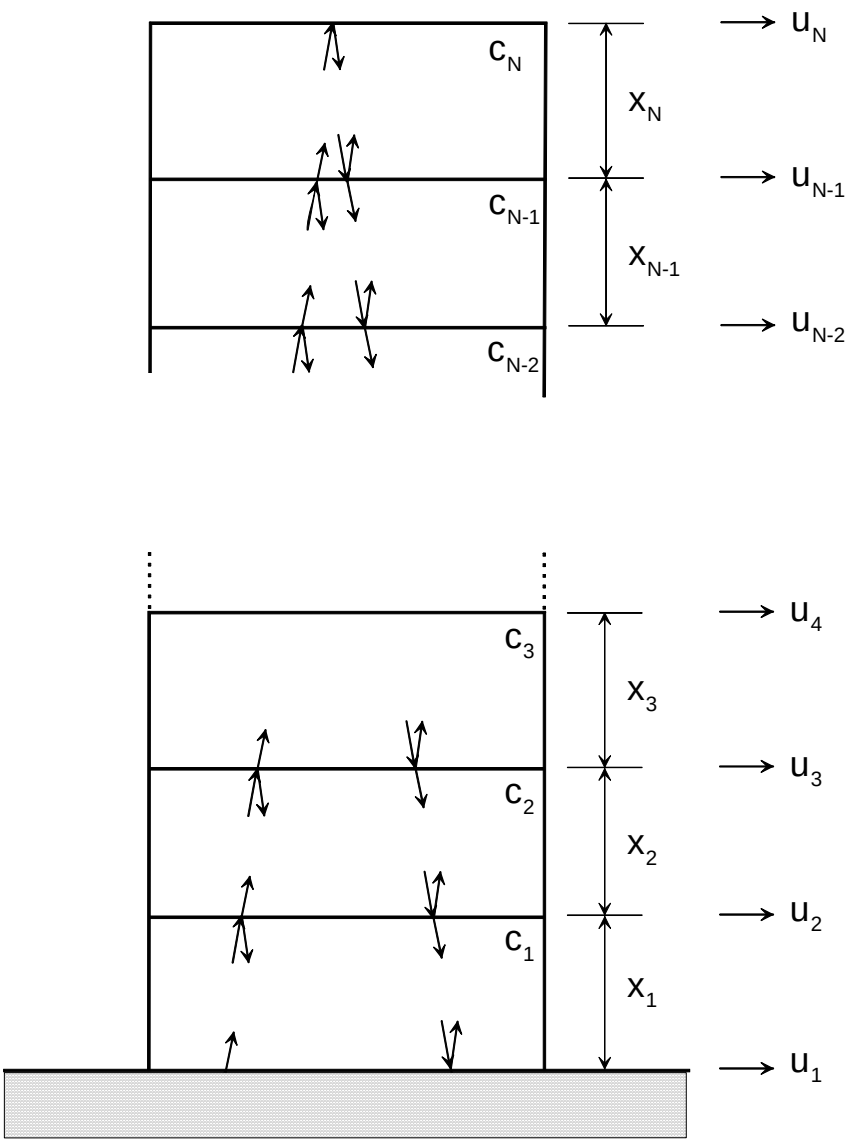

Fig. 3.2.1 An n-layer building model.

Function $\hat{h}_i(\omega)$ is the transfer function between the response at level i and the input, and it represents the Fourier transform of the response to input, such that $\hat{u}_{\text{ref}}(\omega)=1$. The transfer function is the Fourier transform of the impulse response function

$$\hat{h}_i(\omega) = FT\{h_i(t)\} \quad (3.4)$$

The impulse response functions can be computed from any recorded response by taking the inverse Fourier transform of the corresponding transfer function and can be used to simulate the propagation of a pulse through the building, using actual data. The time delays can be measured using these impulse response functions. We note that the response at any level can be used as reference motion, in which case the impulse response function for that level would be a Delta-function.

The impulse response, $h_i(t)$, can be computed using

$$h_i(t) = FT^{-1}\left\{\frac{\hat{u}_i(\omega)\bar{\hat{u}}_{\text{ref}}(\omega)}{\left|\hat{u}_{\text{ref}}(\omega)\right|^2 + \varepsilon}\right\}, \quad (3.5)$$

where the bar indicates complex conjugate, and ε is a regularization parameter used to avoid singularities (Snieder and Şafak 2006). In this work, we used $\varepsilon = 0.1 * \bar{P}$ when u_{ref} is the ground floor record, and $\varepsilon = 0.05 * \bar{P}$ when u_{ref} is the roof record, where $\bar{P}$ is the average power of u_{ref}. Other optimization procedures can also be used to suppress noise in the deconvolution—e.g., such as the NIOM method used to analyze geotechnical borehole data (Haddadi and Kawakami 1998).

3.3 Changes in Wave Travel Times

To identify changes in travel times, some reference travel times are needed as a baseline. For continuously monitored buildings, those can be values obtained from weak-motion data recorded "immediately" before the earthquake, which could then be compared with values obtained from similar amplitude motions recorded after the earthquake. Using recorded strong-motion data, one can estimate "instantaneous" travel times from windowed data and track its changes versus time (Todorovska and Trifunac 2006, 2007a,b). In this work we use strong-motion data from earthquakes recorded in the building and a suitable set of time windows. The limits of these time intervals are chosen intuitively and when possible are based on the results of other independent analyses. In each window, the analysis will give the properties of an equivalent linear system representing the building in the corresponding time window.

3.4 Estimation of Fixed-Base Frequency via Wave Travel Times

A significant product of the impulse response analysis is an estimate of the fundamental fixed-base frequency of vibration, using data from only two horizontal sensors, one at the point of fixity (ground level), and another on the roof. In the following, we will assume that the building response is predominantly one-dimensional (1D), that the point of fixity is at ground level, and that the deformations are mainly in shear. Then, the fundamental *fixed-base* period of vibration T_1 of the building, modeled as a shear beam, is related to the time, τ_{tot}, that it takes a wave to travel between the basement and the roof :

$$T_1 = 4\tau_{\text{tot}}, \tag{3.6}$$

and the corresponding fundamental fixed-base frequency is $f_1 = 1/T_1$.

Snieder and Safak (2006) examined the effect of coupling with the soil on the estimate of f_1 using the impulse travel time. In their model, the building is a shear beam bonded to the soil, which is just another layer in a 1-D wave propagation problem through a layered medium. They showed that, for such a model, the travel time of the impulse is not affected by the coupling with the soil. Such a model is appropriate for anti-plane motions and for in-plane motion by vertically incident waves and a building on a surface foundation, but for the in-plane problem, buildings on rigid, embedded foundations, or on surface rigid foundations, with inclined wave incidence, not only deform but also move as a rigid body (translate and rotate). The motions of the upper floors due to the rigid body rocking cannot be separated from those due to deformation of the building even in the most ideal case of a relatively stiff base and floor slabs, unless there are at least two vertical sensors at the base. Unfortunately, in most buildings, and in Borik-2, there is only one vertical sensor on the ground floor. In this work, we assume that the contributions to the recorded motions we use to compute the impulse responses affect mostly the peak amplitude of the propagating pulse, while the effects on the shape of the pulse—and hence on picking the pulse arrival time—are small and are within the "noise" range (i.e., errors due to all other simplifying assumptions).

Finally, we recall that the maximum concentrations of energy of the relative building response do not occur at the fixed-base frequencies of the building, f_1, but at the frequencies of the soil-structure system. The lowest such frequency, which is a result of the coupling of the soil motion with the fundamental fixed-base frequency, we denote as f_{sys}, and we call it "the first system frequency" or "the system frequency." The two frequencies are related by

$$f_{\text{sys}}^{-2} = f_1^{-2} + f_H^{-2} + f_R^{-2}, \tag{3.7}$$

where f_H and f_R represent the horizontal and rocking frequencies of a rigid building on flexible soil. Equation (3.7) implies that $f_1 > f_{sys}$. In our previous work, we showed that this was the case (1) for the former Imperial County Services building (Todorovska and Trifunac 2007d) and (2) for a seven-story hotel building in Van Nuys (Todorovska and Trifunac 2006, 2007a), both in California, which supports our hypothesis that the f_1 we estimate from the impulse response analysis is approximately the fixed-base frequency. In this work, we again use this hypothesis by analyzing that relationship for 20 events recorded in the Borik-2 building and by comparing the changes in f_1 and f_{sys} from one earthquake event to another.

4. RESULTS AND ANALYSIS

This chapter first presents the plots of the impulse responses for 20 earthquakes and the tabulated arrival and travel times between floors (as read from the impulse response plots). Then, the results are presented for the fundamental fixed-base frequency, f_1, during the 20 earthquakes, with an analysis of its changes from one event to another and over time. The relation of f_1 to the soil-structure system frequency, f_{sys}, during the 20 earthquakes and during forced-vibration and ambient vibration tests is also examined.

4.1 Impulse Responses for Recorded Motions

The motions were recorded at the basement, 7th floor, and 13th floor levels. Figures 4.1.1 through 4.1.20 show results for the impulse response functions, at different levels of the building, computed using Eqn. (3.5). The plots on the left correspond to an input impulse at the ground floor, and those on the right to an input impulse at the 13th floor. The computed impulse response functions are shown only for the early stages of response to emphasize the arrival times of the primary pulses. The plots on the left show the input impulse, at time $t = 0$, on the ground floor, which then propagates up, arriving with some delay at the upper floors, and then propagates down after being reflected from the roof. The input pulse has a finite width because of the effective windowing in time (due to the finite duration of the record) and because of the regularization parameter ε (we used $\varepsilon = 0.1$ for the case of an input impulse at the ground floor and $\varepsilon = 0.05$ for the case of an input impulse at the 13th floor). The plots on the right show the input impulse at time $t = 0$ at the 13th floor, which then propagates down causally (in positive time) and also acausally (in negative time). The acausal wave corresponds to a wave propagating up in the physical model. For earthquake EQ 11 (8/13/1981), which produced the largest relative response at this site, the impulse responses were computed also for different time windows.

The pulse arrival times can be read most clearly for (1) the direct wave going up—when the input impulse is at the base (left part of Figs. 4.1.1–4.1.20), and (2) the direct acausal wave going down—when the input impulse is at the roof (right part of Figs. 4.1–4.20). In the analysis of the Borik-2 building, there is a disadvantage caused by the placement of the top SMA-1 on the 13th floor rather than on the roof. For the pulse originating at the ground floor and propagating up, reflections from the roof then interfere with the wave propagating up, and this makes the reading of the arrival time at the 13th floor difficult and ambiguous. To avoid this problem, in all interpretations of the wave travel times in this report we used only the data for the pulse located on the 13th floor and acausal propagation of the pulse upward (with negative times). The results of the readings of the arrival times for this case are shown in Tables 4.1 through 4.20. The

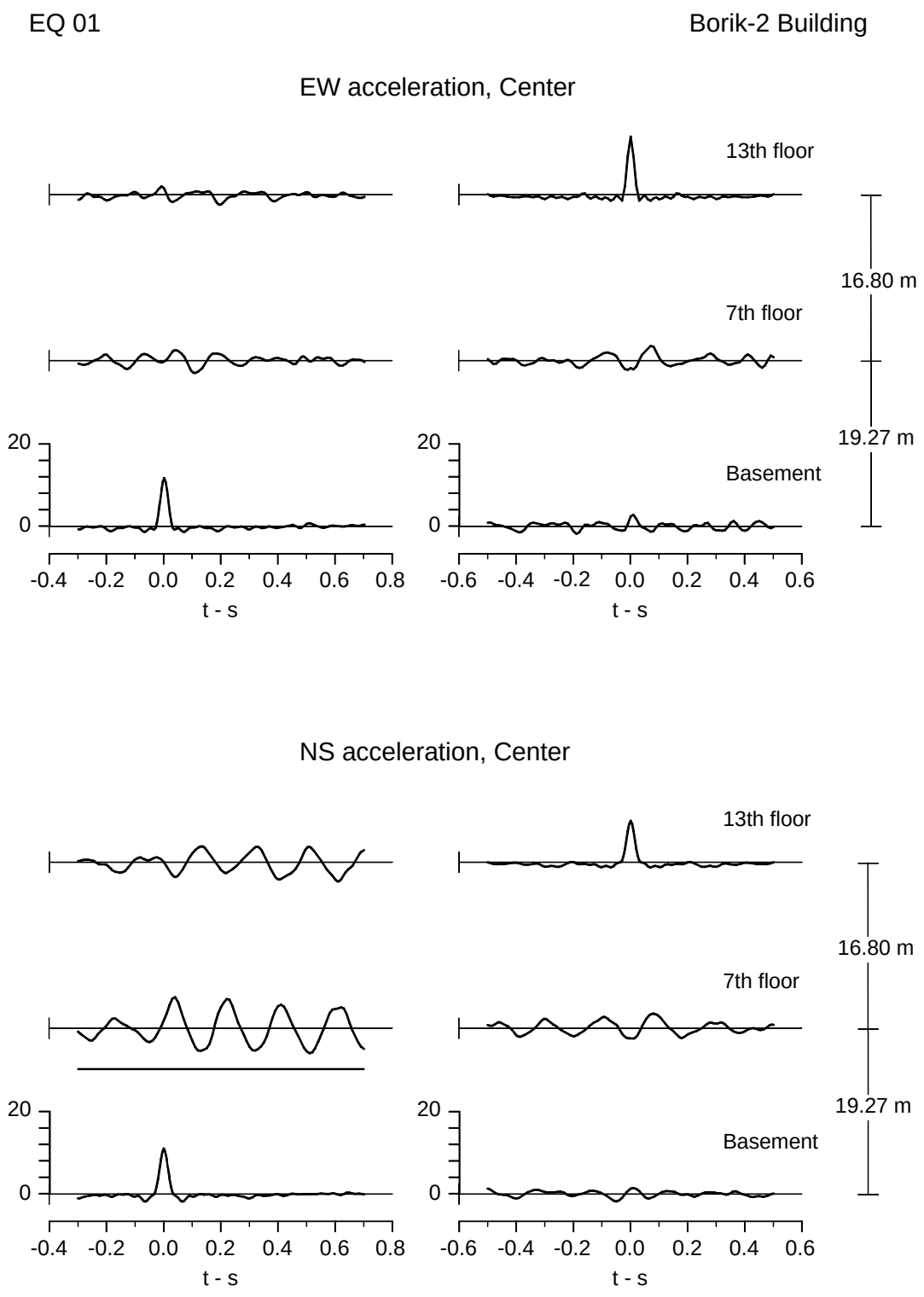

Fig. 4.1.1 Impulse response functions for EW(top) and NS(bottom) motions of the Borik-2 building during earthquake No. 1.

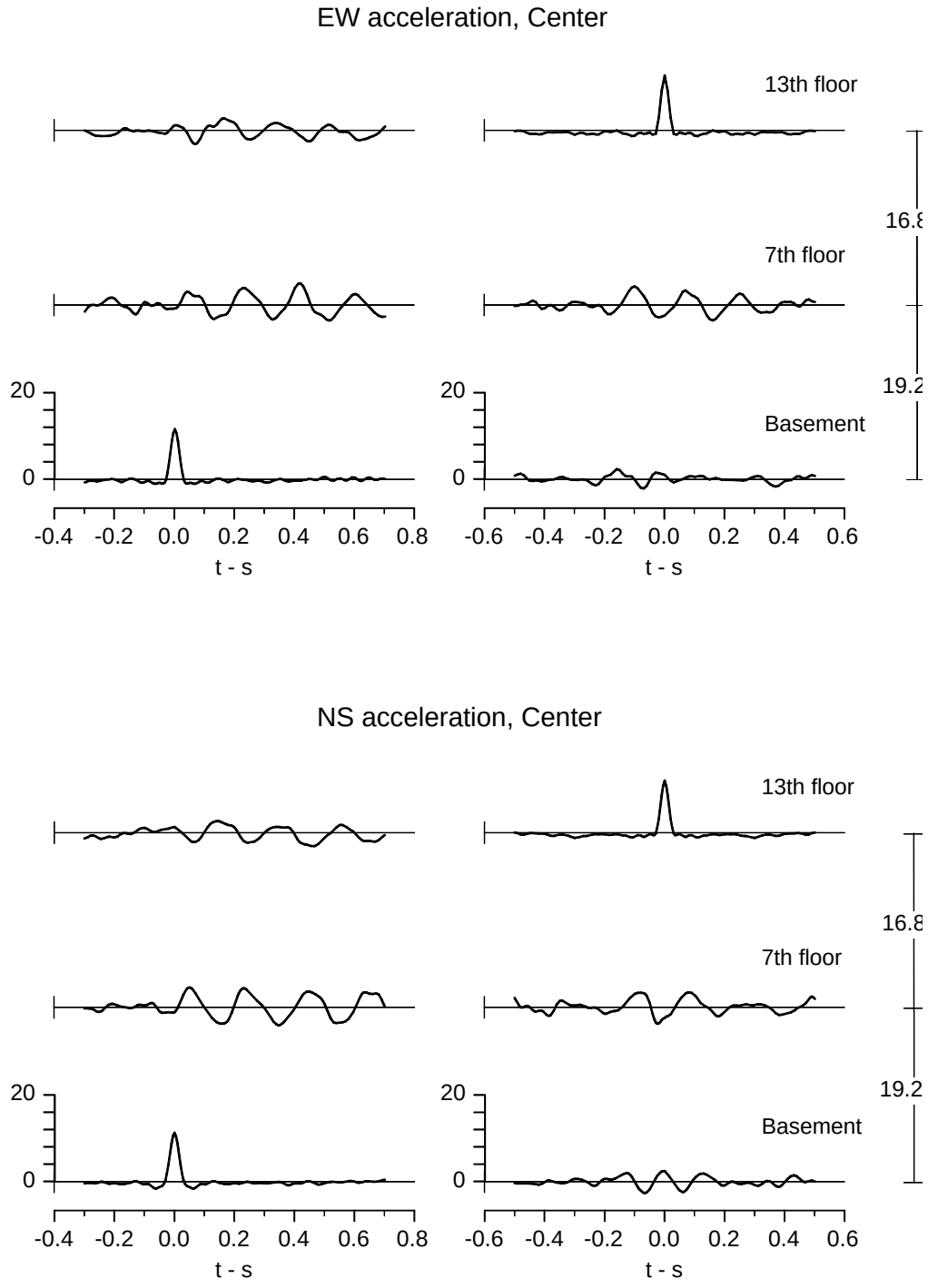

Fig. 4.1.2 Same as Fig. 4.1.1, but for earthquake No. 2.

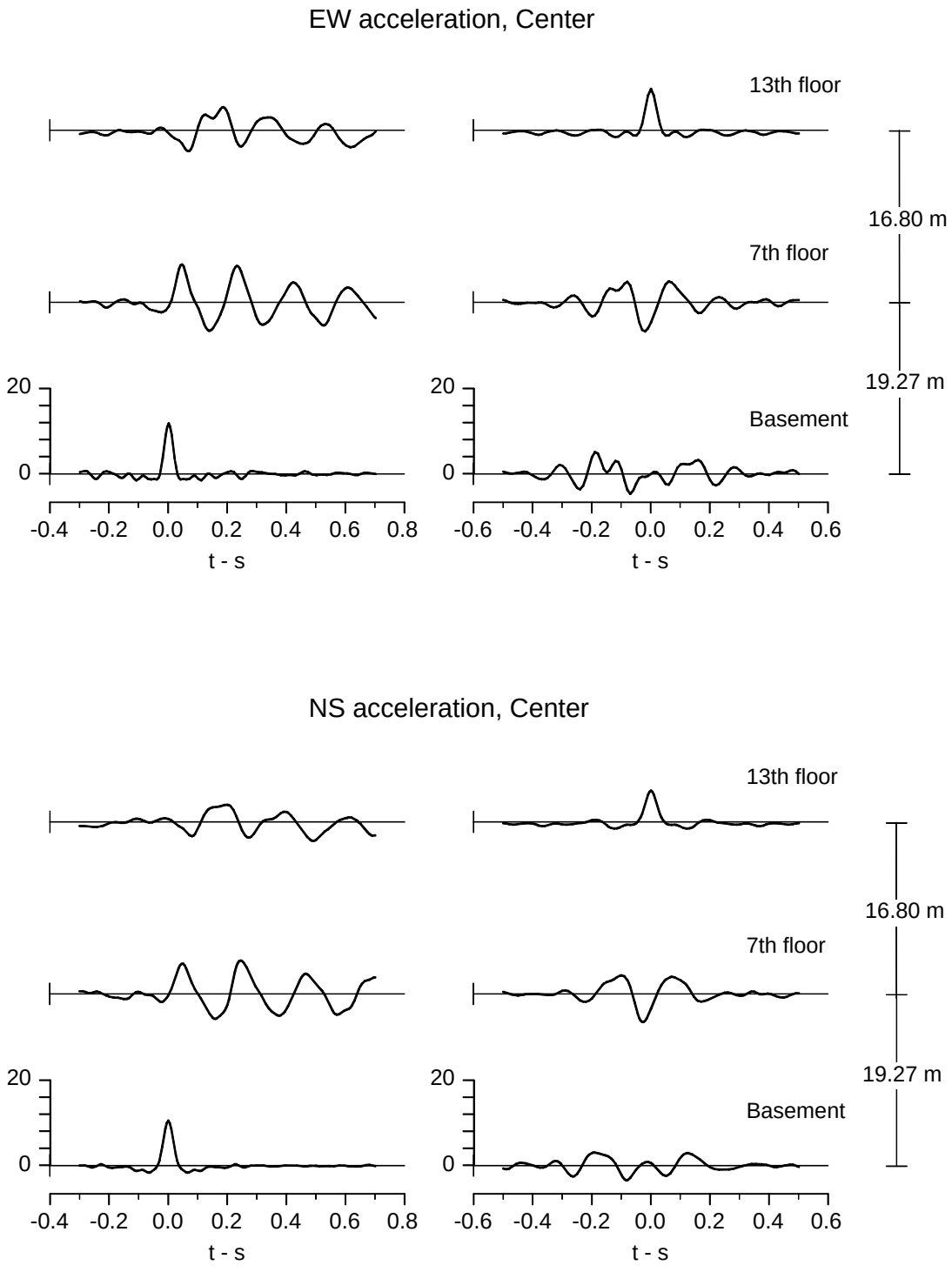

Fig. 4.1.3 Same as Fig. 4.1.1, but for earthquake No. 3.

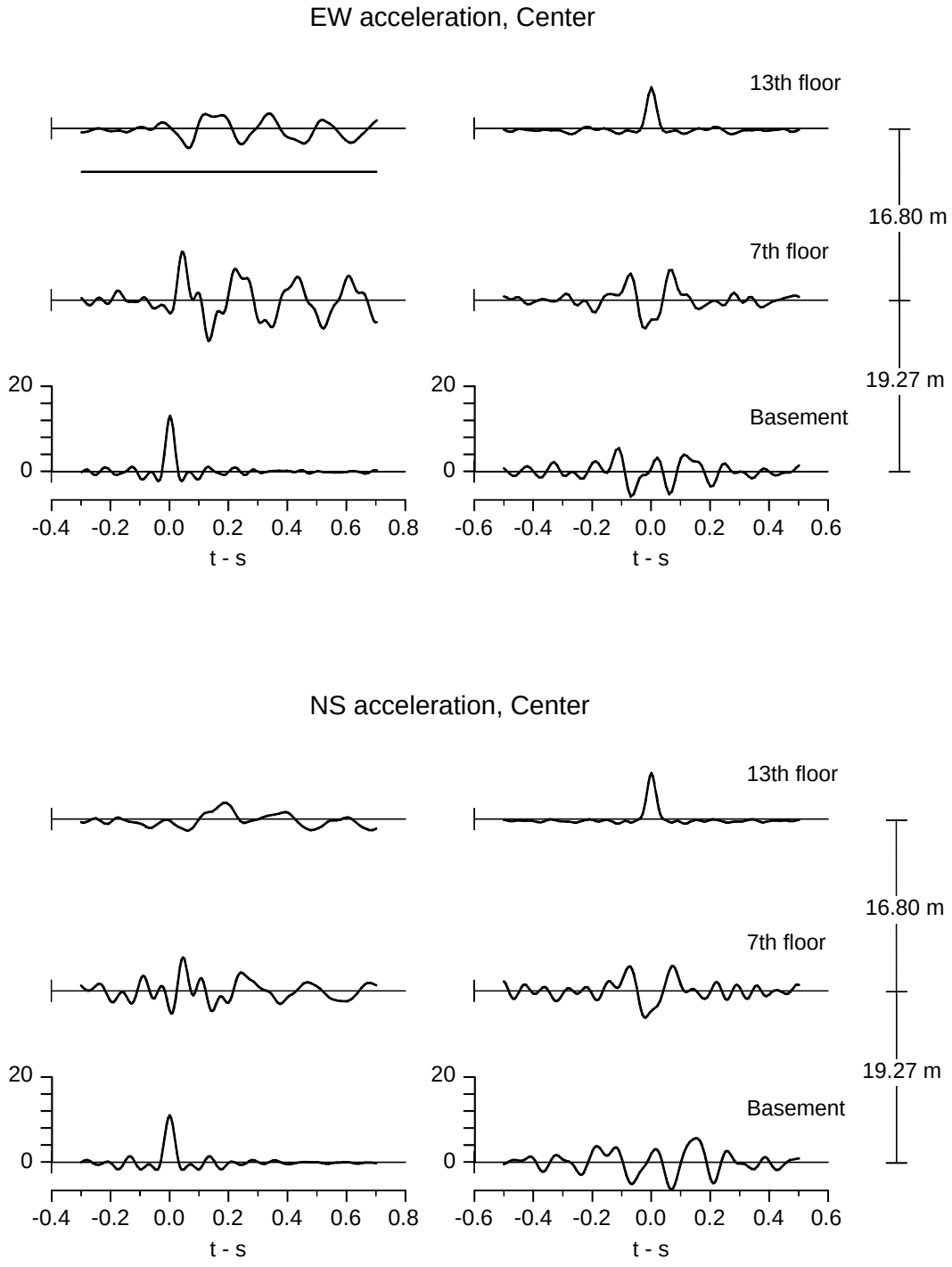

Fig. 4.1.4 Same as Fig. 4.1.1, but for earthquake No. 4.

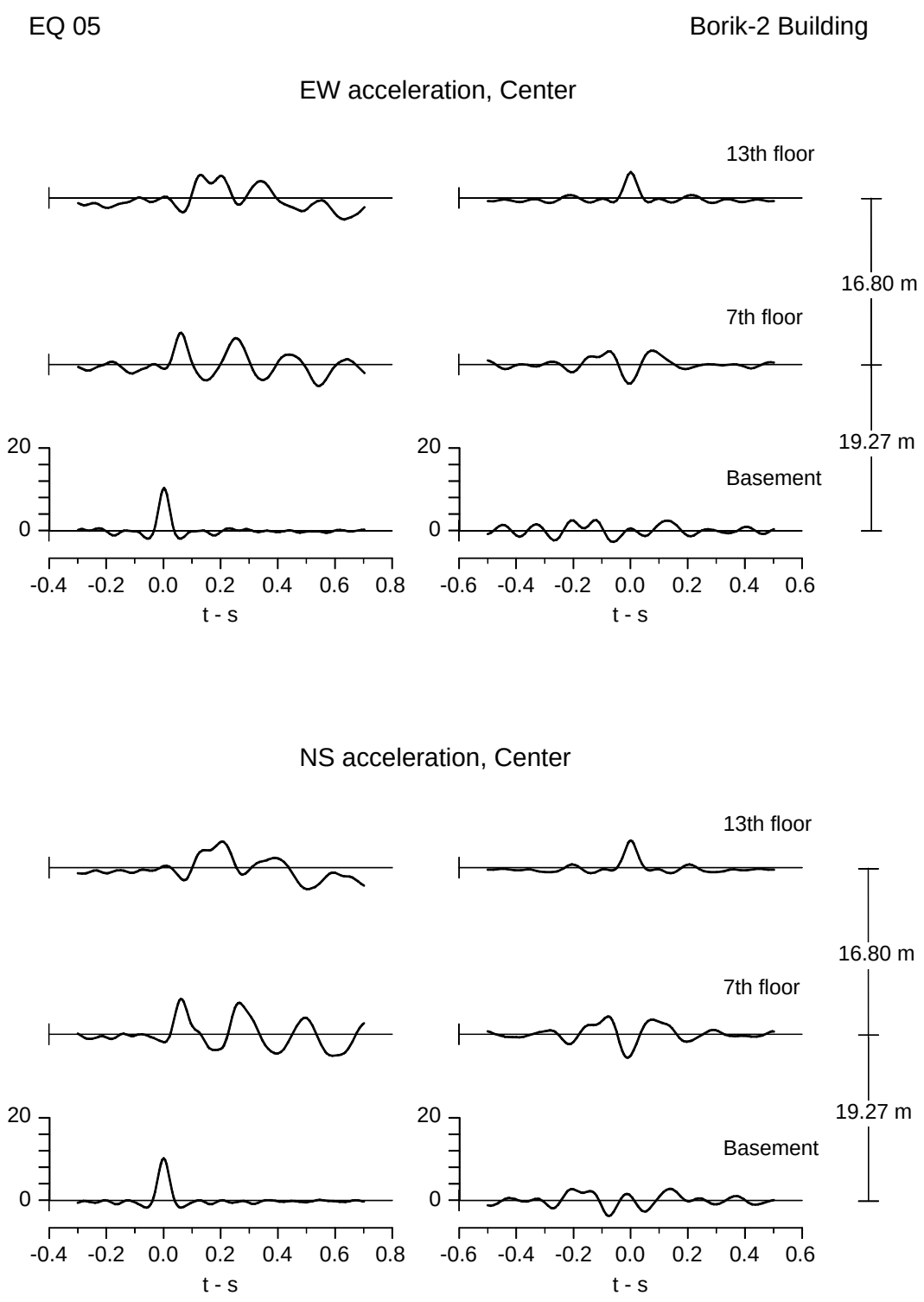

Fig. 4.1.5 Same as Fig. 4.1.1, but for earthquake No.5.

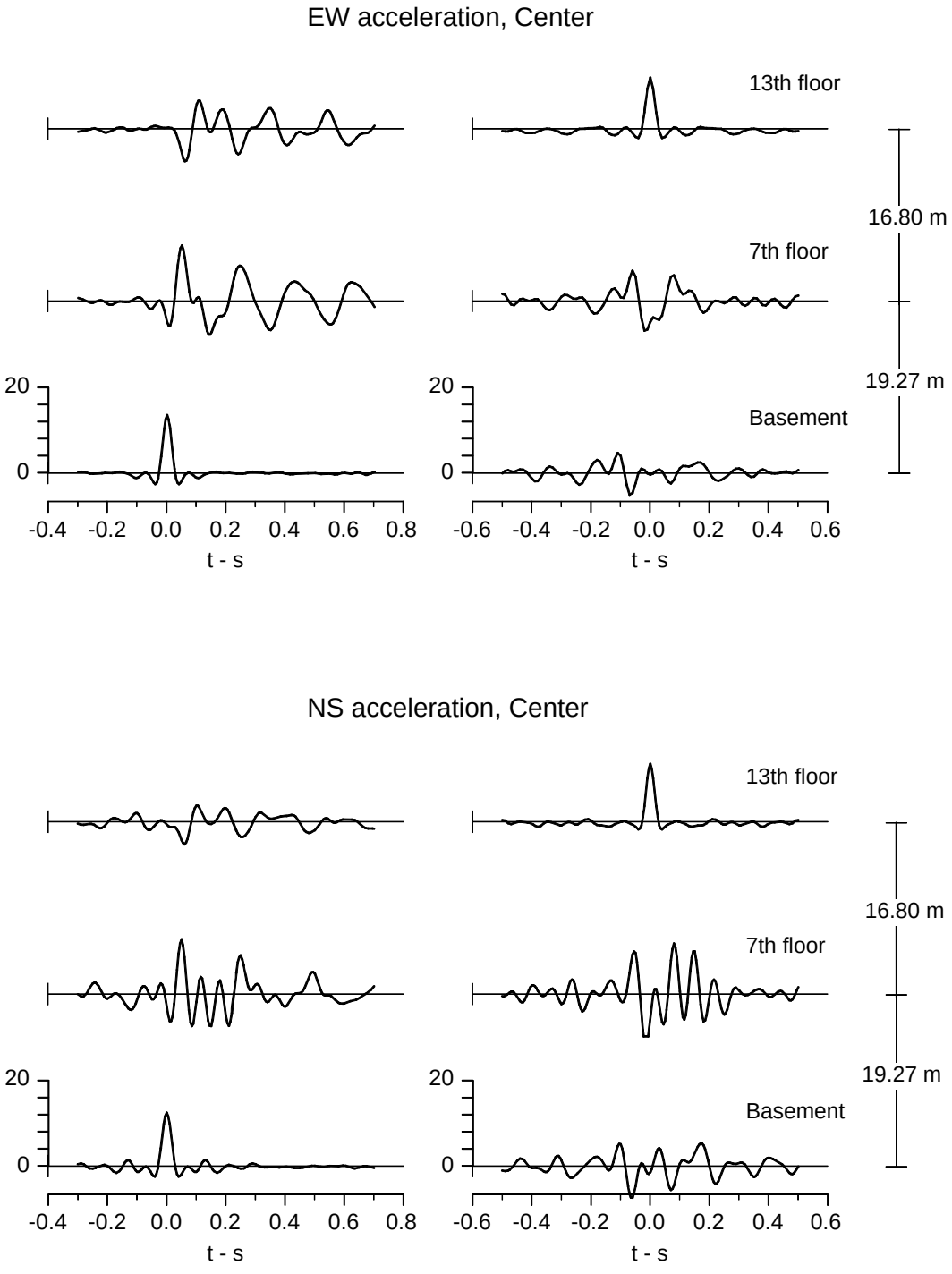

Fig. 4.1.6 Same as Fig. 4.1.1, but for earthquake No.6.

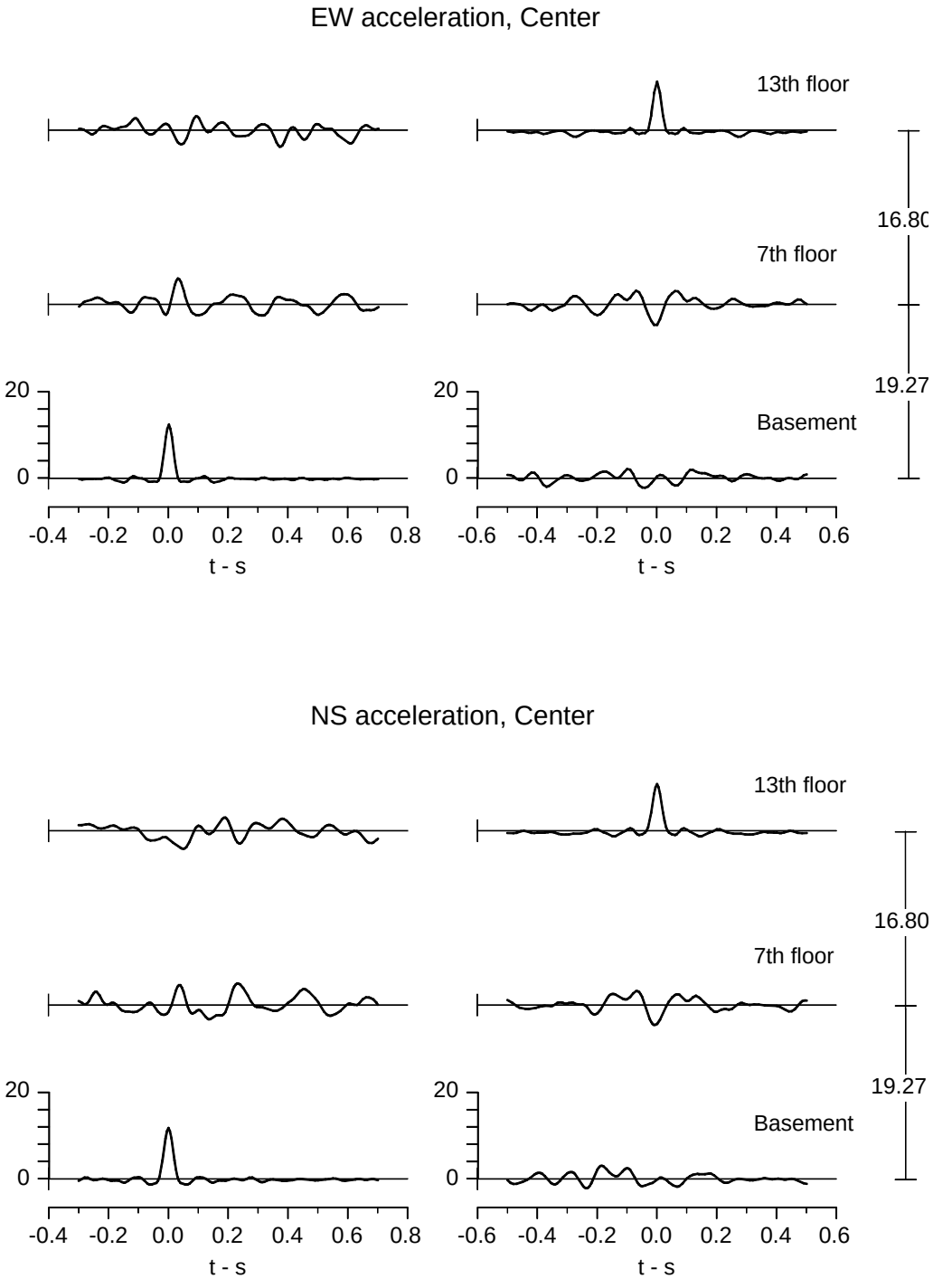

Fig. 4.1.7 Same as Fig. 4.1.1, but for earthquake No.7.

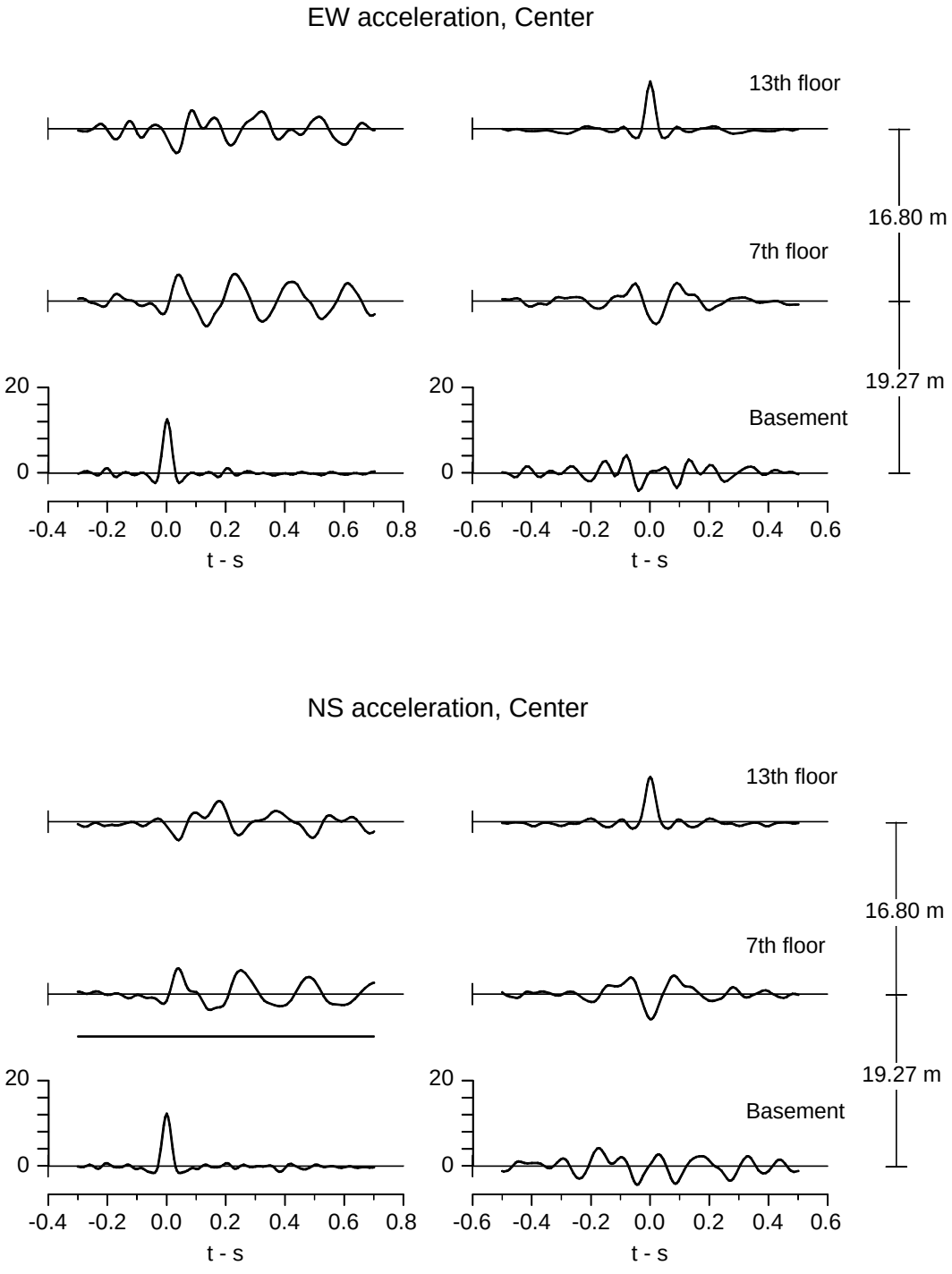

Fig. 4.1.8 Same as Fig. 4.1.1, but for earthquake No.8.

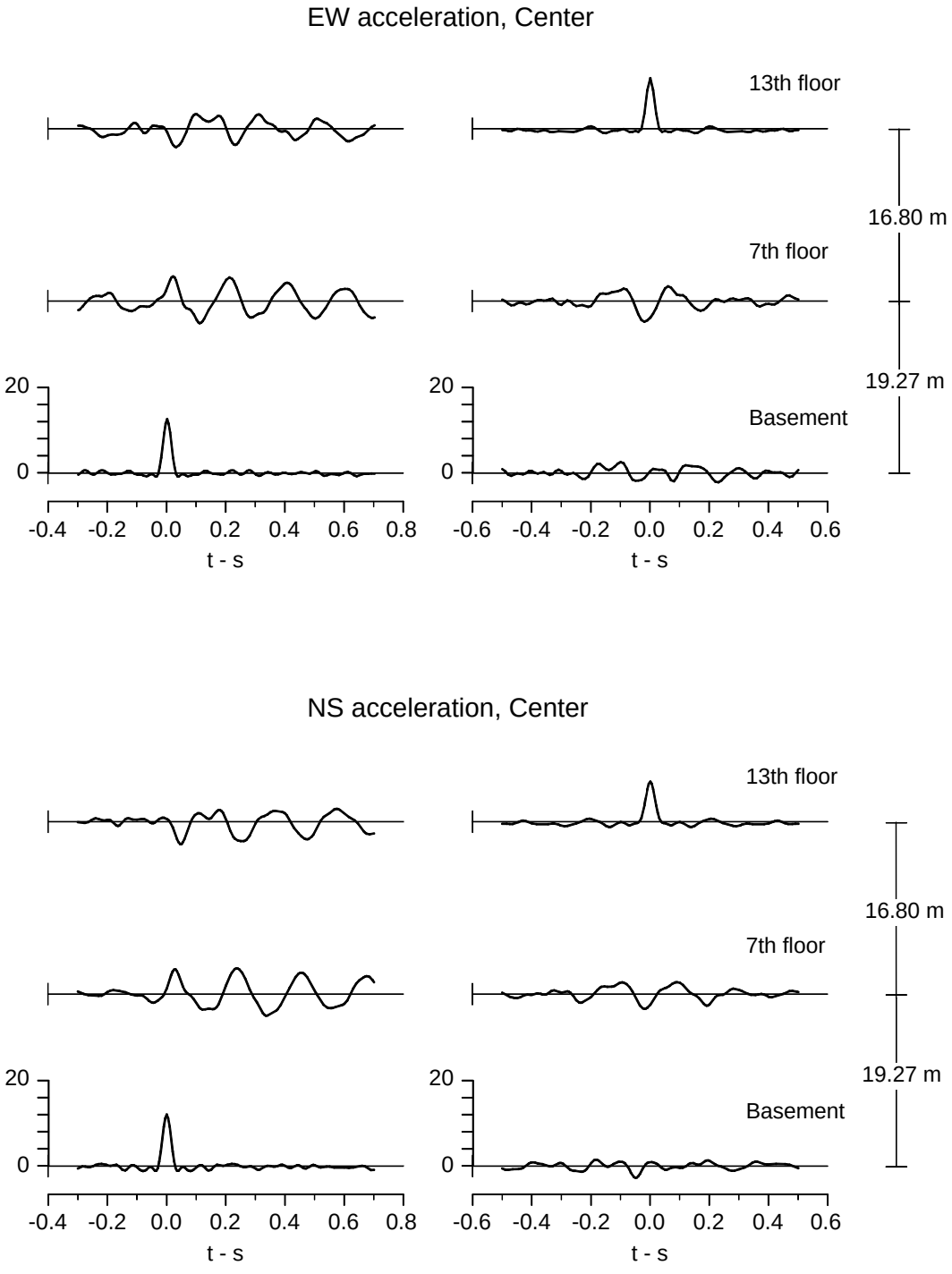

Fig. 4.1.9 Same as Fig. 4.1.1, but for earthquake No.9.

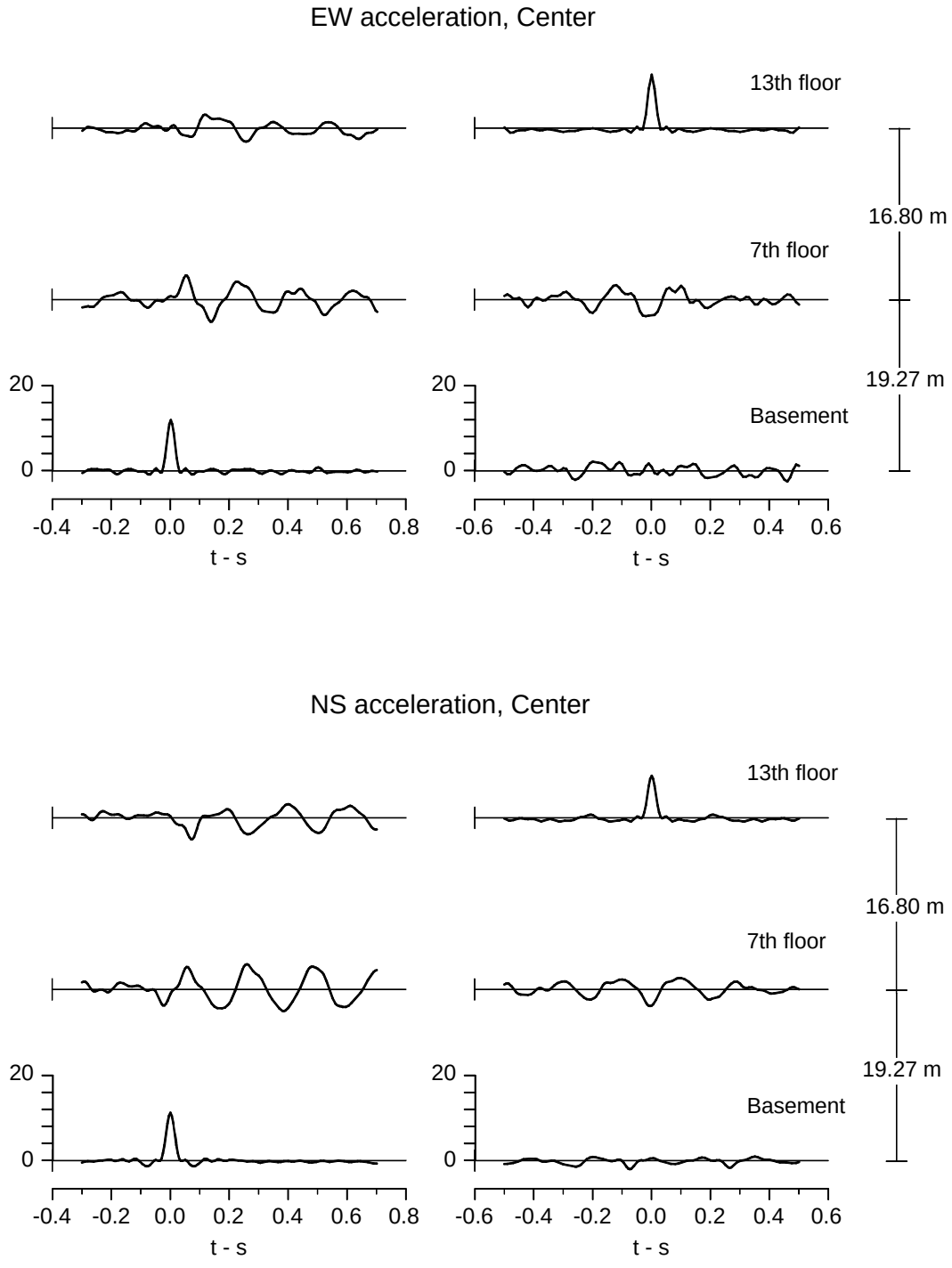

Fig. 4.1.10 Same as Fig. 4.1.1, but for earthquake No.10.

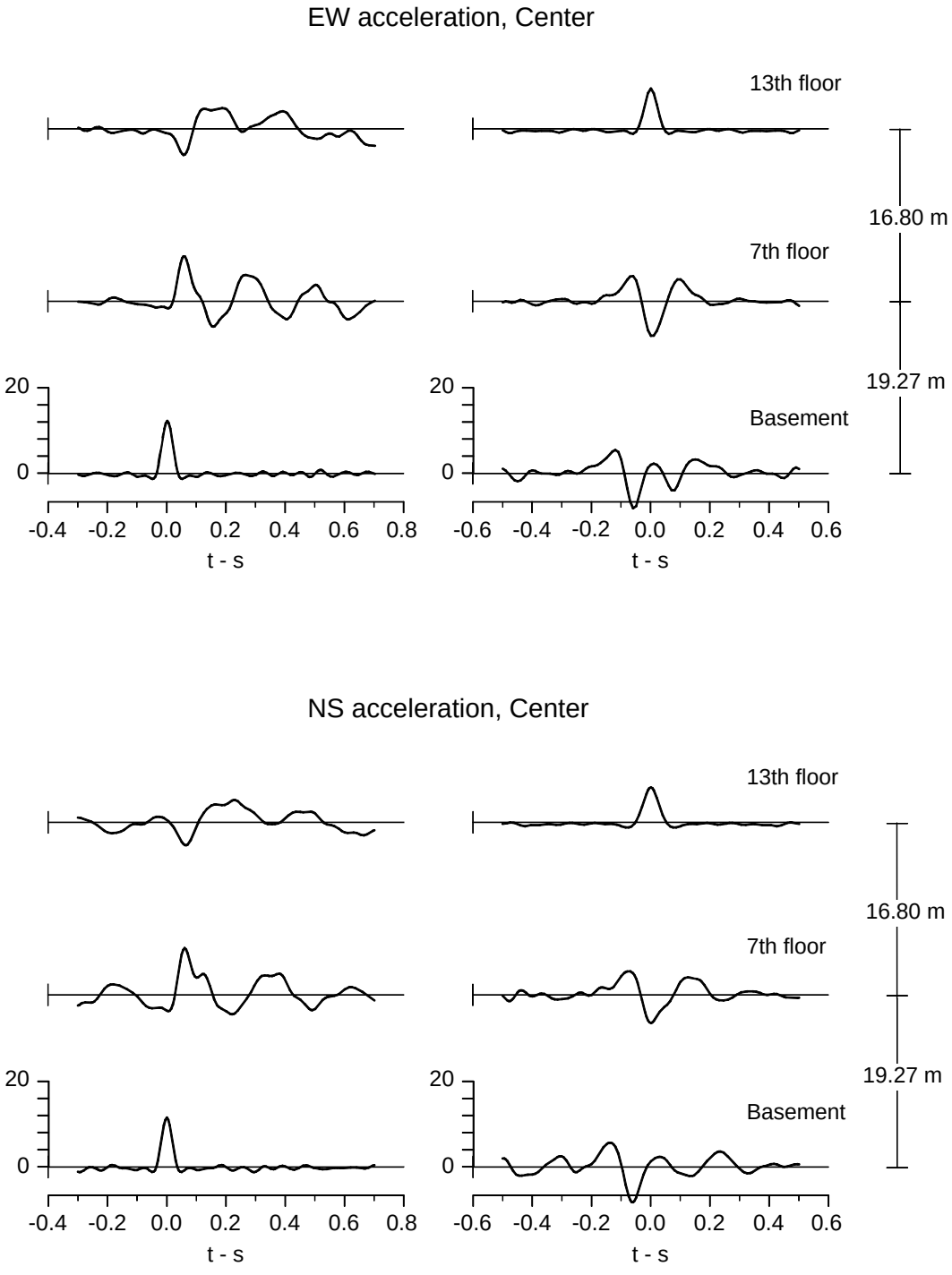

Fig. 4.1.11 Same as Fig. 4.1.1, but for earthquake No.11.

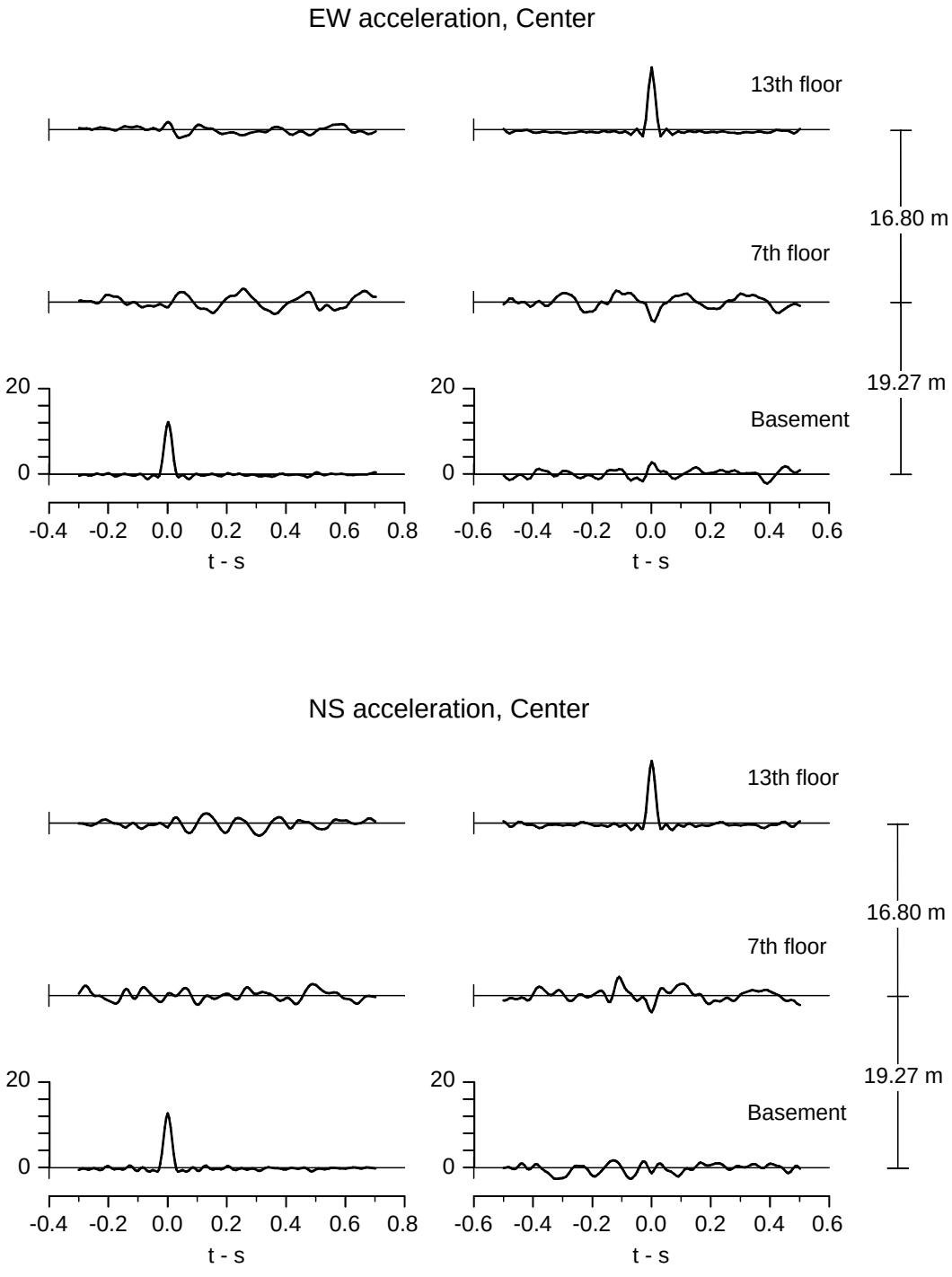

Fig. 4.1.12 Same as Fig. 4.1.1, but for earthquake No.12.

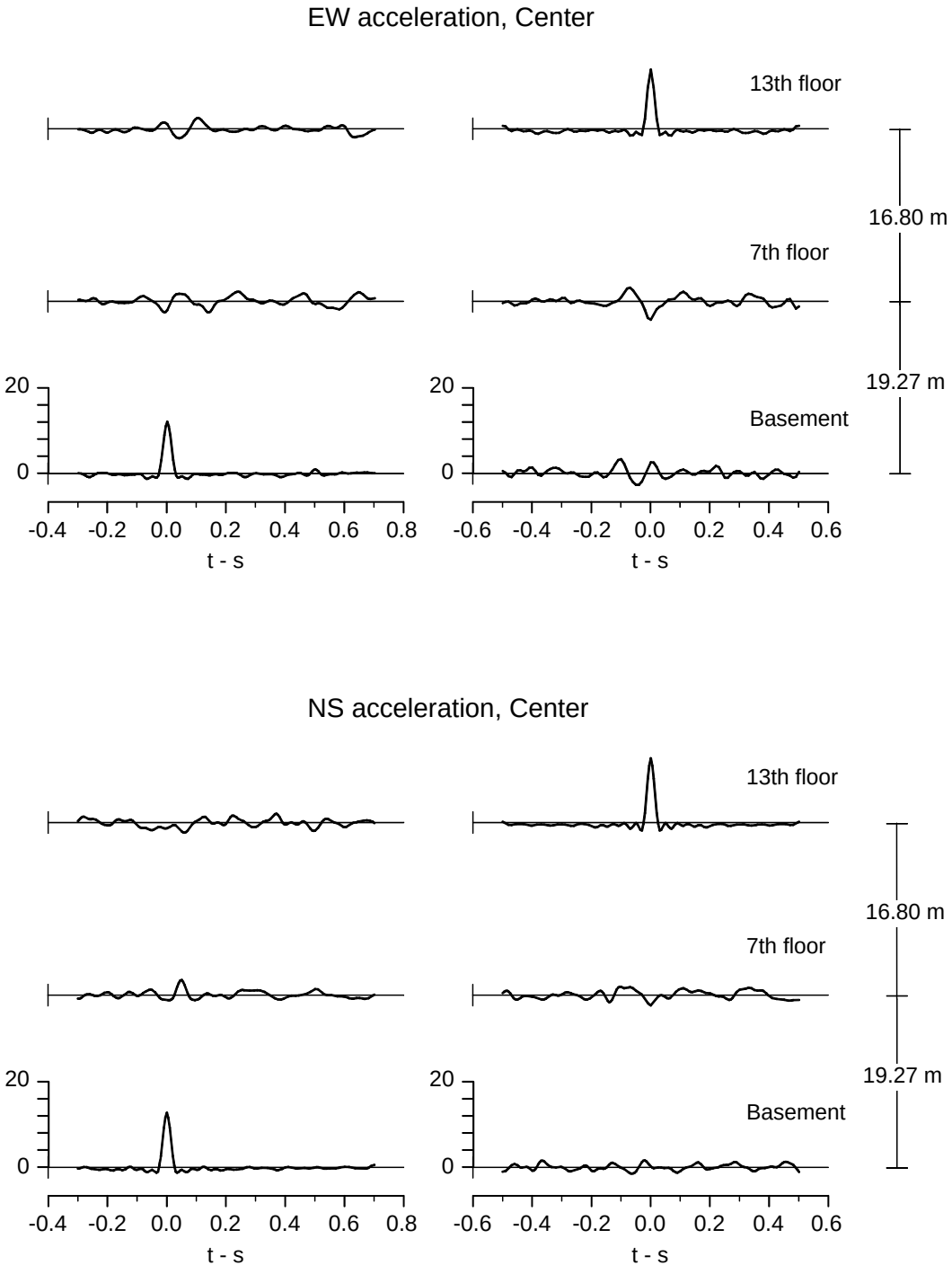

Fig. 4.1.13 Same as Fig. 4.1.1, but for earthquake No.13.

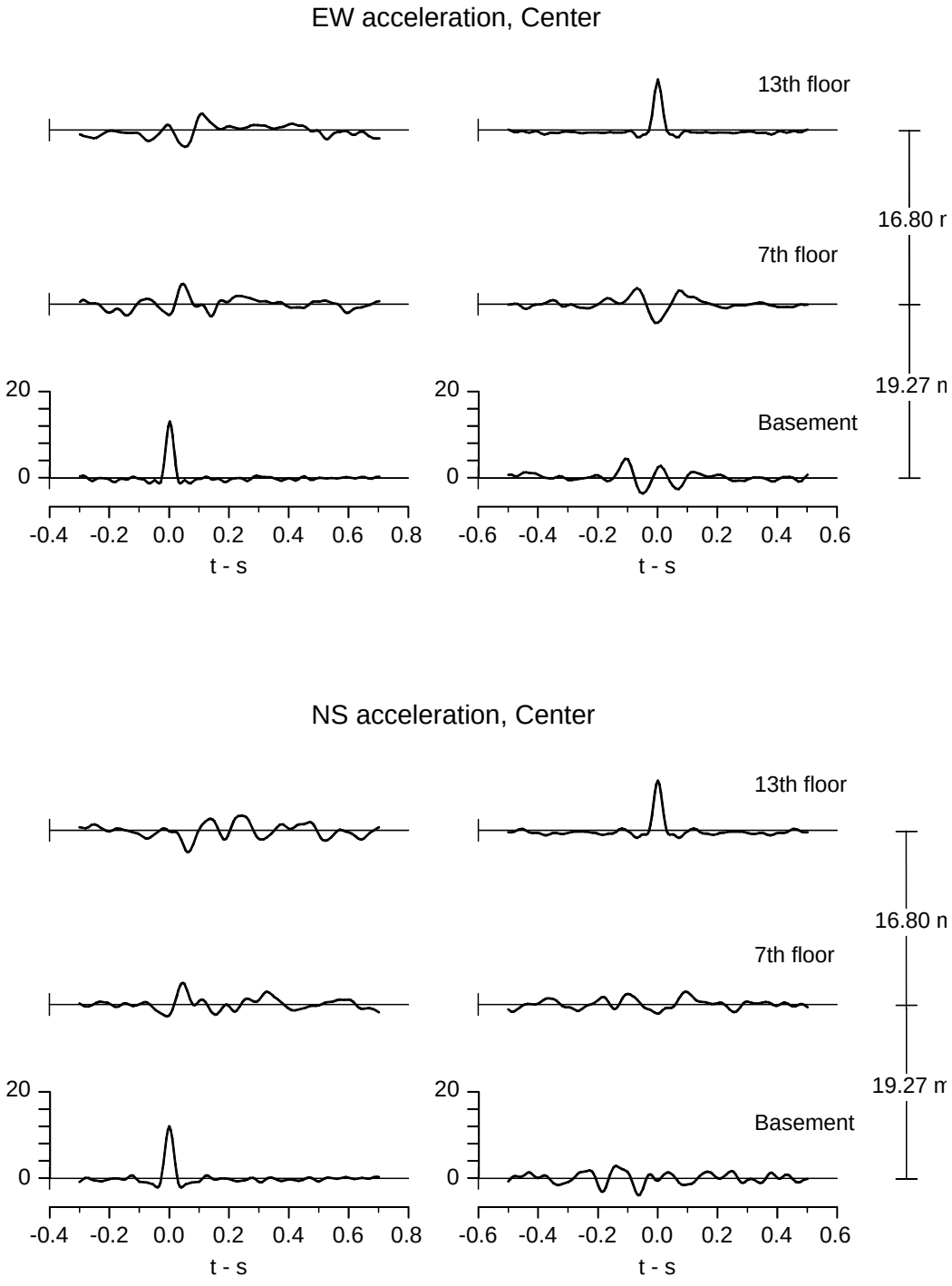

Fig. 4.1.14 Same as Fig. 4.1.1, but for earthquake No.14.

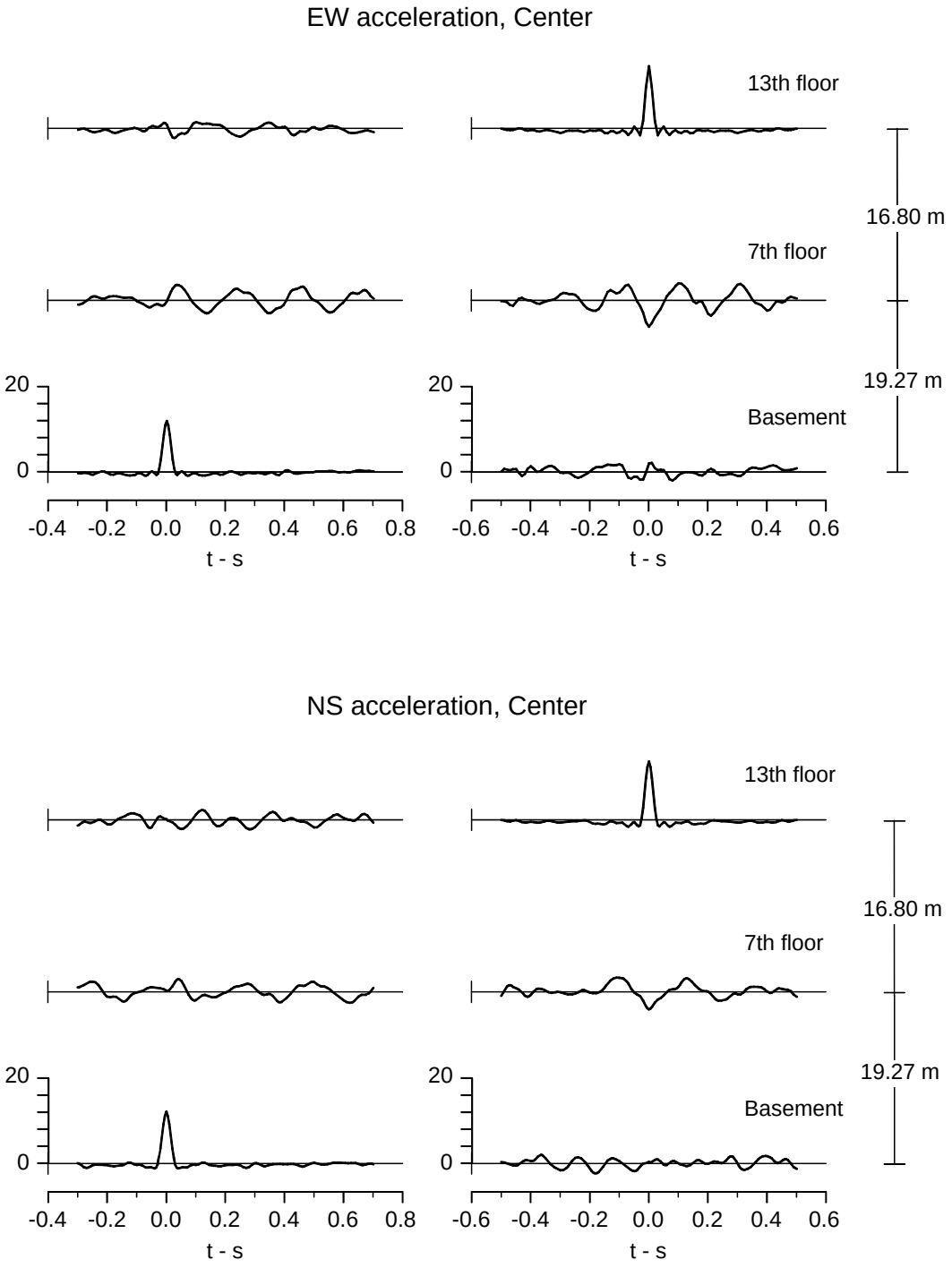

Fig. 4.1.15 Same as Fig. 4.1.1, but for t earthquake No.15.

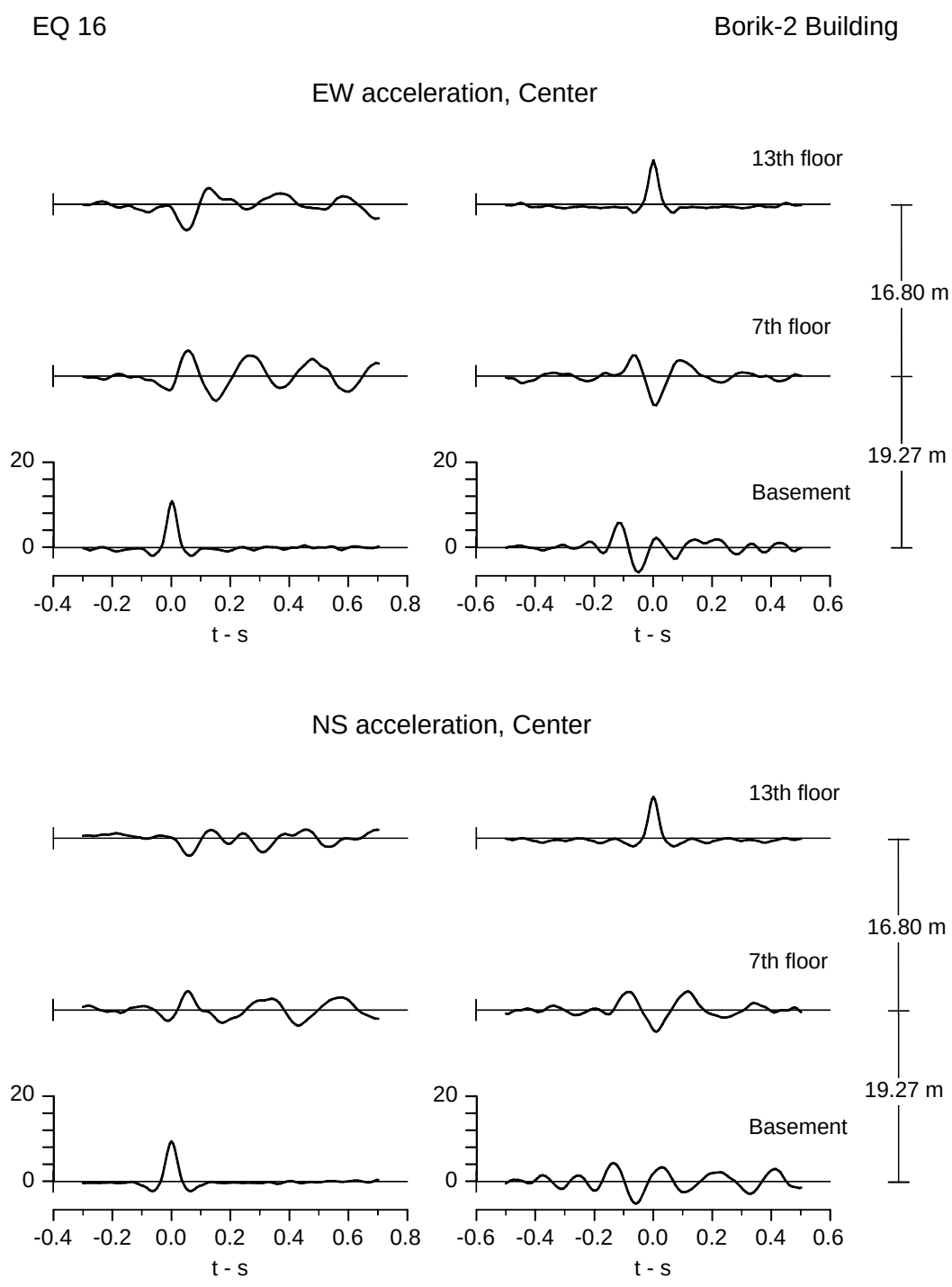

Fig. 4.1.16 Same as Fig. 4.1.1, but for earthquake No.16.

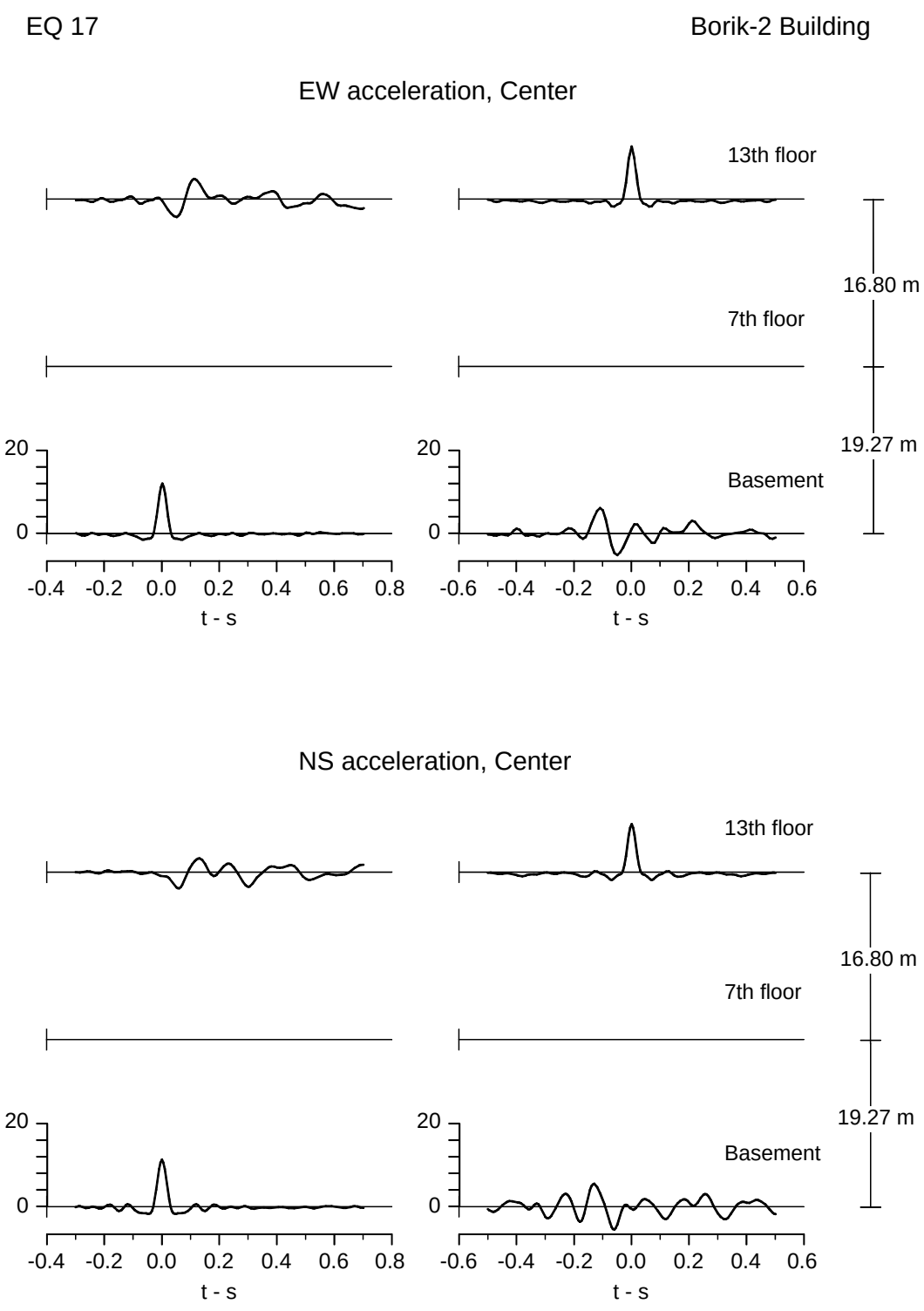

Fig. 4.1.17 Same as Fig. 4.1.1, but for earthquake No.17

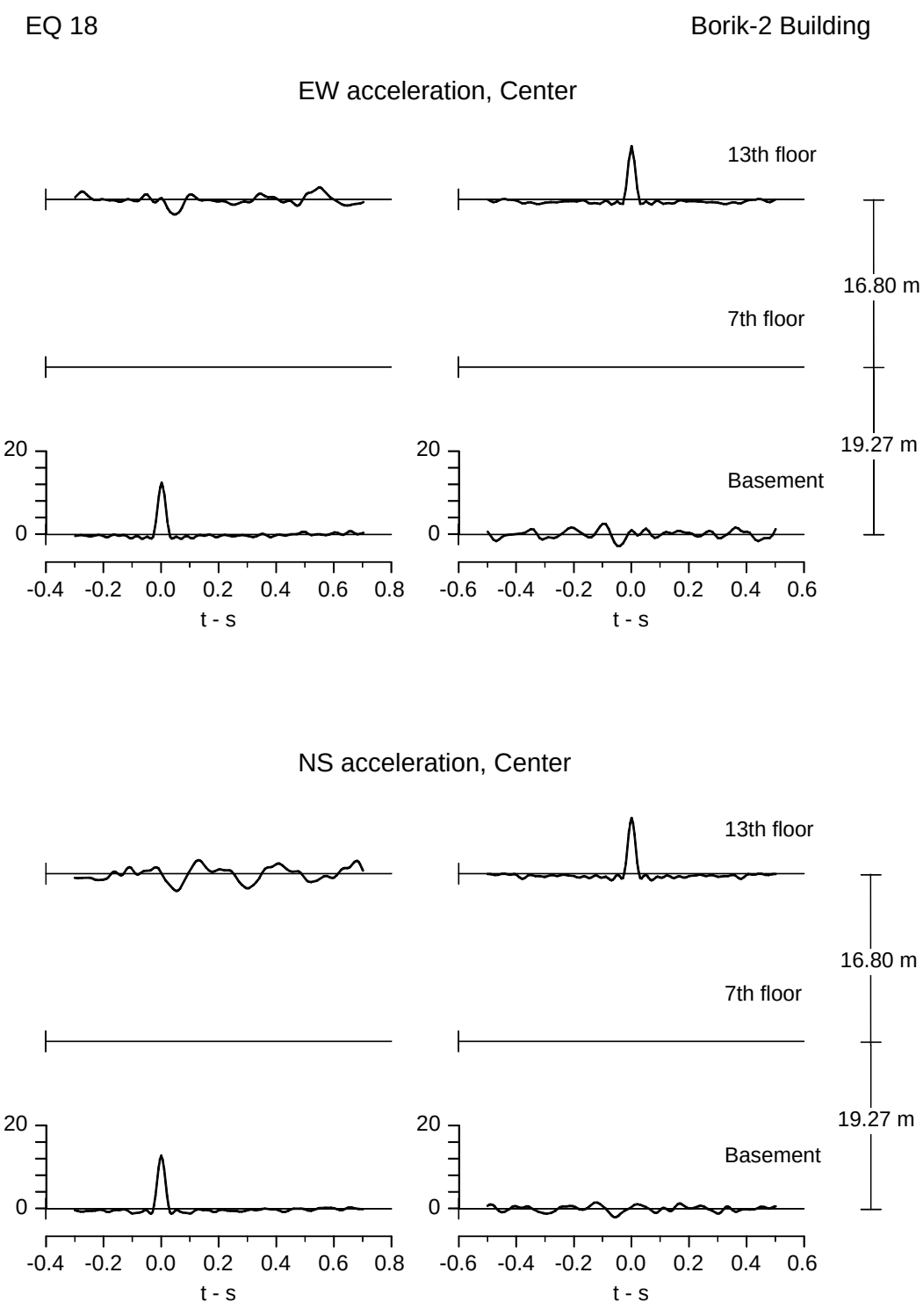

Fig. 4.1.18 Same as Fig. 4.1.1, but for earthquake No.18.

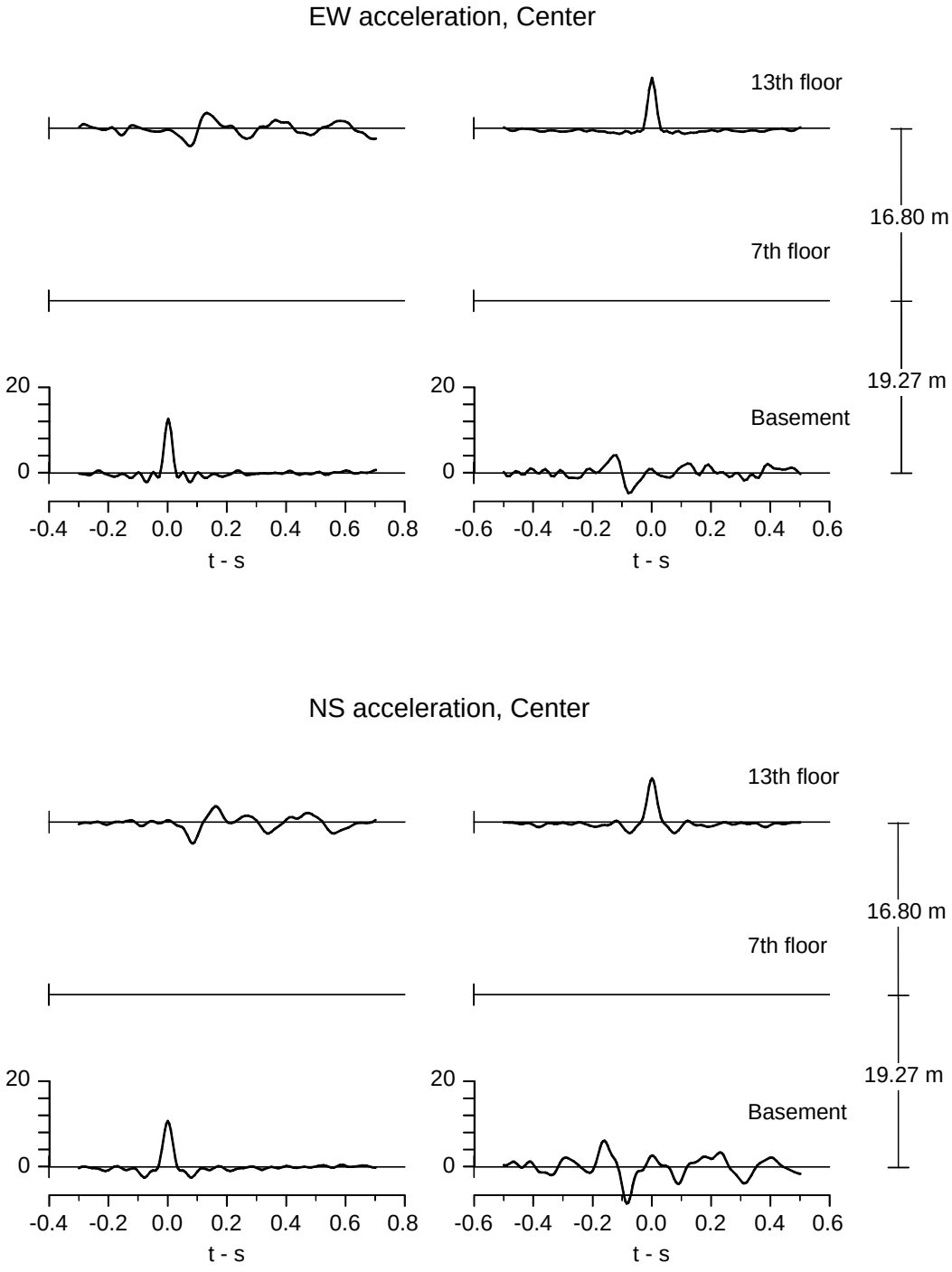

Fig. 4.1.19 Same as Fig. 4.1.1, but for earthquake No.19.

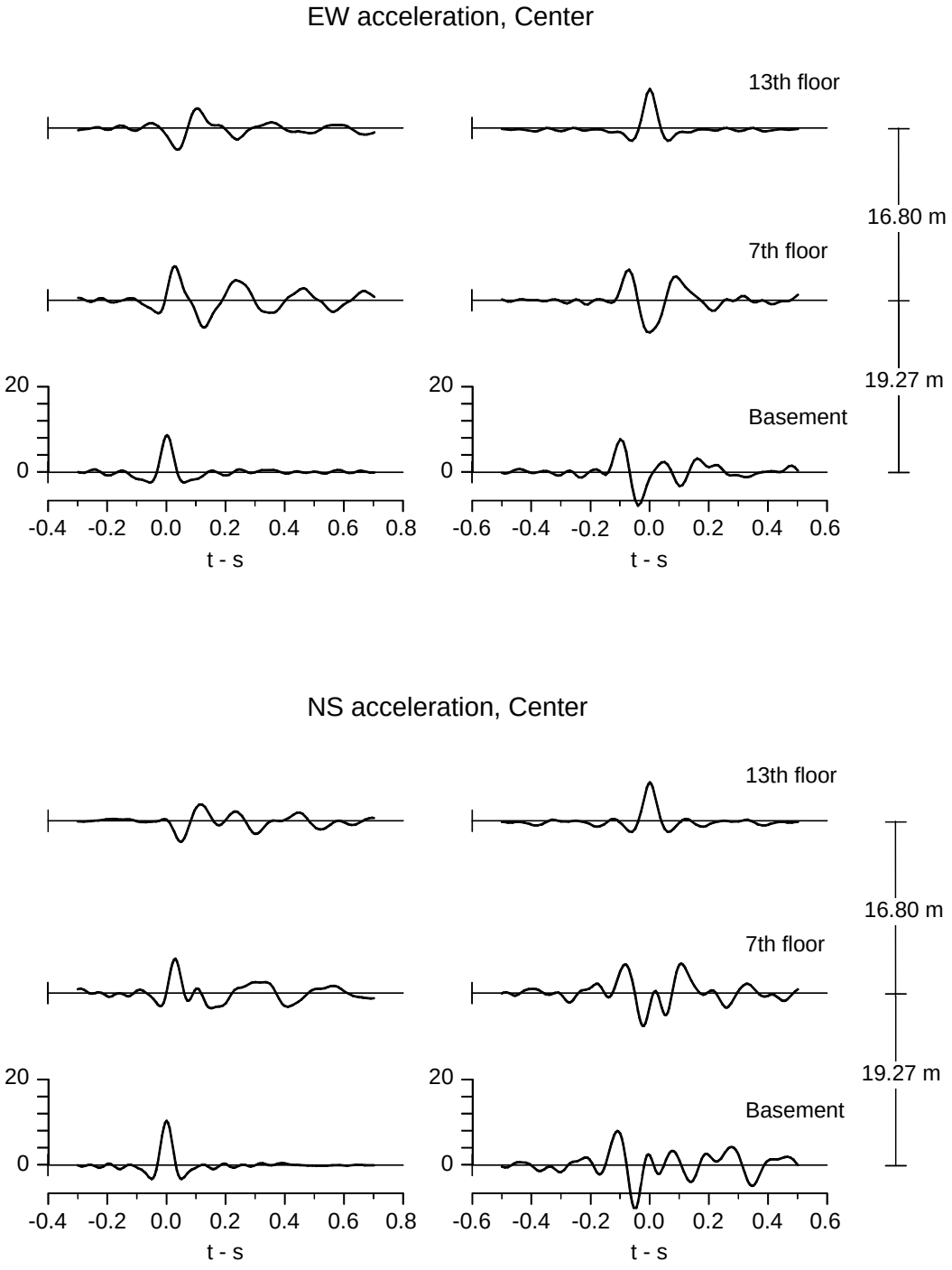

Fig. 4.1.20 Same as Fig. 4.1.1, but for earthquake No.20.

Table 4.1. Earthquake EQ 01: Measured Pulse Arrival Times, t_i, and Wave Travel Times, τ_i

		NS Motions	
	(1)	(2a)	(2b)
Input Impulse	Floor	t_i - s	τ_i - s
Roof, acausal pulse going down	13th floor	0.0	
			0.085
	7th floor	-0.085	
			0.030
	Basement	-0.115	
		EW Motions	
Roof, acausal pulse going down	(1)	(2a)	(2b)
	13th floor	0.0	
			0.080
	7th floor	-0.080	
			0.040
	Basement	-0.120	

Table 4.2. Earthquake EQ 02: Measured Pulse Arrival Times, t_i, and Wave Travel Times, τ_i

		NS Motions	
	(1)	(2a)	(2b)
Input Impulse	Floor	t_i - s	τ_i - s
Roof, acausal pulse going down	13th floor	0.0	
			0.080
	7th floor	-0.080	
			0.040
	Basement	-0.120	
		EW Motions	
Roof, acausal pulse going down	(1)	(2a)	(2b)
	13th floor	0.0	
			0.080
	7th floor	-0.080	
			0.030
	Basement	-0.110 (?)	

Table 4.3. Earthquake EQ 03: Measured Pulse Arrival Times, t_i, and Wave Travel Times, τ_i

		NS Motions	
	(1)	(2a)	(2b)
Input Impulse	Floor	t_i - s	τ_i - s
Roof, acausal pulse going down	13th floor	0.0	
			0.087
	7th floor	-0.087	
			0.038
	Basement	-0.125	
		EW Motions	
Roof, acausal pulse going down	(1)	(2a)	(2b)
	13th floor	0.00	
			0.073
	7th floor	-0.073	
			0.035
	Basement	-0.108	

Table 4.4. Earthquake EQ 04: Measured Pulse Arrival Times, t_i, and Wave Travel Times, τ_i

		NS Motions	
	(1)	(2a)	(2b)
Input Impulse	Floor	t_i - s	τ_i - s
Roof, acausal pulse going down	13th floor	0.0	
			0.075
	7th floor	-0.075	
			0.035
	Basement	-0.110	
		EW Motions	
Roof, acausal pulse going down	(1)	(2a)	(2b)
	13th floor	0.0	
			0.070
	7th floor	-0.070	
			0.042
	Basement	-0.112	

Table 4.5. Earthquake EQ 05: Measured Pulse Arrival Times, t_i, and Wave Travel Times, τ_i

		NS Motions	
	(1)	(2a)	(2b)
Input Impulse	Floor	t_i - s	τ_i - s
Roof, acausal pulse going down	13th floor	0.0	
			0.075
	7th floor	-0.075	
			0.050
	Basement	-0.125 (?)	
		EW Motions	
Roof, acausal pulse going down	(1)	(2a)	(2b)
	13th floor	0.0	
			0.075
	7th floor	-0.075	
			0.045
	Basement	-0.120	

Table 4.6. Earthquake EQ 06: Measured Pulse Arrival Times, t_i, and Wave Travel Times, τ_i

		NS Motions	
	(1)	(2a)	(2b)
Input Impulse	Floor	t_i - s	τ_i - s
Roof, acausal pulse going down	13th floor	0.0	
			0.070
	7th floor	-0.070	
			0.045
	Basement	-0.115	
		EW Motions	
Roof, acausal pulse going down	(1)	(2a)	(2b)
	13th floor	0.0	
			0.068
	7th floor	-0.068	
			0.044
	Basement	-0.112	

Table 4.7. Earthquake EQ 07: Measured Pulse Arrival Times, t_i, and Wave Travel Times, τ_i

		NS Motions	
	(1)	(2a)	(2b)
Input Impulse	Floor	t_i - s	τ_i - s
Roof, acausal pulse going down	13th floor	0.0	
			0.070
	7th floor	-0.070	
			0.045
	Basement	-0.115	
		EW Motions	
Roof, acausal pulse going down	(1)	(2a)	(2b)
	13th floor	0.0	
			0.070
	7th floor	-0.070	
			0.035
	Basement	-0.105	

Table 4.8. Earthquake EQ 08: Measured Pulse Arrival Times, t_i, and Wave Travel Times, τ_i

		NS Motions	
	(1)	(2a)	(2b)
Input Impulse	Floor	t_i - s	τ_i - s
Roof, acausal pulse going down	13th floor	0.0	
			0.072
	7th floor	-0.072	
			0.043
	Basement	-0.115	
		EW Motions	
Roof, acausal pulse going down	(1)	(2a)	(2b)
	13th floor	0.0	
			0.070
	7th floor	-0.070	
			0.037
	Basement	-0.107	

Table 4.9. Earthquake EQ 09: Measured Pulse Arrival Times, t_i, and Wave Travel Times, τ_i

		NS Motions	
	(1)	(2a)	(2b)
Input Impulse	Floor	t_i - s	τ_i - s
Roof, acausal pulse going down	13th floor	0.0	
			0.090
	7th floor	-0.090	
			0.025
	Basement	-0.115	
		EW Motions	
Roof, acausal pulse going down	(1)	(2a)	(2b)
	13th floor	0.0	
			0.073
	7th floor	-0.073	
			0.037
	Basement	-0.110	

Table 4.10. Earthquake EQ 10: Measured Pulse Arrival Times, t_i, and Wave Travel Times, τ_i

		NS Motions	
	(1)	(2a)	(2b)
Input Impulse	Floor	t_i - s	τ_i - s
Roof, acausal pulse going down	13th floor	0.0	
			(?)
	7th floor	(?)	
			(?)
	Basement	-0.117	
		EW Motions	
Roof, acausal pulse going down	(1)	(2a)	(2b)
	13th floor	0.0	
			0.070
	7th floor	-0.070	
			0.040
	Basement	-0.110	

Table 4.11. Earthquake EQ 11: Measured Pulse Arrival Times, t_i, and Wave Travel Times, τ_i

		NS Motions	
	(1)	(2a)	(2b)
Input Impulse	Floor	t_i - s	τ_i - s
Roof, acausal pulse going down	13th floor	0.0	
			0.075
	7th floor	-0.075	
			0.065
	Basement	-0.140	
		EW Motions	
Roof, acausal pulse going down	(1)	(2a)	(2b)
	13th floor	0.0	
			0.080
	7th floor	-0.080	
			0.050
	Basement	-0.130	

Table 4.12. Earthquake EQ 12: Measured Pulse Arrival Times, t_i, and Wave Travel Times, τ_i

		NS Motions	
	(1)	(2a)	(2b)
Input Impulse	Floor	t_i - s	τ_i - s
Roof, acausal pulse going down	13th floor	0.0	
			(?)
	7th floor	(?)	
			(?)
	Basement	-0.125	
		EW Motions	
Roof, acausal pulse going down	(1)	(2a)	(2b)
	13th floor	0.00	
			0.075
	7th floor	-0.075	
			0.030
	Basement	-0.105	

Table 4.13. Earthquake EQ 13: Measured Pulse Arrival Times, t_i, and Wave Travel Times, τ_i

		NS Motions	
	(1)	(2a)	(2b)
Input Impulse	Floor	t_i - s	τ_i - s
Roof, acausal pulse going down	13th floor	0.0	
			0.070
	7th floor	-0.070	
			0.040
	Basement	-0.110	
		EW Motions	
Roof, acausal pulse going down	(1)	(2a)	(2b)
	13th floor	0.0	
			0.070
	7th floor	-0.070	
			0.035
	Basement	-0.105	

Table 4.14. Earthquake EQ 14: Measured Pulse Arrival Times, t_i, and Wave Travel Times, τ_i

		NS Motions	
	(1)	(2a)	(2b)
Input Impulse	Floor	t_i - s	τ_i - s
Roof, acausal pulse going down	13th floor	0.0	
			(?)
	7th floor	(?)	
			(?)
	Basement	-0.115 (?)	
		EW Motions	
Roof, acausal pulse going down	(1)	(2a)	(2b)
	13th floor	0.0	
			0.070
	7th floor	-0.070	
			0.040
	Basement	-0.110	

Table 4.15. Earthquake EQ 15: Measured Pulse Arrival Times, t_i, and Wave Travel Times, τ_i

		NS Motions	
	(1)	(2a)	(2b)
Input Impulse	Floor	t_i - s	τ_i - s
Roof, acausal pulse going down	13th floor	0.0	
			(?)
	7th floor	(?)	
			(?)
	Basement	-0.120	
		EW Motions	
Roof, acausal pulse going down	(1)	(2a)	(2b)
	13th floor	0.0	
			0.070
	7th floor	-0.070	
			0.035
	Basement	-0.105	

Table 4.16. Earthquake EQ 16: Measured Pulse Arrival Times, t_i, and Wave Travel Times, τ_i

		NS Motions	
	(1)	(2a)	(2b)
Input Impulse	Floor	t_i - s	τ_i - s
Roof, acausal pulse going down	13th floor	0.0	
			0.080
	7th floor	-0.080	
			0.040
	Basement	-0.120	
		EW Motions	
Roof, acausal pulse going down	(1)	(2a)	(2b)
	13th floor	0.0	
			0.078
	7th floor	-0.078	
			0.037
	Basement	-0.115	

Table 4.17. Earthquake EQ 17: Measured Pulse Arrival Times, t_i, and Wave Travel Times, τ_i

		NS Motions	
	(1)	(2a)	(2b)
Input Impulse	Floor	t_i - s	τ_i - s
Roof, acausal pulse going down	13th floor	0.0	
			(?)
	7th floor	(?)	
			(?)
	Basement	-0.120	
		EW Motions	
Roof, acausal pulse going down	(1)	(2a)	(2b)
	13th floor	0.0	
			-
	7th floor	-	
			-
	Basement	-0.110	

Table 4.18. Earthquake EQ 18: Measured Pulse Arrival Times, t_i, and Wave Travel Times, τ_i

		NS Motions	
	(1)	(2a)	(2b)
Input Impulse	Floor	t_i - s	τ_i - s
Roof, acausal pulse going down	13th floor	0.0	
			(?)
	7th floor	(?)	
			(?)
	Basement	-0.115	
		EW Motions	
Roof, acausal pulse going down	(1)	(2a)	(2b)
	13th floor	0.0	
			-
	7th floor	-	
			-
	Basement	-0.110	

Table 4.19. Earthquake EQ 19: Measured Pulse Arrival Times, t_i, and Wave Travel Times, τ_i

		NS Motions	
	(1)	(2a)	(2b)
Input Impulse	Floor	t_i - s	τ_i - s
Roof, acausal pulse going down	13th floor	0.0	
			-
	7th floor	-	
			-
	Basement	(?)	
		EW Motions	
Roof, acausal pulse going down	(1)	(2a)	(2b)
	13th floor	0.0	
			-
	7th floor	-	
			-
	Basement	-0.115	

Table 4.20. Earthquake EQ 20: Measured Pulse Arrival Times, t_i, and Wave Travel Times, τ_i

		NS Motions	
	(1)	(2a)	(2b)
Input Impulse	Floor	t_i - s	τ_i - s
Roof, acausal pulse going down	13th floor	0.0	
			0.080
	7th floor	-0.080	
			0.032
	Basement	-0.112	
		EW Motions	
Roof, acausal pulse going down	(1)	(2a)	(2b)
	13th floor	0.0	
			0.077
	7th floor	-0.077	
			0.035
	Basement	-0.112	

Table 4.21. Borok-2 Building. Peak Displacements on 13th Floor (Relative to Sensor in the Basement), d_{max}, Fixed-Base Frequency, f_1, and System Frequency, f_{sys}, During 20 Earthquakes.

EQ Number	NS			EW		
	d_{max} cm	f_1 Hz	f_{sys} Hz	d_{max} cm	f_1 Hz	f_{sys} Hz
01	0.013	2.01	1.40	0.007	1.93	-
02	0.014	1.93	1.35	0.012	2.10	1.32
03	0.062	1.85	1.28	0.066	2.14	1.30
04	0.038	2.10	1.30	0.039	2.07	1.33
05	0.185	1.85	1.21	0.194	1.93	1.21
06	0.051	2.01	1.25	0.033	2.07	1.28
07	0.058	2.01	1.38	0.064	2.20	1.30
08	0.044	2.01	1.28	0.036	2.16	1.30
09	0.040	2.01	-	0.027	2.10	1.26
10	0.027	1.98	-	0.028	2.10	1.25
11	4.250	1.65	0.90	2.407	1.78	0.99
12	0.009	1.85	0.99	0.010	2.20	1.15
13	0.014	2.10	1.20	0.008	2.20	1.19
14	0.032	2.01	1.15	0.030	2.10	1.13
15	0.012	1.93	1.09	0.011	2.20	1.10
16	0.037	1.93	1.10	0.045	2.01	1.15
17	0.026	1.93	1.12	0.019	2.10	1.17
18	0.010	2.01	1.11	0.017	2.10	1.20
19	0.042	-	1.10	0.018	2.01	1.19
20	0.106	2.07	1.11	0.089	2.07	1.18

columns in these tables show: (1) the floor level, (2a) the arrival time t_i of the impulse at the particular floor, and (2b) the propagation time between the respective floors (sensors).

4.2 Reading of the Pulse Arrival Times and Fundamental Fixed-Base Frequency

An increase or decrease in the velocities v_i for interval i relative to some reference velocity v_{ref} of the waves in the building can be computed from the travel times as $\Delta v_i / v_{\text{ref}} = \left(v_i - v_{\text{ref}}\right) / v_{\text{ref}} = \tau_{\text{ref}} / \tau_i - 1$. The corresponding relative change of rigidity can be estimated based on the fact that, for an almost-uniform distribution of density along the height of the building, $\mu_i \sim v_i^2$, where μ_i is the shear modulus for segment i of the building. Then, $\Delta\mu_i / \mu_{\text{ref}} = \left(\tau_{\text{ref}} / \tau_i\right)^2 - 1$ (Todorovska and Trifunac 2006). In this report, we do not analyze the

changes in velocity or the relative changes in rigidity because all of the recorded motions are relatively small, including the largest event, EQ 11, so that all of the responses are essentially linear.

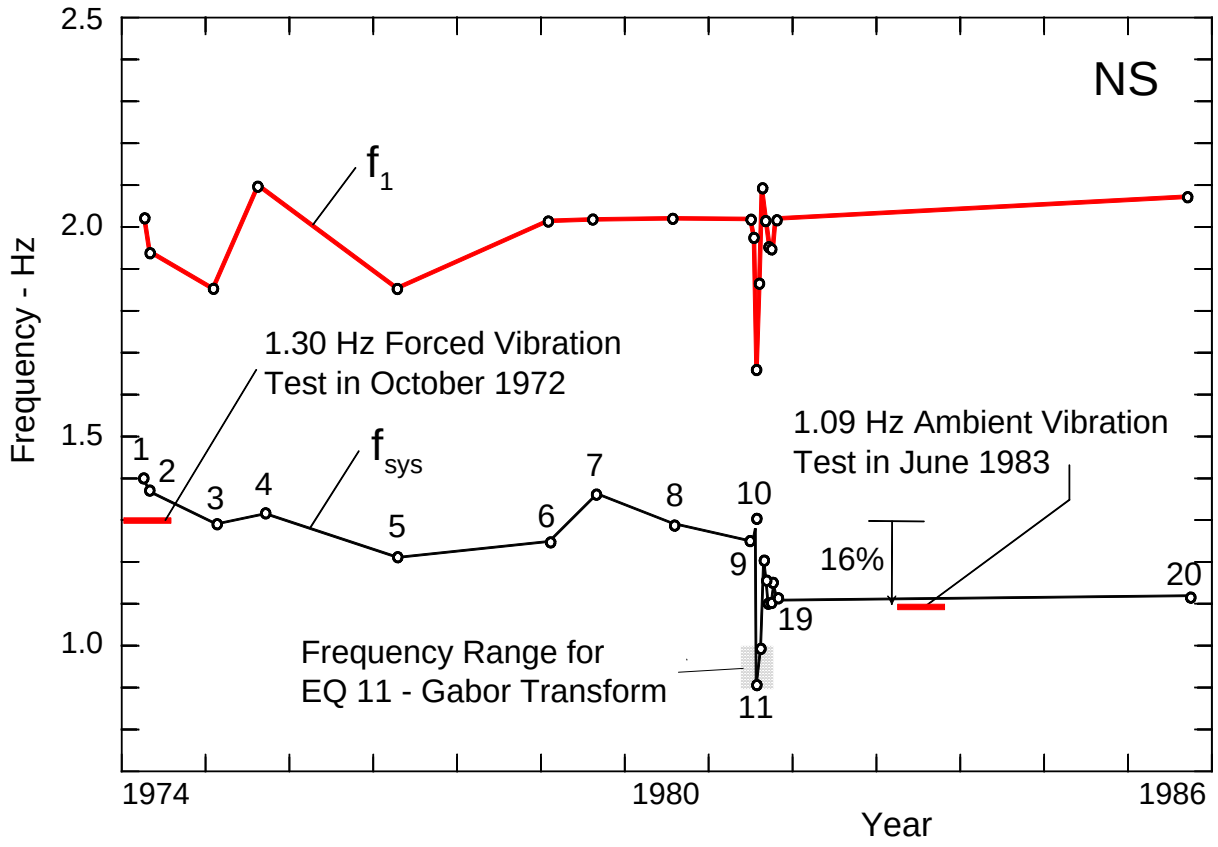

Fig.4.3.1a System frequency f_{sys} and fixed-base frequency f_1 during 20 earthquakes, for the NS response of the Borik-2 building, plotted versus time of the earthquake occurrence in years. Also shown are the results of the forced-vibration test in October 1972 and the ambient vibration test in June 1983. The values of f_1 and of f_{sys} are interconnected by straight lines to help visualize the trends.

Some basic response parameters of the recorded motions during the 20 earthquakes are summarized in Table 4.21. Column (1) identifies the events (see Table 2.4.1). The following two sets of three columns, for NS and for EW motions, show the corresponding peak relative displacements , $d_{\max}$, the estimates of fixed-base frequency, f_1, and the system frequency f_{sys}. We will discuss the changes of f_1 and f_{sys} in what follows.

4.3 Analysis of Changes of f_1 and Comparison with f_{sys} During Earthquakes

Figures 4.3.1 show plots of f_1 versus time during all 20 earthquakes. Figure 4.3.1a shows f_1 for

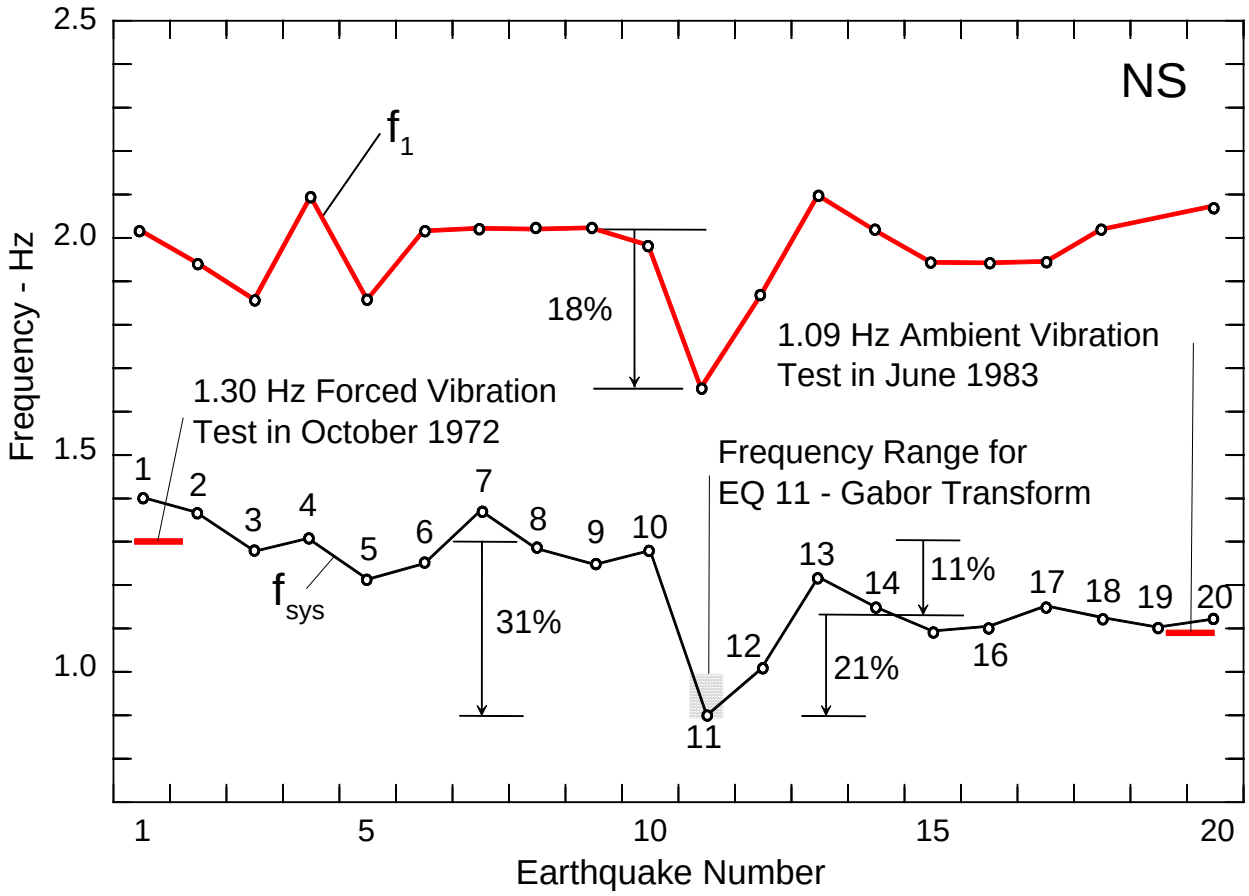

Fig.4.3.1b Same as Fig.4.3.1a, but plotted versus the earthquake event number.

the NS response of the Borik-2 building, plotted versus time of the earthquake occurrence in years. Figure 4.3.1b shows the same, but plotted versus the event number. Figures 4.3.2a and b show the corresponding results for the EW response. In addition, these figures show the soil-structure system frequency f_{sys} during the same earthquakes and also during the forced-vibration test in October 1972 and the ambient vibration test in June 1983. The values of f_1 and of f_{sys} are interconnected by straight lines to help emphasize the trends.

It can be seen from Figs. 4.3.1a and b that the drops of both f_1 and f_{sys} (about 18% and 31%, respectively, for NS motions, and about 16% and 22%, respectively, for EW motions) occur during the largest earthquake, EQ 11. It can also be seen that for all earthquakes $f_{sys} < f_1$, which

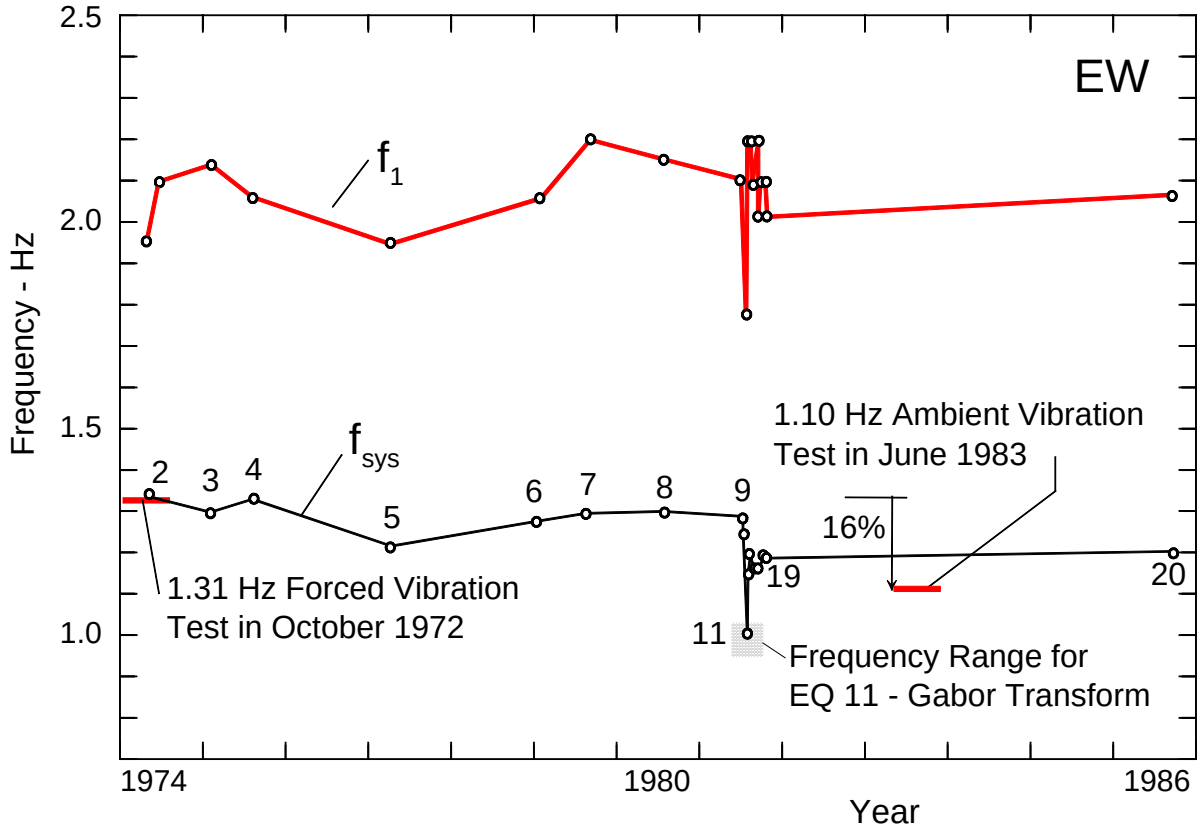

Fig.4.3.2a System frequency f_{sys} and fixed-base frequency f_1 during 20 earthquakes, for the EW response of the Borik-2 building, plotted versus time of the earthquake occurrence in years. Also shown are the results of the forced-vibration test in October 1972 and the ambient vibration test in June 1983. The values of f_1 and of f_{sys} are interconnected by straight lines to help visualize the trends.

is consistent with Eqn. (3.7). We note that *their ratio is approximately constant*, as is suggested by Eqn. (3.7), which corresponds to essentially *linear* soil-structure interaction. Clearly, the non-linearities during this history of response of the Borik-2 building, between 1974 and 1986, were relatively small, and no damage occurred in the building. These trends can be contrasted with our previous studies of the 7-story hotel, in Van Nuys and the Imperial County Services Building in El Centro, both in California (Todorovska and Trifunac 2006, 2007a,d), where we found that in the presence of nonlinear response the ratio between f_1 and f_{sys} changed significantly from one

earthquake to another, and relative to f_1. It can be seen from Figs. 4.3.1a and 4.3.2a that the estimates of f_{sys} from the forced-vibration test in 1972 and from ambient vibration test in 1983

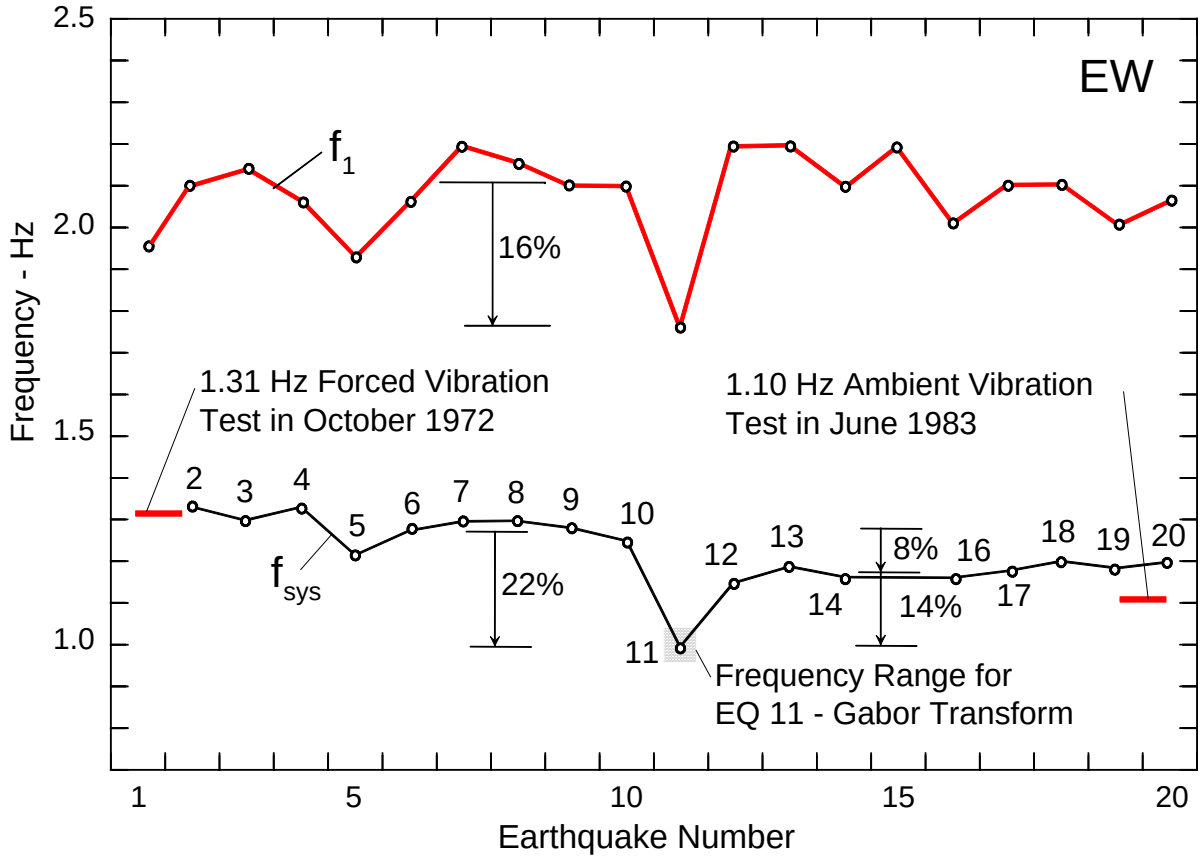

Fig.4.3.2b Same as Fig.4.3.2a, but plotted versus the earthquake event number.

are all consistent with our analysis of the response during 19 small earthquakes. Our estimates of f_{sys} and the ambient tests in 1983 both suggest a slight drop in the system frequency, in the range from 15 to 20%.

In Figs. 4.3.3a and b, we plot $f_{sys}^2 d_{max}$ versus d_{max}. This is equivalent to plotting the normalized peak force acting on the equivalent system representing the Borik-2 building versus the corresponding displacement. Fig. 4.3.3a shows the the slope (tangent) of the straight line through the data points of the 19 small events equals 1.35 and that a drop of this slope to about 0.8 occurred for event 11. This corresponds to the reduction of the system modulus by a factor of about 0.59, which would imply a drop in the corresponding system frequency of about 23%. This

estimate agrees favorably with the drop of 31% shown in Fig. 4.3.1b, during event 11. Fig. 4.3.3b shows the corresponding results for the EW response, with a drop of the slope from 1.42

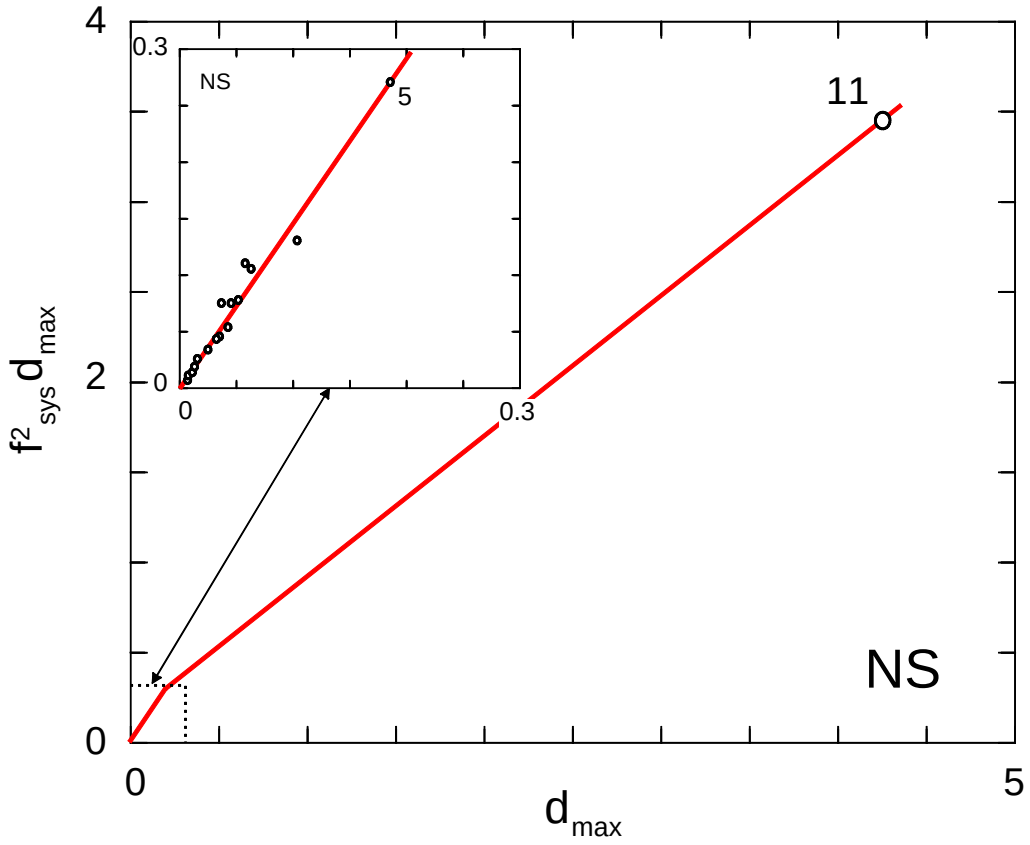

Fig. 4.3.3a Plot of $f_{sys}^2 d_{\max}$ (~ peak force per-unit mass) versus $d_{\max}$ (peak relative displacement) for NS response of the Borik-2 building.

for the 19 small events to about 1 for event 11, or a reduction in modulus by a factor of about 0.70. This would imply a drop in the corresponding system frequency of about 16%, which can be compared with the drop of 22% shown in Fig. 4.3.2b.

4.4 Analysis of f_1 and of f_{sys} During Earthquake EQ 11

Figures. 4.4.1a and b show the time-dependent changes in the fundamental system frequency f_{sys} during the largest earthquake event in the data studied here, EQ 11. The top right segment in these figures shows the recorded acceleration in the basement and computed relative displacement of 13th floor. The plot below shows the signal amplitude and the Gabor transform

skeleton. At the bottom right, these figures show the estimated changes of f_{sys} versus time. The left-hand drawing shows the wandering of Gabor transform amplitudes versus frequency. In Fig. 4.4.1a, we show six points (open circles), and in Fig. 4.4.1b we show eight points chosen to

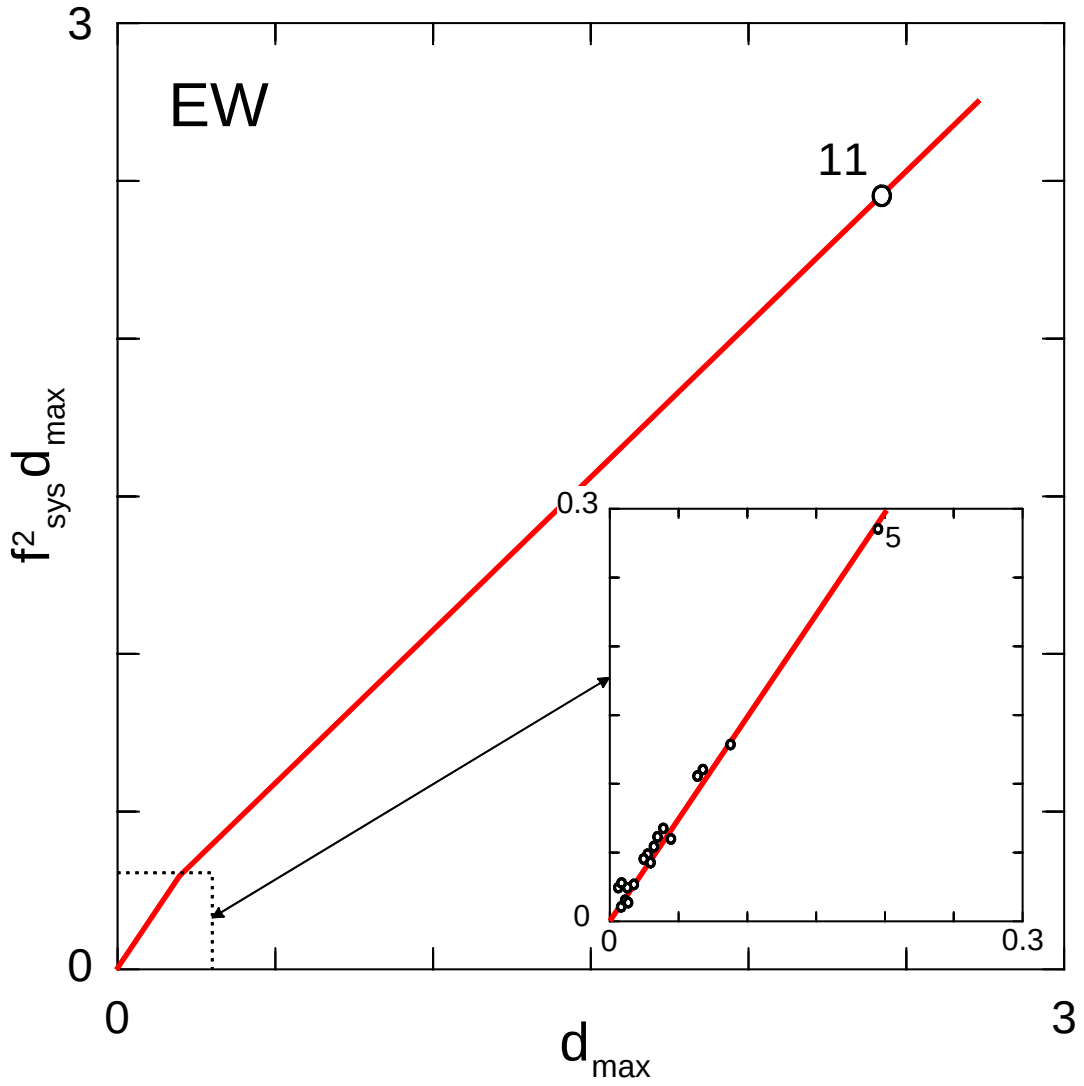

Fig. 4.3.3b Same as Fig. 4.3.3a, but for EW response.

suitably connect the amplitude-time-frequency relationship of the results. Because the recorded signals become large about 2–3 s after the instrument trigger, our analysis does not show the decrease in f_{sys} at the beginning. A slight recovery of f_{sys} can be seen for shaking after about 20 s. Both bottom graphs show essentially constant values of f_{sys} during the first 20 s of strong shaking. Minor local lengthening of system period can be noticed in Fig.4.4.1b during a time interval with low relative response (points 2-3-4), which is consistent with softer system behavior for vibrations within the open gaps.

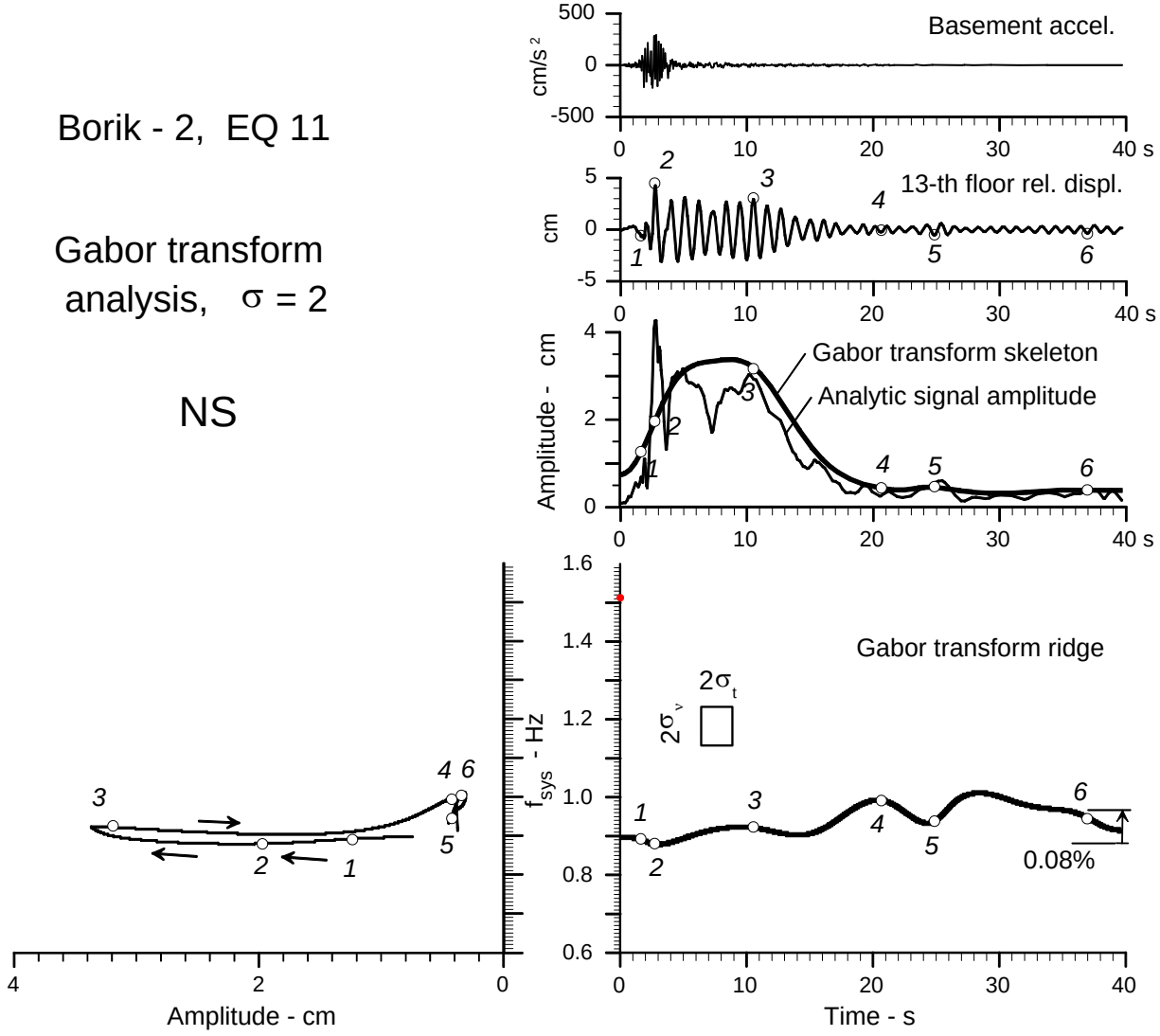

Fig. 4.4.1a Time-frequency analysis for the NS response of the Borik-2 building: Basement acceleration and relative response at the 13th floor (top right), amplitude envelope, and Fourier spectrum of relative response (solid line) and of ground acceleration (light line) (right middle); system frequency versus time (bottom right), and amplitude of relative response versus frequency (bottom left). A square labeled $2\sigma_v$ by $2\sigma_t$ (Todorovska and Trifunac 2007b) describes the frequency-time resolution for these results.

Figs. 4.4.2a,b show a different and more elementary method for estimating the time- and amplitude-dependent changes in the response during event 11. In these figures, we plot peak

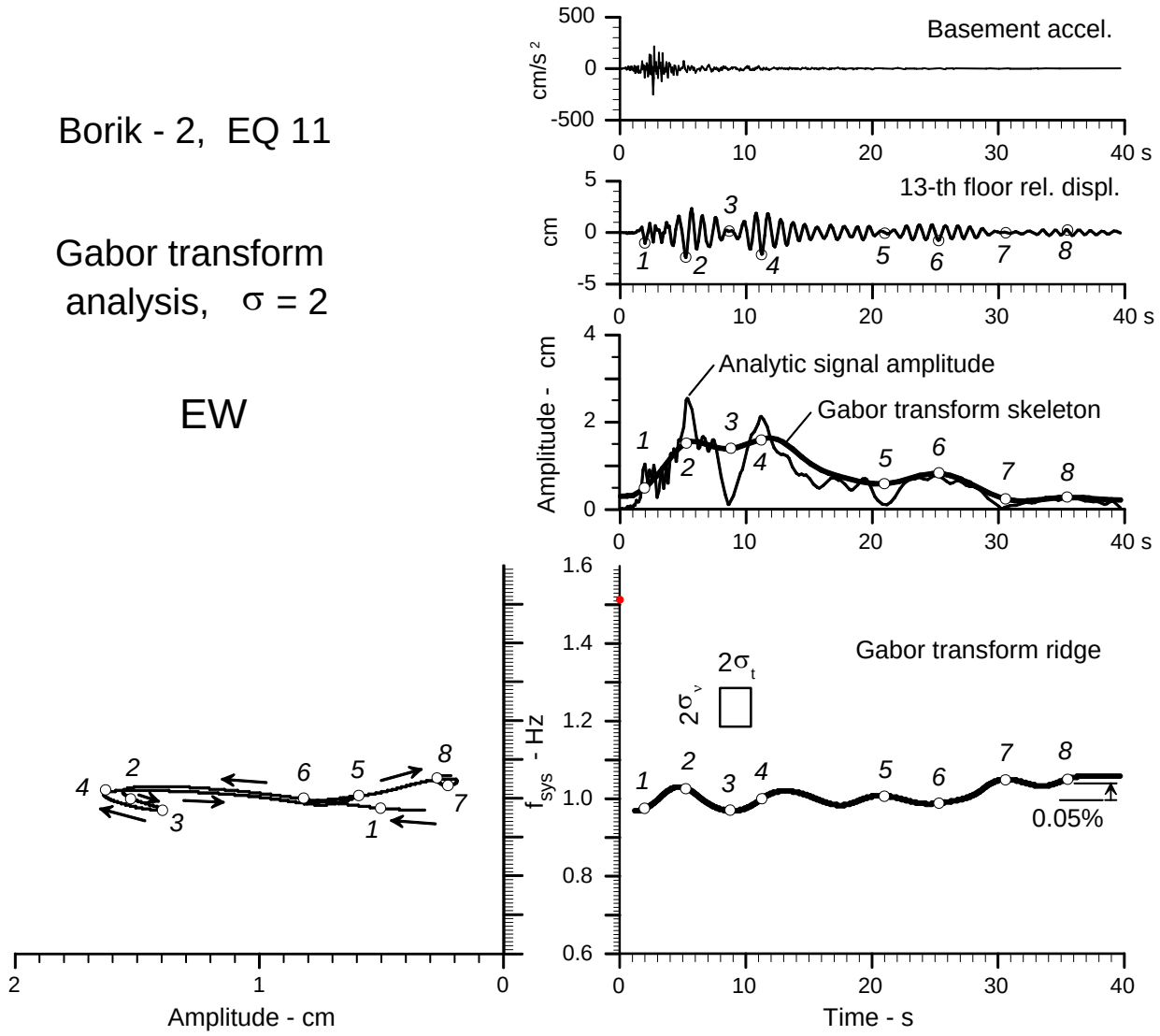

Fig. 4.4.1b Same as Fig. 4.4.1a, but for the EW response.

amplitudes versus instantaneous estimates of the system frequency, which is evaluated by measuring the frequency of the equivalent sinusoidal pulse, from the duration of the two consecutive zero crossings. For this to work, it is necessary to consider only those peaks that are sufficiently "close" to a sinusoid. The peaks that we selected are shown by open circles in the top parts of Figs. 4.4.2a,b and are identified by numbers. The bottom segments in these figures show peak amplitude versus frequency of the relative displacement on the 13th floor. The behavior of

the changes of the peak amplitudes versus instantaneous frequency we find in these plots is typical of many other such analyses (e.g., Trifunac et al. 2001). In the beginning, and again

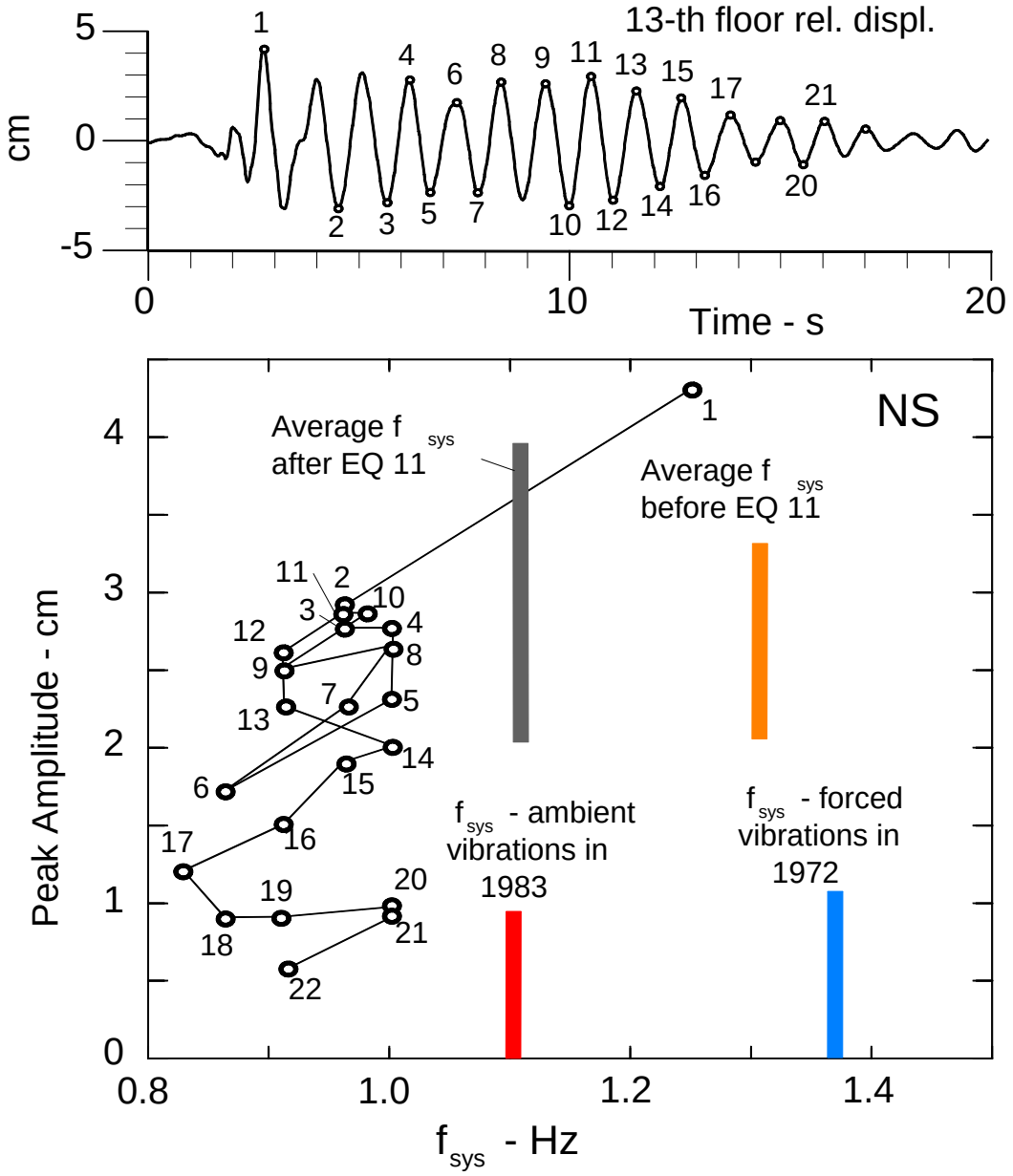

Fig. 4.4.2a Relative NS displacement of 13th floor during EQ 11(top), peak amplitudes of relative response versus instantaneous estimates of system frequency, and averages of system frequency during (a) forced-vibration test in 1972, (b) 8 earthquakes preceding EQ 11, (c) 8 earthquakes following EQ 11, and (d) ambient vibration tests in 1983.

during arrivals of large strong-motion pulses, with onset of sudden ground motion, the system briefly becomes "stiffer" as it engages all of its constituents (all or most of the model "gaps"

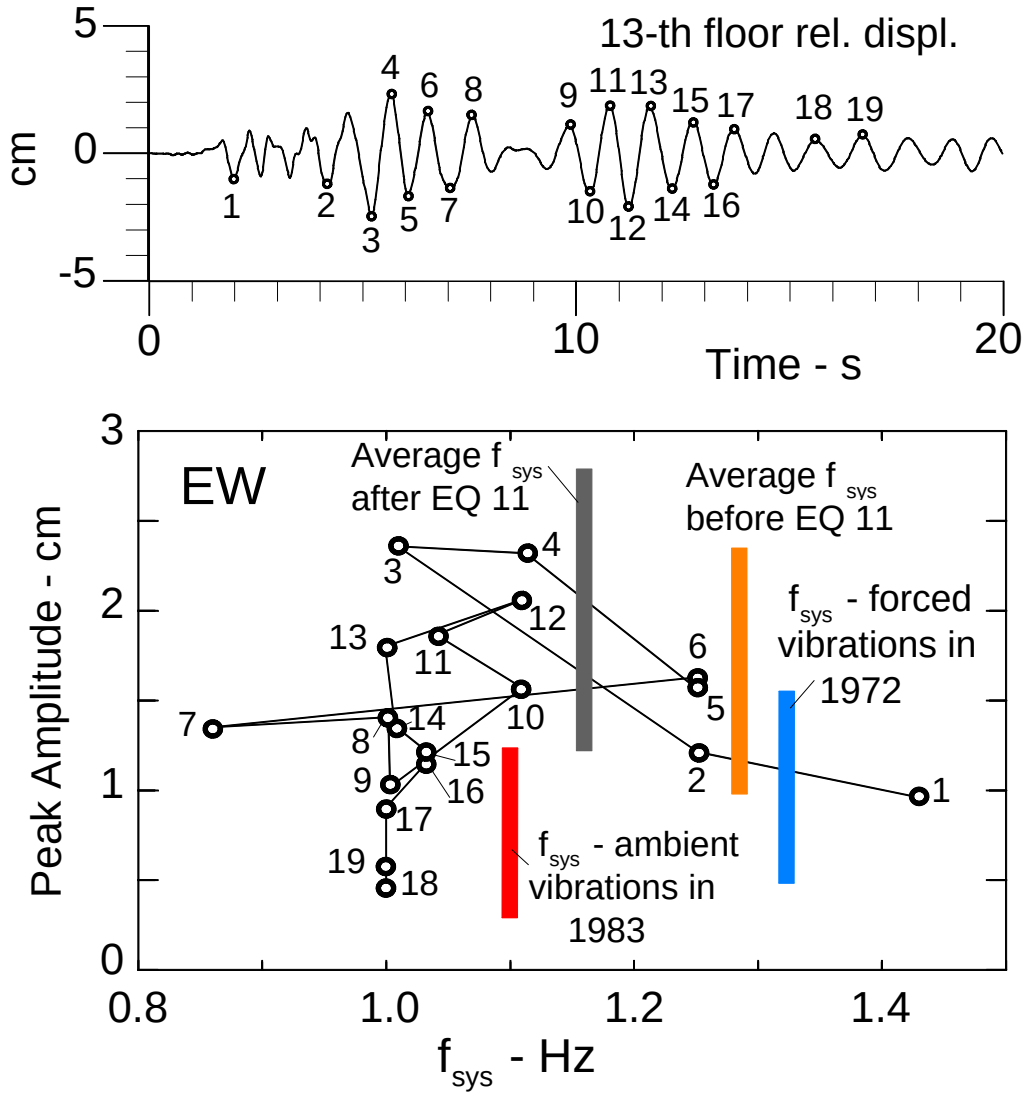

Fig. 4.4.2b Same as Fig. 4.4.2a, but for the EW response.

become closed) in a pseudo linear fashion of elastic-nonlinear or stiffening equivalent spring (e.g., point 1 for NS response and points 1 and 3-4-5 for EW response). During the "quiescent" intervals of strong motion, as the relative response begins to decay, the system progressively opens some or all of its "gaps" and with decaying amplitudes becomes "softer." This can be seen, for example, in Figs. 4.4.2a,b for the sequences of peaks 4-5-6 and 14-15-16-17 for NS

response, and for peaks 5-6-7 and 15-16-17 for EW response. Overall behavior of the amplitude-frequency dependence of all the peaks in these figures is in excellent agreement with the

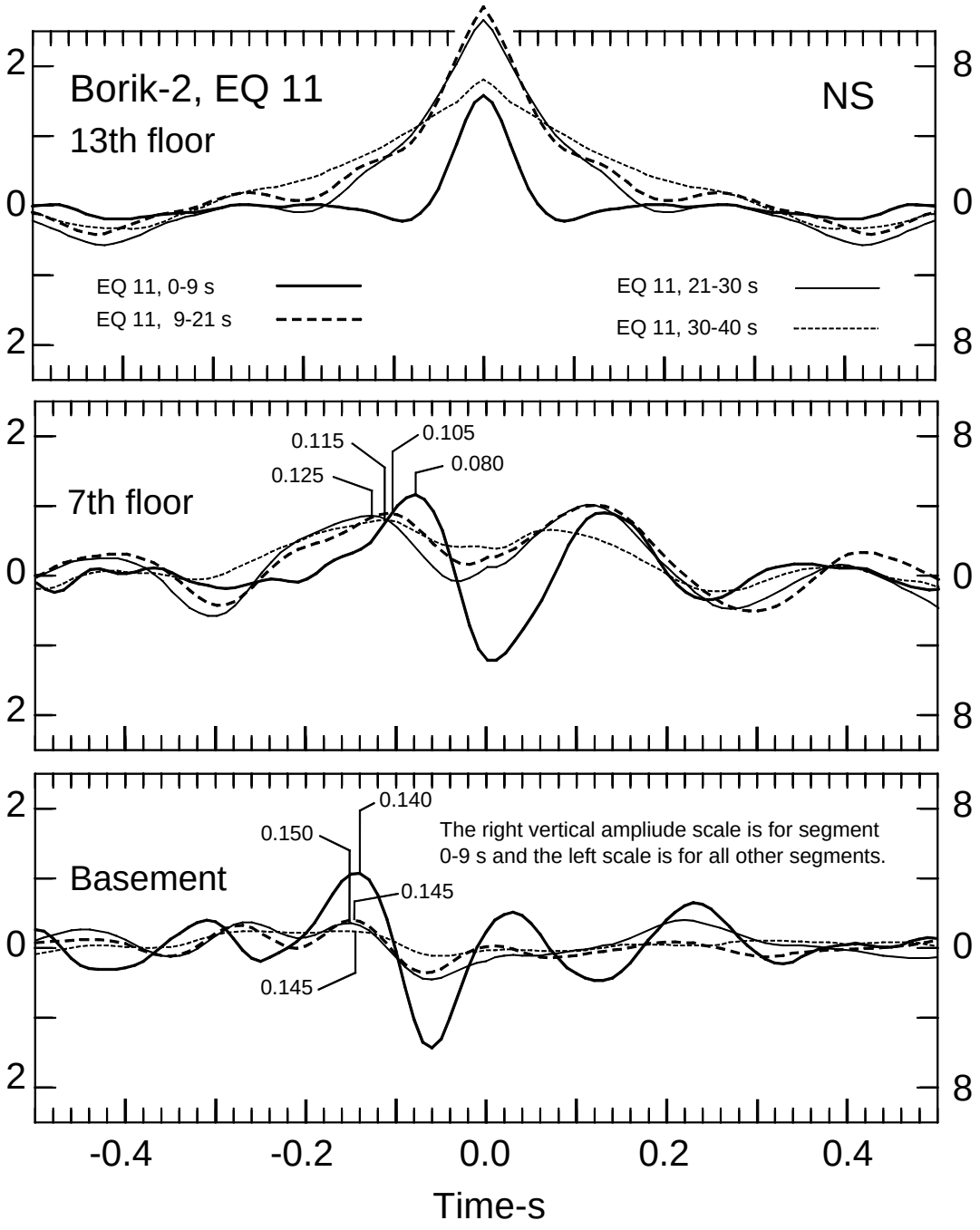

Fig. 4.4.3a Impulse response functions for NS response of the Borik-2 building for four consecutive time intervals during event EQ 11: 0–9 s, 10–21 s, 22–30 s, and 31–40 s.

corresponding smooth representation in terms of the Gabor transform (Figs. 4.4.1a,b), with the pre-EQ 11 conditions (f_{sys} as evaluated during forced-vibration tests in October 1972, and

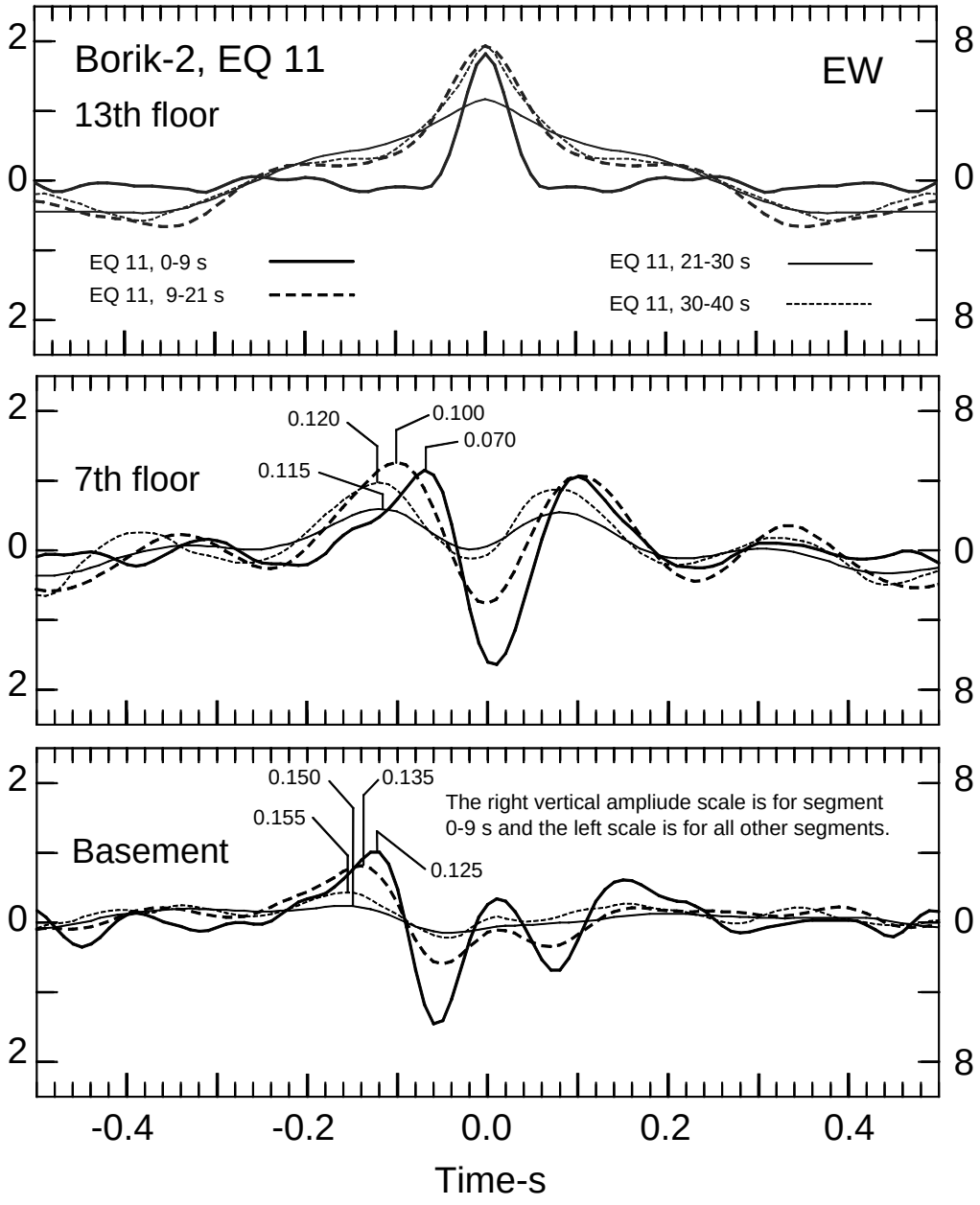

Fig. 4.4.3b Same as Fig. 4.4.3a, but for the EW response.

average f_{sys} during the small earthquakes that preceded the event EQ 11 in 1981) and with post-EQ 11 conditions (average f_{sys} as evaluated during the small earthquakes that followed EQ 11 and average f_{sys} as evaluated during ambient vibration tests in 1983).

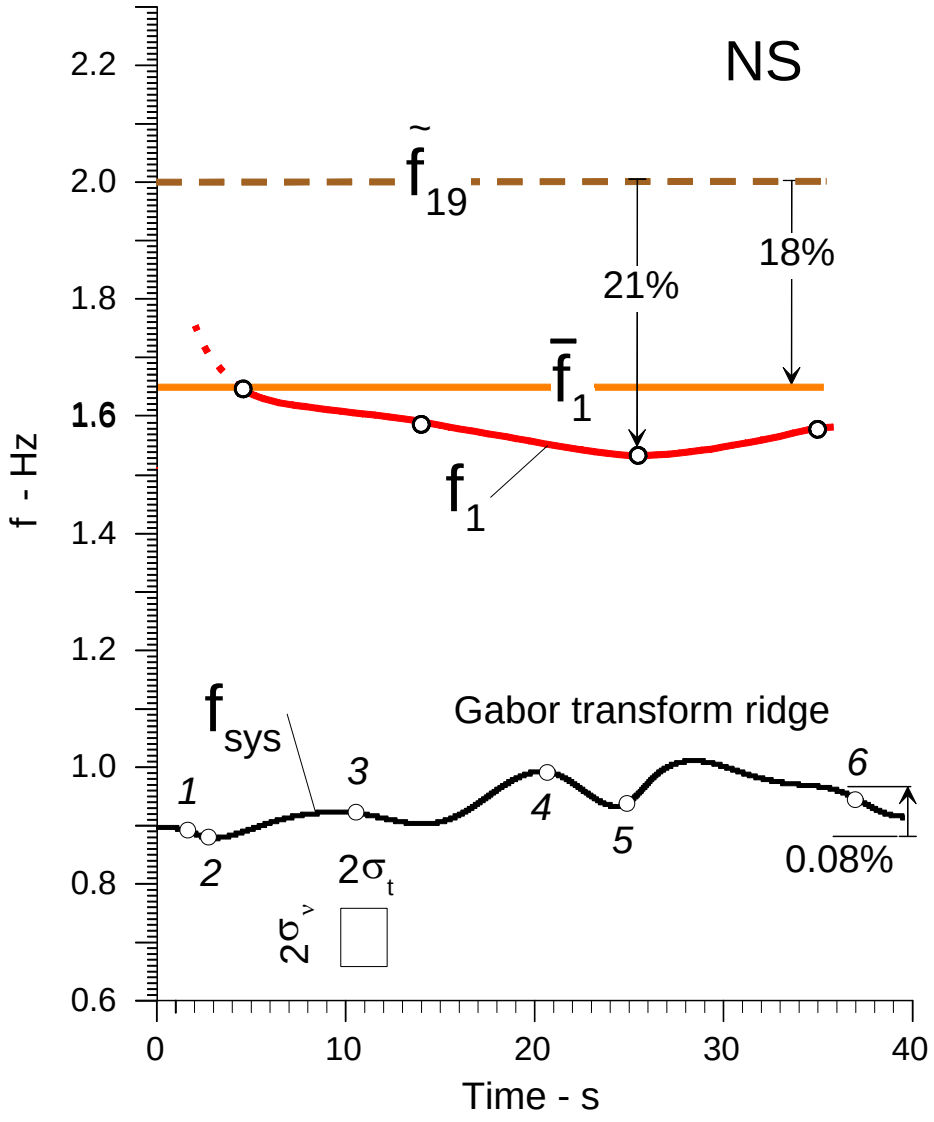

Fig. 4.4.4a Comparison of (a) average value of f_1, designated by $\bar{f}_1$ (computed via impulse response functions and wave travel times for the 40 s-long record from EQ 11; see Tables 4.11 and 4.21); (b) the average trend of f_1 during the 19 small events, designated by $\tilde{f}_{19}$; and (c) the smoothed changes of f_1 during 40 s of NS strong motion (top). Simultaneous changes of f_{sys} estimated via the ridge of the Gabor transform are also shown (bottom).

Figs. 4.4.3a and b show the impulse response functions for four consecutive time intervals during event EQ 11: 0–9 s, 10–21 s, 21–30 s, and 30–40 s. Table 4.4.1 summarizes the arrival times t_i and the estimates of the interval travel times τ_i. Because the top SMA-1 instrument is on the 13th floor (36.07 m above the basement instrument) and not on the roof (38.87 m above the basement

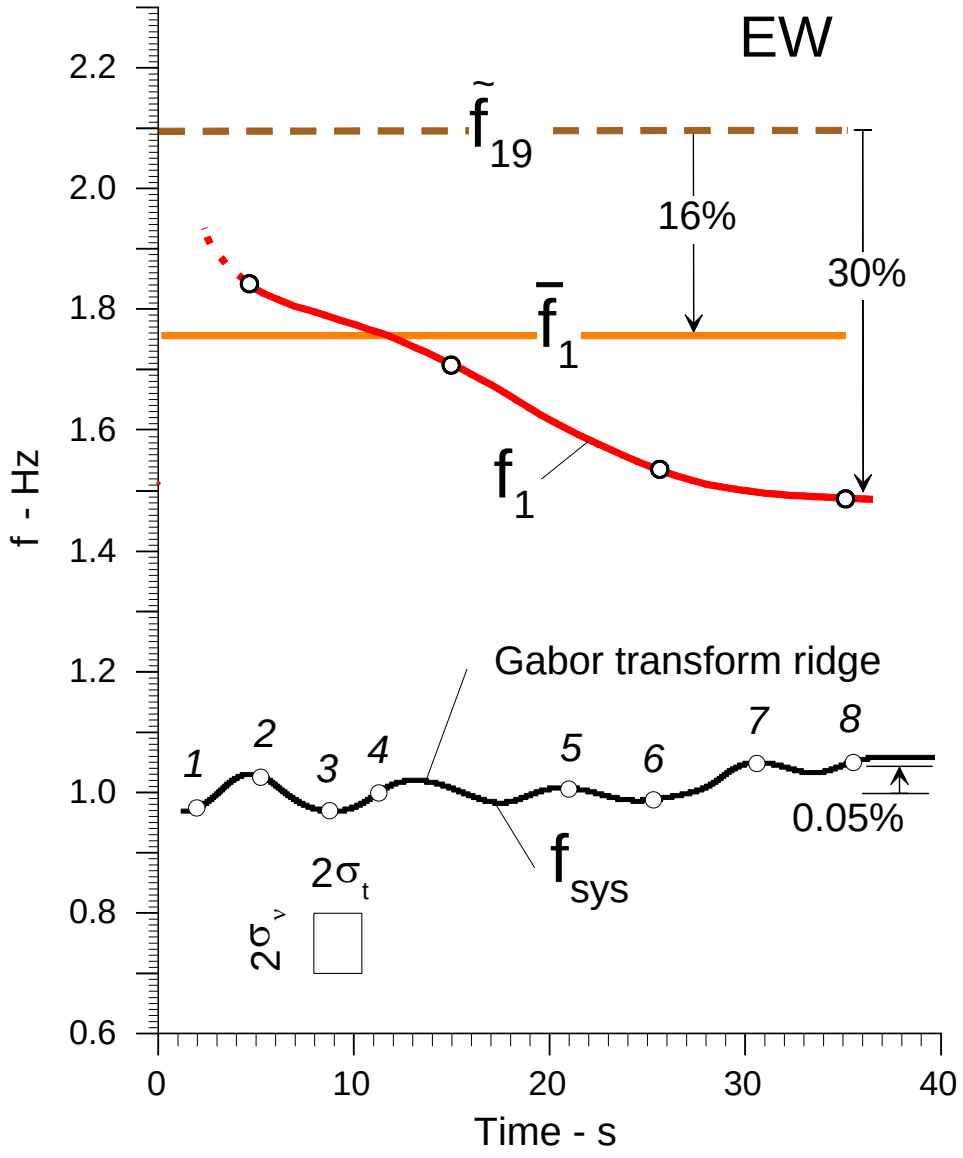

Fig. 4.4.4b Same as Fig.4.4.4a, but for the EW response.

instrument), we prorated the travel times by a factor 38.87/36.07 = 1.08 (note that we are not considering here the additional 3.4 m to the top of the building, which includes the terrace and the elevator equipment on the roof. Those certainly add to the complexities of the impulse response functions at the 13th floor, but they are not part of the structural system and have smaller plan dimensions, so that the waves are expected to effectively reflect off the roof surface). Because the fundamental period of vibration is four times longer than the travel time from the bottom to the top of the building, when we prorate the travel times by 1.08 we obtain the estimates for the NS vibrations f_1 = 1.65, 1.59, 1.54, and 1.59 Hz, and for the EW vibrations f_1 = 1.85, 1.71, 1.54, and 1.49 Hz, respectively, for the time intervals 0 < t < 9 s, 9 < t < 21 s, 21 < t < 30 s, and 30 < t < 40 s. Changes in these frequencies with time are also shown in Figs. 4.4.4a and b. The average values of f_1, designated by $\overline{f_1}$ (computed via impulse response

Table 4.4.1 Event EQ 11, Recorded in the Borik-2 Building (NS and EW Motions): Measured Pulse Arrival Times, t_i, and Corresponding Wave Travel Times, τ_i.

		NS Motions							
		0<t<9 s		9 < t < 21 s		21 < t < 30 s		30 < t < 40 s	
Input Impulse	(1)	(2a)	(2b)	(3a)	(3b)	(4a)	(4b)	5(a)	(5b)
	Floor	t_i - s	τ_i - s	t - s	τ_i - s	t_i - s	τ_i - s	t_i - s	τ_i - s
Roof, acusal pulse going down	13th floor	0.0		0.0		0.0		0.0	
			0.080		0.105		0.125		0.115
	7th floor	-0.080		-0.105		-0.125		-0.115	
			0.060		0.040		0.025		0.030
	Basement	-0.140		-0.145		-0.150		-0.145	
Motions									
Roof, acusal pulse going down	13th floor	0.0		0.0		0.0		0.0	
			0.070		0.100		0.115		0.120
	7th floor	-0.070		-0.100		-0.115		-0.120	
			0.055		0.035		0.035		0.035
	Basement	-0.125		-0.135		-0.150		-0.155	

functions and wave travel times for the 40 s-long records; see Tables 4.11 and 4.21), are also shown in Figs. 4.4.4a and b. The overall average trend of f_1 during all other 19 small events,

designated by $\widetilde{f_{19}}$ is also shown for both NS and EW motions. While the overall average drop of f_1 was only 18% and 16% for NS and EW responses, respectively (see also Figs. 4.3.1b and 4.3.2b), time-dependent changes during event EQ 11 show considerably larger short-time drops—21% for NS and 30% for EW responses. During these changes, f_{sys} was almost constant, between 0.9 and 1.0 Hz for NS (Fig. 4.4.2a) and between 0.97 and 1.10 Hz for EW (Fig.4.4.2b) responses.

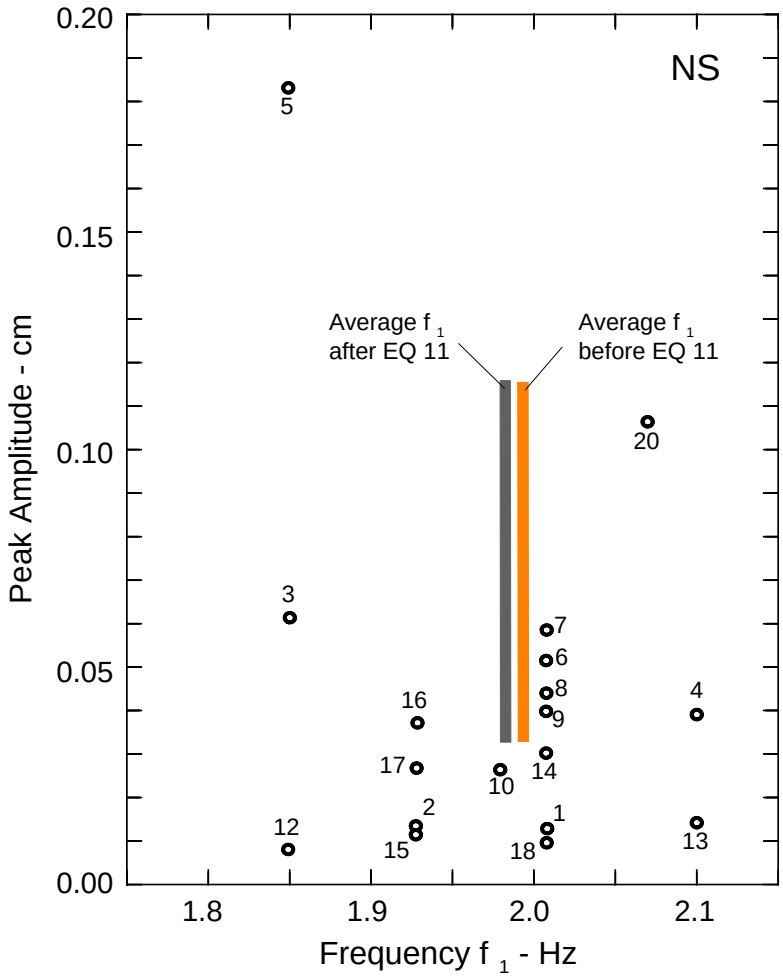

Fig.4.4.5a Peak amplitudes of the relative NS response, $d_{\max}$, at the 13th floor versus f_1. Average values of f_1 before (for nine events, excluding EQ 05), and after (for eight events, see Table 4.21) earthquake EQ 11 are also shown.

The above trends imply that the primary source of changes of the system frequencies in the response of the Borik-2 building during event EQ 11 is caused by the changes in f_1, while small permanent changes after this event are associated with f_{sys} and appear to result from changes in the soil surrounding the building foundation. Compared with our previous findings for the buildings in Southern California (Todorovska and Trifunac 2006, 2007a,d), this constitutes a new and interesting observation, which we will discuss further in what follows.

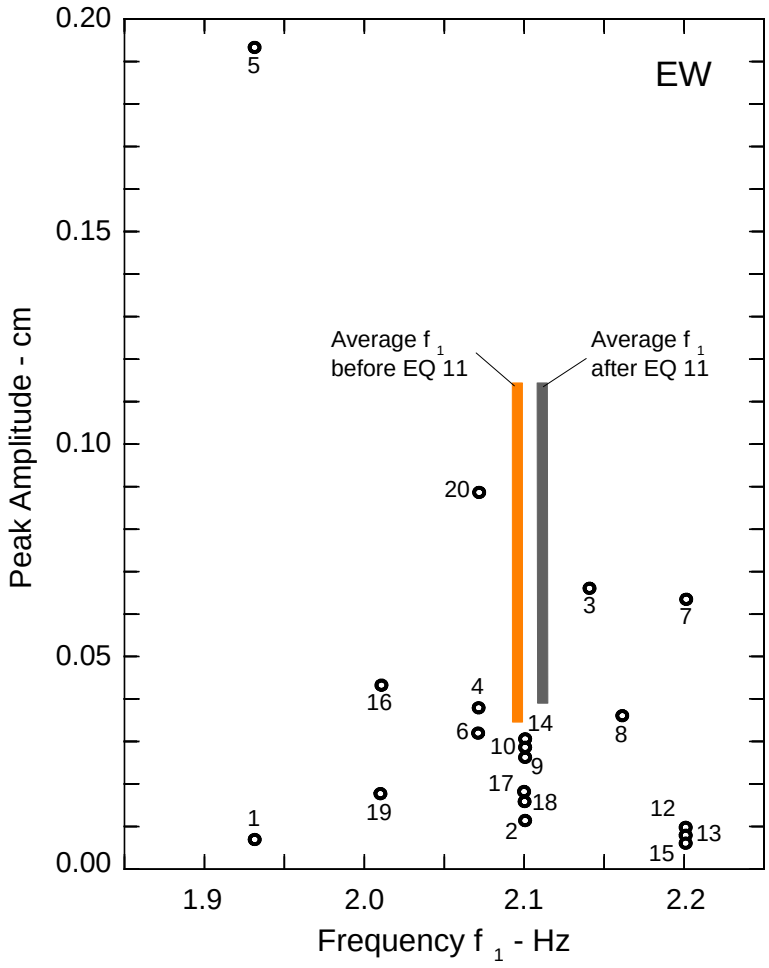

Fig. 4.4.5b Same as Fig. 4.4.5a, but for the EW response.

In Figs. 4.4.3a,b, we show the travel times from the basement to the 13th floor and from 7th floor to the 13th floor, in seconds. These travel times have been chosen to correspond to local peaks in the transfer functions at the basement and the 7th floor, and they have been selected by eye, using "educated empirical" interpretation, based on past experience in working with other buildings

and with various forms of filtering and plotting of this type of data. These times are therefore neither unique nor can their accuracy be easily quantified by some simple error analysis. A more reproducible method of selecting these travel times would require modeling of wave pulses propagating up and down the building and then fitting the model arrival times with the transfer functions shown in Figs. 4.4.3a,b. This more accurate way of selecting the travel times is beyond the scope of this work but will be addressed in our future analyses. As we noted in Todorovska and Trifunac (2006), our aim at present is to document the data for buildings with multiple recordings and to gain insight and experience with regard to what can be done with such data.

In Figs. 4.4.5a, and b, we show peak amplitude of the relative response at the 13th floor versus f_1, which was calculated using the wave travel times from impulse response functions (see Table 4.21). Visual perusal of all peaks shows no obvious dependence of f_1 on peak displacements, and the scatter of points in these two figures appear to be related only to the reading errors in the travel times. This is consistent with our interpretation that for all 19 earthquakes (excluding EQ 11) the Borik-2 building behaved as a linear system with a constant equivalent stiffness (see Figs. 4.3.3a,b) before and after earthquake EQ 11 in 1981. In Figs. 4.4.5a, and b, we also show average values of f_1 for small earthquakes before and after event EQ 11, and excluding the larger event EQ 05 (M = 4.7). Assuming that f_1 indeed did not change, from Figs. 4.4.5a and b we are left with an impression that the standard deviation of the reading errors for f_1 in this study are about 0.1 Hz.

Figures 4.3.1a,b and 4.3.2a,b imply reasonable accuracy of our measurements of f_1 in terms of their consistency with the completely independent estimates of f_{sys}. The estimates of f_1 are based on our subjective reading of the travel times by eye, using impulse response plots. The estimates of f_{sys} are based on a straightforward reading of the peaks in the Fourier spectrum amplitudes of relative displacements at the 13th floor (see Figs. 2.4.5a through 2.4.6e). Figures 4.3.1a,b and 4.3.2a,b show how f_1 and f_{sys} both essentially and consistently follow all small fluctuations of frequency from one event to the next. This consistency assures us that the simple and subjective procedure we used in this work to "read" the values of f_1 is adequate for the purpose and, in qualitative terms, accurate and consistent from one reading to the next, as well as being reproducible. Small fluctuations that show up consistently in the values of f_1 and f_{sys} might be caused by changes in occupancy, rainfall (Todorovska and Al Rjoub 2006), temperature, or a combination of these factors.

The trends of f_{sys} in Figs. 4.3.1b and 4.3.2b show a permanent drop following EQ 11 in 1981 that is about 11% for the NS and 8% for the EW direction. The trends of f_1 in the same figures

show fluctuations but no systematic drop after EQ 11. The systematic change in f_{sys} is even more pronounced for the 2nd system frequency, as shown in Fig. 2.4.7. This may be yet another difference in overall dynamic behavior of this building relative to what we are used to seeing in Southern California, where for small and intermediate levels of shaking f_{sys} often gradually returns to its pre-earthquake values. The difference may be caused by the nature of the site conditions, which beneath the Borik-2 building include considerable gravel deposits. It may be of interest to note here that in our studies of the spectral amplitudes of strong motion in the former Yugoslavia relative to southern California the sites of typical Yugoslav accelerograph stations appear to be "stiffer" (Lee and Trifunac 1992; 1993; Manić 2003).

4.5 Global and Local Indicators of Damage—When Does Damage Occur?

In our previous work, we proposed that the trends of f_1 versus time can be used as a simple *global* indicator of damage (Todorovska and Trifunac 2006, 2007a,d). We stated that a drop in f_1 of more than a certain percentage (about 20% for the Van Nuys building in California) relative to the value of the initial time interval of weaker shaking would be an indicator that damage has occurred. Such an algorithm, implemented in a real-time health-monitoring system, would have indicated that damage occurred in the Van Nuys building during the San Fernando and Northridge earthquakes as early as about 10 s after trigger of strong-motion recorders. We also noted in Todorovska and Trifunac (2007a,d) that such a rule applied to $f_{\rm sys}$ would not work because it would have resulted in a false alarm during other earthquakes. Although Eqn. (3.7) suggests a constant relationship between $f_{\rm sys}$ and f_1 during linear and almost-linear levels of response, that is not necessarily true for strong earthquake shaking because soil can experience nonlinear response, and thus $f_{\rm sys}$ can experience temporary and long-term decreases.

In the case of the Borik-2 building studied here, we found the average drop of f_1 to be equal to 18% for the NS and 16% for the EW responses, respectively. During the strongest shaking by event EQ 11, the largest "instantaneous" drops of f_1 were 21% and 30%, respectively. Based on the reports on the state of this building after the EQ 11 event, which indicated no structural damage, this suggests that the threshold levels for the percentage drop of f_1 will have to be empirically calibrated in terms of the structural types, and possibly relative to the stiffness of the underlying soil.

4.6 Force-Displacement Relationships Inferred From Wave Travel Times

The true nature of the earthquake response of virtually all structures can be described best in terms of *nonlinear* wave propagation (Gičev and Trifunac 2007a,b). The engineering formulation of the corresponding *linear* problem has instead tended to use the vibrational approach, formulated as the Response Spectrum Superposition method, which was proposed in early 1930s (Biot 1932; 1933; 1934; 1941; 1942; Trifunac 2003; 2006). A general theory of the nonlinear response of multi-degree-of-freedom systems has yet to be developed. In the meantime, simplified representations and approximate gross modeling of structures, formulated around various extensions of the response spectrum method, are used in seismic design. One such simplified method for estimation of nonlinear response uses push-over analyses. A typical push-over analysis presents the base shear coefficient versus the displacement of the top of the structure and describes a "force-displacement relationship" of an "equivalent" single-degree-of-freedom system. The results of our analysis can also be viewed in such a form for comparison with previous results and to gain an understanding of how the two approaches compare. For that purpose, we presented in Figures 4.3.3a and b plots showing normalized force-displacement relationships. In the case of the Borik-2 building, our full-scale experimental results show essentially a linear relationship, consistent with small amplitudes of response for the data set studied here.

5. DISCUSSION AND CONCLUSIONS

This report describes our third detailed study of a new structural health-monitoring method based on detecting changes in the stiffness of the structural members by measuring changes in the travel times of seismic waves propagating through these members. The wave travel times are estimated from impulse response analysis. The changes can also be translated into changes of the fundamental fixed-base frequency of the structure. In this study, we applied the method to strong-motion data recorded in the Borik-2 building, which was not damaged by a sequence of earthquakes occurring between 1974 and 1986. The subject of our first previous study included the transverse and longitudinal response of the Imperial County Services Building, in El Centro, California, which was a 6-story reinforced-concrete building damaged by the Imperial Valley earthquake of 1979 (Todorovska and Trifunac 2007d). The subject of our second study was the longitudinal (EW) response of a 7-story reinforced-concrete hotel building located in the city of Van Nuys, in the Los Angeles metropolitan area, which was damaged by the San Fernando earthquake of 1971 and by the Northridge earthquake of 1994. For the latter building, we also analyzed its response for nine other earthquakes. For both previously studied buildings, the results for the system frequencies measured during ambient vibration tests were also available.

In all of these exploratory studies, we applied the impulse response method in its most rudimentary form, based on several simplifying assumptions. The first assumption is that one-dimensional wave propagation up and down the structure can capture the principal features of the response and that side reflections of the non-vertically propagating waves (Todorovska et al. 1988) can be neglected. The second assumption is that it is sufficient to work only with the recorded horizontal translations. Another group of assumptions is related to the transmittal of the incident waves through the foundation. In that regard, we assumed that the effects associated with the horizontal propagation of seismic waves incident through the foundation can be neglected (Gičev 2005; Trifunac et al. 1999), that the structural response resulting from warping and deformation of the foundation can be neglected (Gičev, 2005), and that the rotational waves in the building, caused by soil-structure interaction and by the rotational components of the ground motion (associated with body P and SV waves and Rayleigh surface waves) can be neglected. Finally, we did not consider explicitly the detailed nature of the contributions of torsion and rocking to the recorded horizontal NS and EW translations.

The spatial resolution of the impulse response method depends upon the number and the separation distance of the sensors, while its temporal resolution depends upon the length of the time window chosen for the analysis. We measured the wave travel times by manually reading the impulse arrival times at different sensors, with error of about $\Delta\tau \approx 0.01$ s. As can be seen from Tables 4.1 through 4.20, the wave travel time over the height of the building was between τ_{tot} = 0.105 s and 0.155 s for all 20 events. During the largest event, τ_{tot} was 0.155 s. This

implies that the error in reading the change in the pulse arrival times, $\Delta\tau$, is about five times smaller than the change in τ_{tot} for most events studied here. Translating these errors into the

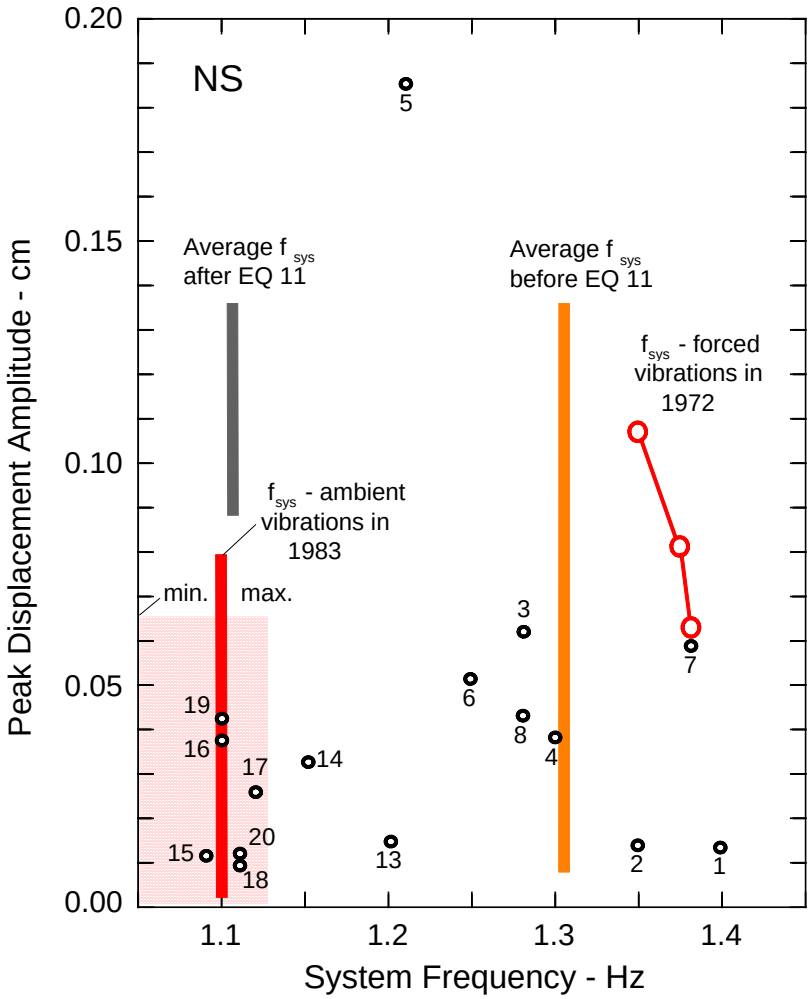

Fig. 5.1a Summary of the changes in system frequency f_{sys} for the NS response of the Borik-2 building during the period 1972–1986. Shown are (a) amplitude dependence of f_{sys} for three force amplitudes (the corresponding peak displacements at resonance are shown by large open circles) during the forced-vibration tests in October 1972; (b) peak relative displacements on 13th floor, d_{max}, versus the corresponding frequencies f_{sys} for 19 "small" earthquakes (open circles); (c) average values of f_{sys} during these "small" earthquakes, before and after EQ 11 in 1981; and (d) minimum, maximum (shown by a shaded zone in bottom left), and average values of measured f_{sys} during ambient vibration tests of the building in June 1983.

resulting errors in the estimates of f_1 gives 0.1 Hz for f_1 near 1.5 Hz, and 0.2 Hz for f_1 near 2.5 Hz, which is in agreement with what we found from the scatter in the estimates of f_1 in Figs. 4.4.5a and b. As we have already noted, the determination of the wave travel times can be made more accurate and automated by fitting a model to the data, but this refinement is beyond the scope of this report.

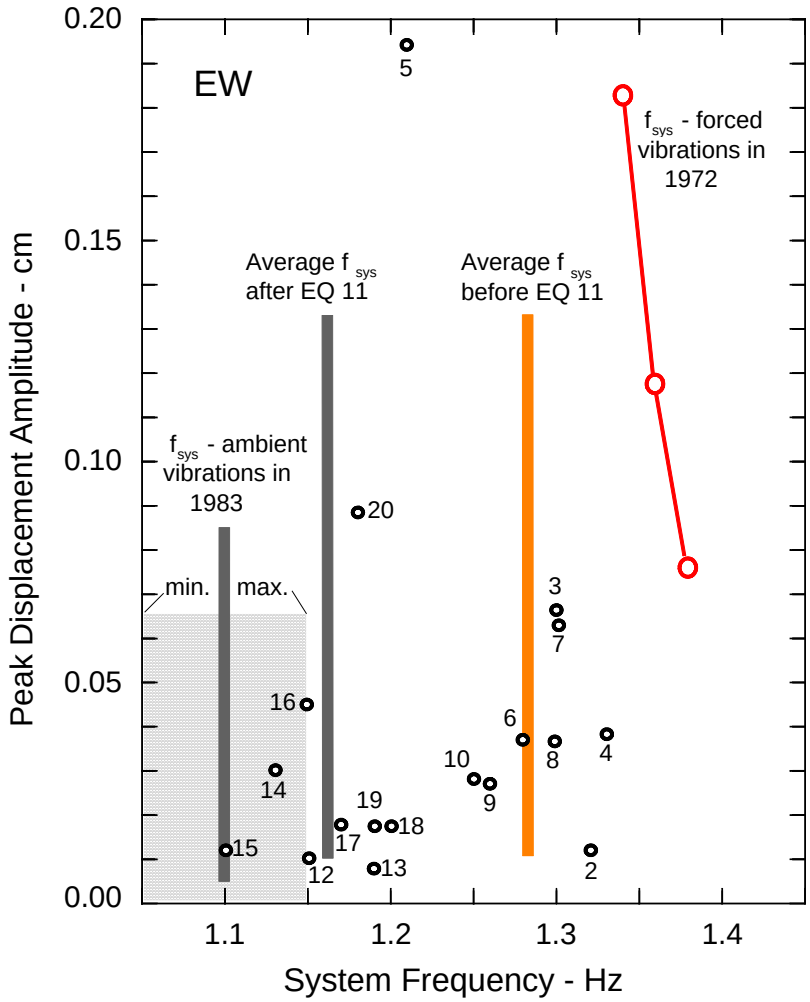

Fig. 5.1b Same as Fig. 5.1a, but for the EW response.

The results in this work confirm the findings of our first study (Todorovska and Trifunac 2006) that, despite the simplifying assumptions, even for time windows as short as about 5 s the impulse response method yields physically meaningful impulse responses and wave travel times. The estimates of fixed-base frequency from the measured wave travel times we found to be consistent with the concurrent estimates of soil-structure system frequency. Our analysis of the

Borik-2 building response to 19 small earthquakes was also found to be in excellent agreement with the estimates of f_{sys} based on forced-vibration tests following the construction (and preceding the first earthquake excitations), and with the estimates of f_{sys} based on the ambient vibration experiments, which took place about two years after the earthquake of 1981 and before a small earthquake (EQ 20), which was recorded in 1986 (Figs. 5.1a and b).

We found that the fixed-base frequency f_1 of the Borik-2 building did not change following earthquake EQ 11 in 1981 but that the f_{sys} was reduced permanently. For the NS system response, its average value (using events 1 through 8, see Table 4.21) was 1.306 Hz before and1.108 Hz (using events 12 through 20) after event EQ 11, which represents a drop of about 15%. For the EW system response, it was 1.283 Hz (using events 2 through 10) before and 1.162 Hz (using events 12 through 20) after event EQ 11, for a drop of about 10%.

Figures 5.1a and b teach us another important lesson, which is that invaluable information can be extracted about the dynamic behavior of structures from analyses of many small recordings of their earthquake response. As these figures show, except for earthquakes 5 and 11 (see Figs.2.4.1 and 2.4.2) all peak displacements at the 13th floor of the Borik-2 building during 18 earthquakes were smaller than those during the forced-vibration tests of October 1972. Accurate digital processing of the very small accelerograms in buildings obviously can provide exceptionally useful information about the structural response. It is therefore the responsibility of all agencies engaged in archiving the strong-motion data in buildings and in other structures to recognize this fact and to process and release this data to the engineering community for analysis and further study.

Considering (1) how much more valuable the data from full-scale observations in real buildings is relative to even the most sophisticated laboratory experiments, (2) that this data is already recorded, and (3) that we have accurate digitization and processing capabilities that enable us to use this data, there should be no further delay in the systematic publication and release of such data on all buildings where multiple recordings have been archived. The only way the science of predicting the earthquake response of structures can be advanced is through creation of a sound and comprehensive database on actual response. This will provide an unquestionable—and the only acceptable—basis for testing various theoretical models and will provide a realistic picture of the nature and extent of changes in structural behavior over time. Without such a database, it is impossible to develop robust and reliable structural health-monitoring systems and to calibrate the required damage detection thresholds. Most structural health-monitoring algorithms are based on detecting some change(s) relative to the conditio quo ante, but as we have shown here for the Borik-2 building, and for the Van Nuys hotel in California (Todorovska and Trifunac 2006, 2007a), those prior conditions also change with time. If those changes are too large or we

do not know what they are because we did not monitor their variations over time, there will be no reliable conditio quo ante, and this will interfere with the detection algorithms and could render them useless.

We conclude that the analysis of wave travel times in a building undergoing earthquake response via impulse response functions, computed from the recorded seismic response, can provide useful and reliable information about the degree and spatial distribution of the changes in its stiffness. This method should be further improved and refined.

ACKNOWLEDGEMENTS

We are grateful to B. Petrović, one of the designers of the IMS system, for his useful discussions and comments about the Borik-2 building. We are grateful to P. Fajfar for sending us his article with the results of dynamic analyses of the Borik-2 building. We are indebted to Lj. Taškov and L. Krstevska for their invaluable help in interpreting the 1983 report on ambient vibration measurements in the Borik-2 building and for many useful discussions and comments. Last but not the least, we thank the director and the staff of the Seismological Observatory in Skopje for their hospitality during August 2006, while we digitized the Borik-2 data there.

REFERENCES

Aničić, D., Fajfar, P., Petrović, Szavits-Nossan, A., and Tomaževič, M. (1990). Zemljotresno Inženjerstvo (visokogradnja), Građjevinska Knjiga, Beograd.

Biot, M.A. (1932). Vibrations of buildings during earthquake, Chapter II in Ph.D. Thesis No. 259, entitled *Transient Oscillations in Elastic System*, Aeronautics Department, Calif. Inst. of Tech., Pasadena, California.

Biot, M.A. (1933). Theory of elastic systems vibrating under transient impulse with an application to earthquake-proof buildings, *Proc. National Academy of Sciences*, 19(2), 262–268.

Biot, M.A. (1934). Theory of vibration of buildings during earthquakes, *Zeitschrift für. Angewandte Matematik und Mechanik*, 14(4), 213–223.

Biot, M.A. (1941). A mechanical analyzer for the prediction of earthquake stresses, *Bull. Seism. Soc. Amer*., 31, 151–171.

Biot, M.A. (1942). Analytical and experimental methods in engineering seismology, *ASCE Transactions*, 108, 365–408.

Browning, J.A., Li, R.Y., Lynn, A., and Moehle, J.P. (2000). Performance assessment for a reinforced concrete frame building, *Earthquake Spectra*, 16(3), 541–555.

Chang P.C., Flatau A., and Liu S.C. (2003). Review paper: Health monitoring of civil infrastructure, *Structural Health Monitoring*, 2(3), 257–267.

Čaušević, M. (1988). Mathematical modeling of reinforced concrete structures subjected to earthquakes, Univ. Đuro Pucar Stari, Publication No. JFP 519E, Banja Luka, Yugoslavia.

De la Llera, J.C., Chopra, A.K., and Almazan, J.L. (2001). Three-dimensional inelastic response of an RC building during the Northridge earthquake. *J. Structural Eng.*, ASCE, 127(5), 482–489.

Dimitrijević, R. (1982). Primana montažnog skeleta od prednapregnutog betona u sssr-u na bazi jugoslovenskog sistema IMS, *Bilten IMS*, Godina IX, Broj 1, 2–7.

Dimitrijević, R. (2002). *World Housing Encyclopedia Report* (country: Yugoslavia), Earthquake Engineering Research Institute and International Association of Earthquake Engineering.

Doebling S.W., Farrar C.R., Prime M.B., and Shevitz D.W. (1996). Damage identification and health monitoring of structural and mechanical systems from changes in their vibration characteristics: A literature review, *Report LA-13070-MS*, Los Alamos National Laboratory, Los Alamos, NM.

Fajfar, P., Čaušević, M., and Jiang, Y. (1987). Comparison of analytically and experimentally determined dynamic behavior of a multistory RC building, *Proceedings of the EUROBUIL 87*, Dubrovnik, 134–139.

Gičev, V. (2005). *Investigation of Soil-Flexible Foundation-Structure Interaction for Incident Plane SH Waves*, Ph.D. Dissertation, Dept. of Civil Engineering, Univ. Southern California, Los Angeles, California.

Gičev, V., and Trifunac, M.D. (2007a). Permanent deformations and strains in a shear building excited by a strong motion pulse, *Soil Dynamics and Earthquake Engineering,* 27(8), 774–792.

Gicev, V., and Trifunac, M.D. (2007b). Energy and power of nonlinear waves in a seven story reinforced concrete building, *Indian Society of Earthquake Technology Journal*, 44(1), (in Press).

Haddadi, H.R., and Kawakami, H. (1998). Modeling wave propagation by using normalized input-output minimization (NIOM) method for multiple linear systems, *Structural Eng./ Earthquake Eng.*, JSCE, 15(1), 29–39

Hudson, D.E. (1970). Dynamic tests of full-scale structures, Chapter 7 in *Earthquake Engineering*, R. Wiegel (ed.), New Jersey: *Prentice Hall*.

Islam, M.S. (1996). Analysis of the response of an instrumented 7-story nonductile concrete frame building damaged during the Northridge earthquake, *Professional paper 96-9*, Los Angeles Tall Building Structural Design Council, 1996 Annual Meeting.

Ivanović, S., Trifunac, M.D., and Todorovska, M.I. (2001). On identification of damage in structures via wave travel times, *Proc. NATO Workshop on Strong Motion Instrumentation for Civil Engineering Structures*, June 2–5, 1999, Istanbul Turkey, Kluwer Academic Pub., Dordrecht, 447–468.

Jordanovski, L.R., Lee, V.W., Manić, M.I., Olumčeva, T., Sinadinovski, C., Todorovska, M.I., and Trifunac, M.D. (1987). Strong earthquake ground motion data in EQINFOS: Yugoslavia, Part 1*, Dept. of Civil Eng. Rep., No. 87-15*, Univ. of Southern California, Los Angeles, California.

Jurukovski, D.V., Taškov, Lj. A., and Trajkovski, V.K. (1984). Mathematical model formulation of a fourteen story rc building using strong motion records and parameter system identification,

Proceedings of the 8th World Conference on Earthquake Engineering, San Francisco, IV, 615–619.

Kanai, K. (1965). Some new problems of seismic vibrations of a structure, *Proc. Third World Conf. on Earthquake Engineering*, Auckland and Wellington, New Zealand, January 22–February 1, 1965, II-260 to II-275.

Kojic,S., Trifunac, M.D., and Anderson, J.C. (1984) *A Post Earthquake Response Analysis of the Imperial County Services Building*, Department of Civil Engineering, Report CE 84-02, University of Southern Calif., Los Angeles, California.

Lee, V.W, and Trifunac, M.D. (1990). *Automatic Digitization and Processing of Accelerograms Using PC*, Dept. of Civil Eng. Report 90-03, Univ. Southern California, Los Angeles, California.

Lee, V.W., and Trifunac, M.D. (1992). Frequency dependent attenuation of strong earthquake ground motion in Yugoslavia, *European Earthquake Eng*., VI(1), 3–13.

Lee, V.W., and Trifunac, M.D. (1993). Empirical scaling of Fourier amplitude spectra in former Yugoslavia, *European Earthquake Eng*., VII(2), 47–61.

Li, Y.R., and Jirsa, J.O. (1998). Nonlinear analyses of an instrumented structure damaged in the 1994 Northridge earthquake, *Earthquake Spectra*, 14(2), 265N283.

Luco, J.E., Wong, H.L., and Trifunac, M.D. (1986). *Soil Structure Interaction Effects on Forced Vibration Tests*, Department of Civil Engineering, Report CE 86-05, University of Southern Calif., Los Angeles, California.

Ma, J., and Pines, D.J. (2003). Damage detection in a building structure model under seismic excitation using dereverberated wave machines, *Engineering Structures*, 25, 385–396.

Manić, M. (2003). *Prilog kon definiranje na empiriskite modeli za ocenka na Furievite spektri na zabrzuvanjeto na počvata so primena za teritorijata na balkanskiot region*, Ph.D. Dissertation, Institut za zemjotresno inženerstvo i inženerska seizmologija (IZIIS), Univerzitet "Sv. Kiril i Metodij", Skopje, Makedonija.

Petrović, B. (1982). Ispitivanje veza u sistemu IMS, *Bilten IMS*, Godina IX, Broj 1, 8–17.

Petrović, B. (1989). *Odabrana Poglavlja iz Zemljotresnog Gradjevinarstva* (II izdanje), IRO Gradjevinska Knjiga, Beograd.

Petrovski, J., Jurukovski, D., and Perčinkov, S. (1975). *Forced-Vibration Test of a 13 Story Building in Banja Luka, Constructed by the System IMS-Zezelj*, Report DTL 3-75, Institute of Earthquake Engineering and Engineering Seismology, Univ. "Kiril and Metodij," Skopje, Yugoslavia.

Şafak, E. (1999). Wave propagation formulation of seismic response of multi-story buildings. *J. of Structural Eng*., ASCE, 125(4), 426–437.

Snieder, R., and Şafak, E. (2006). Extracting the building response using interferometry: Theory and applications to the Millikan Library in Pasadena, California, *Bull. Seism. Soc. Am*., 96(2), 586–598.

Taškov, Lj., and Krstevska, L. (1983). Dinamičko ispitivanje objekta BS-2 i BS-4 spratnosti P+12 Banja Luka, metodom ambijent vibracija, Institut za zemjotresno inženerstvo i inženerska seizmologija, Univerzitet "Kiril i Metodij", Izveštaj IZIIS 83-86, Skopje, Macedonija.

Todorovska, M.I., and Lee, V.W. (1989). Seismic waves in buildings with shear walls or central core, *J. Engrg Mech.*, ASCE, 115(12), 2669–2686.

Todorovska, M.I, and Al-Rjoub, Y. (2006). Effects of rainfall on soil-structure system frequency: examples based on poroelasticity and a comparison with full-scale measurements, *Soil Dynamics and Earthquake Engineering*, 26(6-7), 708–717.

Todorovska, M.I., and Trifunac, M.D. (1989). Antiplane earthquake waves in long structures, *J. Engrg Mech.*, ASCE, 115(12), 2687–2708.

Todorovska, M.I., and Trifunac, M.D. (1990). A note on the propagation of earthquake waves in buildings with soft first floor, *J. Engrg Mech*., ASCE, 116(4), 892–900.

Todorovska, M.I., and Trifunac, M.D. (2006). *Impulse Response Analysis of the Van Nuys 7-Story Hotel During 11 Earthquakes (1971-1994): One-dimensional Wave Propagation and Inferences on Global and Local Reduction of Stiffness Due to Earthquake Damage*, Dept. of Civil Eng. Report, CE 06-01, University of Southern California, Los Angeles, California.

Todorovska, M.I., and Trifunac, M.D. (2007a). Impulse response analysis of the Van Nuys 7-story hotel during 11 earthquakes and earthquake damage detection, *Structural Control and Health Monitoring* (in press).

Todorovska, M.I., and Trifunac, M.D. (2007b). Earthquake damage detection in the Imperial County Services Building I: The data and time-frequency analysis, *Soil Dynam. and Earthquake Engrg.*(submitted for publication).

Todorovska, M.I., and Trifunac, M.D. (2007c). Earthquake damage detection in the Imperial County Services Building II: analysis of novelties via wavelets, *Soil Dynam. and Earthquake Engrg* (submitted for publication).

Todorovska, M.I. and Trifunac, M.D. (2007d). Earthquake damage detection in the Imperial County Services Building III: Analysis of wave travel times via impulse response functions, *Soil Dynam. and Earthquake Engrg* (in press).

Todorovska, M.I., Lee, V.W., and Trifunac, M.D. (1988). *Investigation of Earthquake Response of Long Buildings*, Dept. of Civil Engineering Report CE 88-02, Univ. of Southern California, Los Angeles, California.

Trajkovski, V. (1992). *Definiranje na mathematički model na konstruktiven sistem vrz baza na registracija na silen zemjotres so pomoš na parametarska identifikacija na sistemot*, M.S. Dissertation, Institut za zemjotresno inženerstvo i inženerska seizmologija, Univerzitet "Sv. Kiril i Metodij," Skopje, Makedonija.

Trifunac, M.D. (2003). 70th Anniversary of Biot Spectrum, 23rd Annual ISET Lecture, *J. Indian Society of Earthquake Technology*, 40(1), 19–50.

Trifunac, M.D. (2006). Biot response spectrum, *Soil Dynamics and Earthquake Engineering,* 26(6-7), 491–500.

Trifunac, M.D., and Ivanović, S.S. (2003a). Reoccurrence of site specific response in former Yugoslavia – Part I: Montenegro, *Soil Dynamics and Earthquake Eng*., 23(8), 637–661.

Trifunac, M.D., and Ivanović, S.S. (2003b). Reoccurrence of site specific response in former Yugoslavia – Part II: Friuli, Banja Luka, and Kopaonik, *Soil Dynamics and Earthquake Eng*., 23(8), 663–681.

Trifunac, M.D., and Ivanović, S.S. (2003c). *Analysis of Drifts in a Seven-Story Reinforced Concrete Structure*, Dept. of Civil Eng. Report CE 03-01, Univ. of Southern California, Los Angeles, California.

Trifunac, M.D., and Lee, V.W. (1979). *Automatic Digitization and Processing of Strong-Motion Accelerograms*, Part I, pp. 1–259, Part II, pp. 260–379, Dept. of Civil Eng. Report CE 79-15, Univ. of Southern California, Los Angeles, California.

Trifunac, M.D., and Todorovska, M.I. (2001). Recording and interpreting earthquake response of full-scale structures, *Proc. NATO Workshop on Strong Motion Instrumentation for Civil Engineering Structures*, June 2–5, 1999 Istanbul, Turkey, Kluwer Pub. Dordreeht, 131–155.

Trifunac, M.D., and Lee, V.W. (1990). *Automatic Digitization and Processing of Accelerograms Using PC*, Dept. of Civil Eng., Report CE 90-03, Univ. Southern California, Los Angeles, California.

Trifunac, M.D., Ivanović, S.S., Todorovska, M.I., Novikova, E.I., and Gladkov, A.A. (1999). Experimental evidence for flexibility of a building foundation supported by concrete friction piles, *Soil Dynam. and Earthquake Eng*., 18, 169–187.

Trifunac, M.D., Ivanović, S.S., and Todorosvka, M.I. (2001). Apparent periods of a building II: time-frequency analysis, *J. of Struct. Engrg*, ASCE, 127(5), 527–537.

Trifunac, M.D., Ivanović, S.S., and Todorosvka, M.I. (2003). Wave propagation in a seven-story reinforced concrete building: III—damage detection via changes in wave numbers, *Soil Dyn. And Earthquake Eng.*, 23(1), 65–75.

Vojnović, B. (1982). Sigurnost IMS skeletne konstrukcije pri neregularnim opterećenjima i građenju, *Bilten IMS*, Godina IX, Broj 1, 18–25.